Chaos in Hamiltonian systems

Haris Skokos

Department of Mathematics and Applied Mathematics
University of Cape Town
Cape Town, South Africa

E-mail: haris.skokos@uct.ac.za
URL: http://math_research.uct.ac.za/~hskokos/

28th Summer School - Conference 'Dynamical Systems and Complexity', Greece, 19 July 2022

Outline

- **Chaos**
- **Autonomous Hamiltonian systems. Example: Hénon-Heiles system**
- **Regular vs Chaotic motion**
- **Visualization of chaos: Poincaré Surface of Section (PSS)**
- **Chaos Indicators**
  - ✓ **Variational equations and Tangent map**
  - ✓ **Lyapunov exponents**
  - ✓ **Smaller ALignment Index – SALI**
  - ✓ **Generalized ALignment Index – GALI**

Chaos

Definition [Devaney (1989)]

Let V be a set and $f : V \to V$ a map on this set.

We say that f is chaotic on V if

Chaos

Definition [Devaney (1989)]

Let V be a set and $f : V \to V$ a map on this set.

We say that f is chaotic on V if

1. **f has sensitive dependence on initial conditions.**

Chaos

Definition [Devaney (1989)]

Let V be a set and $f : V \to V$ a map on this set.

We say that f is chaotic on V if

1. **f has sensitive dependence on initial conditions.**
2. **f is topologically transitive.**

Chaos

Definition [Devaney (1989)]

Let V be a set and $f : V \to V$ a map on this set.

We say that f is chaotic on V if

1. **f has sensitive dependence on initial conditions.**
2. **f is topologically transitive.**
3. **periodic points are dense in V.**

Chaos

1. f has sensitive dependence on initial conditions.

Chaos

1. f has sensitive dependence on initial conditions.

$\mathbf{f} : V \to V$ has *sensitive dependence on initial conditions* if there exists $\delta > 0$ such that, for any $\mathbf{x} \in V$ and any neighborhood Δ of $\mathbf{x}$, there exist $\mathbf{y} \in \Delta$ and $n \geq 0$, such that $|\mathbf{f}^n(\mathbf{x}) - \mathbf{f}^n(\mathbf{y})| > \delta$, where $\mathbf{f}^n$ denotes n successive applications of $\mathbf{f}$.

Chaos

1. f has sensitive dependence on initial conditions.

$\mathbf{f} : V \rightarrow V$ has *sensitive dependence on initial conditions* if there exists $\delta > 0$ such that, for any $\mathbf{x} \in V$ and any neighborhood Δ of $\mathbf{x}$, there exist $\mathbf{y} \in \Delta$ and $n \geq 0$, such that $|\mathbf{f}^{n}(\mathbf{x}) - \mathbf{f}^{n}(\mathbf{y})| > \delta$, where $\mathbf{f}^{n}$ denotes n successive applications of **f**.

There exist points arbitrarily close to **x** which eventually separate from **x** by at least δ under iterations of **f**.

Chaos

1. f has sensitive dependence on initial conditions.

f : $V \to V$ has *sensitive dependence on initial conditions* if there exists $\delta > 0$ such that, for any $\mathbf{x} \in V$ and any neighborhood Δ of **x**, there exist $\mathbf{y} \in \Delta$ and $n \geq 0$, such that $|\mathbf{f}^n(\mathbf{x}) - \mathbf{f}^n(\mathbf{y})| > \delta$, where $\mathbf{f}^n$ denotes n successive applications of **f**.

There exist points arbitrarily close to **x** which eventually separate from **x** by at least δ under iterations of **f**.

Not all points near **x** need eventually move away from **x** under iteration, but there must be at least one such point in every neighborhood of **x**.

Chaos

2. f is topologically transitive.

Chaos

2. f is topologically transitive.

$\mathbf{f} : V \to V$ is said to be *topologically transitive* if for any pair of open sets $U, W \subset V$ there exists $n > 0$ such that $\mathbf{f}^{\,n}(U) \cap W \neq \emptyset$.

Chaos

2. f is topologically transitive.

$\mathbf{f} : V \rightarrow V$ is said to be *topologically transitive* if for any pair of open sets $U, W \subset V$ there exists $n > 0$ such that $\mathbf{f}^{\,n}(U) \cap W \neq \emptyset$.

This implies the existence of points which eventually move under iteration from one arbitrarily small neighborhood to any other.

Chaos

2. f is topologically transitive.

$\mathbf{f} : V \rightarrow V$ is said to be *topologically transitive* if for any pair of open sets $U, W \subset V$ there exists $n > 0$ such that $\mathbf{f}^{\,n}(U) \cap W \neq \emptyset$.

This implies the existence of points which eventually move under iteration from one arbitrarily small neighborhood to any other.

Consequently, the dynamical system cannot be decomposed into two disjoint invariant open sets.

Chaos

A chaotic system possesses three ingredients:

Chaos

A chaotic system possesses three ingredients:

1. **Unpredictability because of the sensitive dependence on initial conditions**

Chaos

A chaotic system possesses three ingredients:

1. **Unpredictability because of the sensitive dependence on initial conditions**
2. **Indecomposability because it cannot be decomposed into noninteracting subsystems due to topological transitivity**

Chaos

A chaotic system possesses three ingredients:

1. **Unpredictability** because of the sensitive dependence on initial conditions
2. **Indecomposability** because it cannot be decomposed into noninteracting subsystems due to topological transitivity
3. **An element of regularity** because it has periodic points which are dense.

Chaos

A chaotic system possesses three ingredients:

1. **Unpredictability because of the sensitive dependence on initial conditions**
2. **Indecomposability because it cannot be decomposed into noninteracting subsystems due to topological transitivity**
3. **An element of regularity because it has periodic points which are dense.**

Usually, in physics and applied sciences, people use the notion of chaos in relation to the sensitive dependence on initial conditions.

Autonomous Hamiltonian systems

Consider an N degree of freedom autonomous Hamiltonian system having a Hamiltonian function of the form:

$$H(\underbrace{q_1,q_2,\ldots,q_N}_{\text{positions}},\ \underbrace{p_1,p_2,\ldots,p_N}_{\text{momenta}})$$

Autonomous Hamiltonian systems

Consider an N degree of freedom autonomous Hamiltonian system having a Hamiltonian function of the form:

$$H(\underbrace{q_1,q_2,\ldots,q_N}_{\text{positions}},\ \underbrace{p_1,p_2,\ldots,p_N}_{\text{momenta}})$$

The time evolution of an orbit (trajectory) with initial condition

$$P(0)=(q_1(0),\ q_2(0),\ldots,q_N(0),\ p_1(0),\ p_2(0),\ldots,p_N(0))$$

is governed by the Hamilton's equations of motion

$$\frac{dp_i}{dt} = -\frac{\partial H}{\partial q_i}\ ,\qquad \frac{dq_i}{dt} = \frac{\partial H}{\partial p_i}$$

Autonomous Hamiltonian systems

Consider an N degree of freedom autonomous Hamiltonian system having a Hamiltonian function of the form:

$$\underbrace{}_{}\overbrace{}^{}H(\overbrace{q_1,q_2,\ldots,q_N}^{\text{positions}},\ \overbrace{p_1,p_2,\ldots,p_N}^{\text{momenta}})$$

The time evolution of an orbit (trajectory) with initial condition

$$P(0)=(q_1(0),\ q_2(0),\ldots,q_N(0),\ p_1(0),\ p_2(0),\ldots,p_N(0))$$

is governed by the Hamilton's equations of motion

$$\frac{dp_i}{dt} = -\frac{\partial H}{\partial q_i}\ ,\qquad \frac{dq_i}{dt} = \frac{\partial H}{\partial p_i}$$

Phase space: the 2N dimensional space defined by variables $q_1,q_2,\ldots,q_N,\ p_1,p_2,\ldots,p_N$

Example (Hénon-Heiles system)

Example (Hénon-Heiles system)

$$H = \frac{1}{2}\left(p_x^2 + p_y^2\right) + \frac{1}{2}\left(x^2 + y^2\right) + x^2 y - \frac{1}{3} y^3$$

Example (Hénon-Heiles system)

$$H = \frac{1}{2}\left(p_x^2 + p_y^2\right) + \frac{1}{2}\left(x^2 + y^2\right) + x^2 y - \frac{1}{3}y^3$$

THE ASTRONOMICAL JOURNAL VOLUME 69, NUMBER 1 FEBRUARY 1964

The Applicability of the Third Integral Of Motion: Some Numerical Experiments

MICHEL HÉNON* AND CARL HEILES

Princeton University Observatory, Princeton, New Jersey

(Received 7 August 1963)

The problem of the existence of a third isolating integral of motion in an axisymmetric potential is investigated by numerical experiments. It is found that the third integral exists for only a limited range of initial conditions.

Example (Hénon-Heiles system)

$$H = \frac{1}{2}\left(p_x^2 + p_y^2\right) + \frac{1}{2}\left(x^2 + y^2\right) + x^2 y - \frac{1}{3} y^3$$

THE ASTRONOMICAL JOURNAL VOLUME 69, NUMBER 1 FEBRUARY 1964

The Applicability of the Third Integral Of Motion: Some Numerical Experiments

MICHEL HÉNON* AND CARL HEILES

Princeton University Observatory, Princeton, New Jersey

(Received 7 August 1963)

The problem of the existence of a third isolating integral of motion in an axisymmetric potential is investigated by numerical experiments. It is found that the third integral exists for only a limited range of initial conditions.

Hamilton's equations of motion:

$$\frac{dp_i}{dt} = -\frac{\partial H}{\partial q_i}, \quad \frac{dq_i}{dt} = \frac{\partial H}{\partial p_i}$$

Example (Hénon-Heiles system)

$$H = \frac{1}{2}\left(p_x^2 + p_y^2\right) + \frac{1}{2}\left(x^2 + y^2\right) + x^2 y - \frac{1}{3}y^3$$

THE ASTRONOMICAL JOURNAL VOLUME 69, NUMBER 1 FEBRUARY 1964

The Applicability of the Third Integral Of Motion: Some Numerical Experiments

Michel Hénon* and Carl Heiles

Princeton University Observatory, Princeton, New Jersey

(Received 7 August 1963)

The problem of the existence of a third isolating integral of motion in an axisymmetric potential is investigated by numerical experiments. It is found that the third integral exists for only a limited range of initial conditions.

Hamilton's equations of motion:

$$\frac{dp_i}{dt} = -\frac{\partial H}{\partial q_i}, \quad \frac{dq_i}{dt} = \frac{\partial H}{\partial p_i} \Rightarrow \begin{cases} \dot{x} = p_x \\ \dot{y} = p_y \\ \dot{p}_x = -x - 2xy \\ \dot{p}_y = -y - x^2 + y^2 \end{cases}$$

Regular vs Chaotic orbits

Hénon-Heiles system

$$H = \frac{1}{2}\left(p_x^2 + p_y^2\right) + \frac{1}{2}\left(x^2 + y^2\right) + x^2 y - \frac{1}{3} y^3$$

Regular vs Chaotic orbits

Hénon-Heiles system

$$H = \frac{1}{2}\left(p_x^2 + p_y^2\right) + \frac{1}{2}\left(x^2 + y^2\right) + x^2 y - \frac{1}{3} y^3$$

For H=0.125 we get a regular and a chaotic orbit with initial conditions (ICs):

$x=0$, $y=0.1$, $p_y=0$ and **$x=0$, $y=-0.25$, $p_y=0$.**

Regular vs Chaotic orbits

Hénon-Heiles system

$$H = \frac{1}{2}\left(p_x^2 + p_y^2\right) + \frac{1}{2}\left(x^2 + y^2\right) + x^2 y - \frac{1}{3} y^3$$

For H=0.125 we get a regular and a chaotic orbit with initial conditions (ICs):

$x=0, y=0.1, p_y=0$ and **$x=0, y=-0.25, p_y=0.$**

We perturb both ICs by **$\delta p_y = 10^{-11}$** (!) and check the evolution of x

Regular vs Chaotic orbits

Hénon-Heiles system

$$H = \frac{1}{2}\left(p_x^2 + p_y^2\right) + \frac{1}{2}\left(x^2 + y^2\right) + x^2 y - \frac{1}{3}y^3$$

For H=0.125 we get a regular and a chaotic orbit with initial conditions (ICs):

$x=0$, $y=0.1$, $p_y=0$ and **$x=0$, $y=-0.25$, $p_y=0$.**

We perturb both ICs by **$\delta p_y=10^{-11}$** (!) and check the evolution of x

Orbit **Perturbed**

Regular vs Chaotic orbits

Hénon-Heiles system

$$H = \frac{1}{2}\left(p_x^2 + p_y^2\right) + \frac{1}{2}\left(x^2 + y^2\right) + x^2 y - \frac{1}{3}y^3$$

For H=0.125 we get a regular and a chaotic orbit with initial conditions (ICs):

$x=0, y=0.1, p_y=0$ and **$x=0, y=-0.25, p_y=0$.**

We perturb both ICs by **$\delta p_y=10^{-11}$** (!) and check the evolution of x

		Orbit	Perturbed
t=	100	x= 0.13299571833307644	0.13299571833717263064

Regular vs Chaotic orbits

Hénon-Heiles system

$$H = \frac{1}{2}\left(p_x^2 + p_y^2\right) + \frac{1}{2}\left(x^2 + y^2\right) + x^2 y - \frac{1}{3}y^3$$

For H=0.125 we get a regular and a chaotic orbit with initial conditions (ICs):

$x=0$, $y=0.1$, $p_y=0$ and **$x=0$, $y=-0.25$, $p_y=0$.**

We perturb both ICs by **$\delta p_y=10^{-11}$** (!) and check the evolution of x

		Orbit	Perturbed
t=	100	x= 0.13299571833307644	0.13299571833 7263064
t=	5000	x= 0.37699928389102310	0.37699928370156576

Regular vs Chaotic orbits

Hénon-Heiles system

$$H = \frac{1}{2}\left(p_x^2 + p_y^2\right) + \frac{1}{2}\left(x^2 + y^2\right) + x^2 y - \frac{1}{3}y^3$$

For H=0.125 we get a regular and a chaotic orbit with initial conditions (ICs):

$x=0$, $y=0.1$, $p_y=0$ and **$x=0$, $y=-0.25$, $p_y=0$.**

We perturb both ICs by **$\delta p_y=10^{-11}$** (!) and check the evolution of x

		Orbit	**Perturbed**
t=	100	x= 0.13299571833307644	0.13299571833726306 4
t=	5000	x= 0.37699928389102310	0.37699928370156576
t=	10000	x=-0.15909458335685522 4	-0.15909458334126030 9

Regular vs Chaotic orbits

Hénon-Heiles system

$$H = \frac{1}{2}\left(p_x^2 + p_y^2\right) + \frac{1}{2}\left(x^2 + y^2\right) + x^2 y - \frac{1}{3} y^3$$

For H=0.125 we get a regular and a chaotic orbit with initial conditions (ICs):

$x=0$, $y=0.1$, $p_y=0$ and **$x=0$, $y=-0.25$, $p_y=0$.**

We perturb both ICs by **$\delta p_y=10^{-11}$** (!) and check the evolution of x

		Orbit	Perturbed
t=	100	x= 0.13299571833307644	0.13299571833726306 4
t=	5000	x= 0.37699928388910231 0	0.37699928387015657 6
t=	10000	x=-0.15909458335685522 4	-0.15909458334126030 9
t=	50000	x= 0.10199240073995576 0	0.10199240025396132 1

Regular vs Chaotic orbits

Hénon-Heiles system

$$H = \frac{1}{2}\left(p_x^2 + p_y^2\right) + \frac{1}{2}\left(x^2 + y^2\right) + x^2 y - \frac{1}{3} y^3$$

For H=0.125 we get a regular and a chaotic orbit with initial conditions (ICs):

$x=0, y=0.1, p_y=0$ and **$x=0, y=-0.25, p_y=0.$**

We perturb both ICs by **$\delta p_y=10^{-11}$** (!) and check the evolution of x

	Orbit	Perturbed
t= 100	x= 0.13299571833307644	0.132995718337263064
t= 5000	x= 0.37699928389102310	0.37699928370156576
t= 10000	x=-0.159094583356855224	-0.159094583341260309
t= 50000	x= 0.101992400739955760	0.101992400253961321
t=100000	x=-0.381120533746511780	-0.381120533327258870

Regular vs Chaotic orbits

Hénon-Heiles system

$$H = \frac{1}{2}\left(p_x^2 + p_y^2\right) + \frac{1}{2}\left(x^2 + y^2\right) + x^2 y - \frac{1}{3}y^3$$

For H=0.125 we get a regular and a chaotic orbit with initial conditions (ICs):

$x=0, y=0.1, p_y=0$ and **$x=0, y=-0.25, p_y=0.$**

We perturb both ICs by **$\delta p_y=10^{-11}$** (!) and check the evolution of x

	Orbit	Perturbed
t= 100	x= 0.13299571833307644	0.13299571833727263064
t= 5000	x= 0.37699928389102310	0.37699928370156576
t= 10000	x=-0.15909458335685522 4	-0.15909458334126030 9
t= 50000	x= 0.10199240073995576 0	0.10199240025396132 1
t=100000	x=-0.38112053374651178 0	-0.38112053332725887 0
t= 100	x= 0.09027281773516783 5	0.09027282135576866 8

Regular vs Chaotic orbits

Hénon-Heiles system

$$H = \frac{1}{2}\left(p_x^2 + p_y^2\right) + \frac{1}{2}\left(x^2 + y^2\right) + x^2 y - \frac{1}{3}y^3$$

For H=0.125 we get a regular and a chaotic orbit with initial conditions (ICs):

$x=0,\ y=0.1,\ p_y=0$ and **$x=0,\ y=-0.25,\ p_y=0.$**

We perturb both ICs by $\delta p_y=10^{-11}$ (!) and check the evolution of x

	Orbit	Perturbed
t= 100	x= 0.13299571833307644	0.13299571833726306
t= 5000	x= 0.37699928389102310	0.37699928370156576
t= 10000	x=-0.15909458335685522	-0.15909458334126030
t= 50000	x= 0.10199240073995576	0.10199240025396132
t=100000	x=-0.38112053374651178	-0.38112053332725887
t= 100	x= 0.09027281773516783	0.09027282135576866
t= 200	x= 0.29503168748224928	0.29503188485862563

Regular vs Chaotic orbits

Hénon-Heiles system

$$H = \frac{1}{2}\left(p_x^2 + p_y^2\right) + \frac{1}{2}\left(x^2 + y^2\right) + x^2 y - \frac{1}{3}y^3$$

For H=0.125 we get a regular and a chaotic orbit with initial conditions (ICs):

$x=0, y=0.1, p_y=0$ and **$x=0, y=-0.25, p_y=0.$**

We perturb both ICs by **$\delta p_y=10^{-11}$** (!) and check the evolution of x

	Orbit	**Perturbed**
t= 100	x= 0.13299571833307644	0.13299571833263064
t= 5000	x= 0.37699928389102310	0.37699928370156576
t= 10000	x=-0.15909458335685522	-0.1590945833412603
t= 50000	x= 0.10199240073995576	0.10199240025396132
t=100000	x=-0.38112053374651178	-0.38112053332725887
t= 100	x= 0.09027281773516783	0.09027282135576866
t= 200	x= 0.29503168748224928	0.29503188485862563
t= 300	x= 0.51522633010945018	0.51522544048069329

Regular vs Chaotic orbits

Hénon-Heiles system

$$H = \frac{1}{2}\left(p_x^2 + p_y^2\right) + \frac{1}{2}\left(x^2 + y^2\right) + x^2 y - \frac{1}{3} y^3$$

For H=0.125 we get a regular and a chaotic orbit with initial conditions (ICs):

$x=0$, $y=0.1$, $p_y=0$ and **$x=0$, $y=-0.25$, $p_y=0$.**

We perturb both ICs by $\delta p_y=10^{-11}$ (!) and check the evolution of x

	Orbit	Perturbed
t= 100	x= 0.132995718333307644	0.132995718337263064
t= 5000	x= 0.376999283889102310	0.376999283870156576
t= 10000	x=-0.159094583356855224	-0.159094583341260309
t= 50000	x= 0.101992400739955760	0.101992400253961321
t=100000	x=-0.381120533746511780	-0.381120533327258870
t= 100	x= 0.090272817735167835	0.090272821355768668
t= 200	x= 0.295031687482249283	0.295031884858625637
t= 300	x= 0.515226330109450181	0.515225440480693297
t= 400	x= 0.063441889347425867	0.061359558551008345

Regular vs Chaotic orbits

Hénon-Heiles system

$$H = \frac{1}{2}\left(p_x^2 + p_y^2\right) + \frac{1}{2}\left(x^2 + y^2\right) + x^2 y - \frac{1}{3}y^3$$

For H=0.125 we get a regular and a chaotic orbit with initial conditions (ICs):

$x=0, y=0.1, p_y=0$ and **$x=0, y=-0.25, p_y=0.$**

We perturb both ICs by $\delta p_y=10^{-11}$ (!) and check the evolution of x

		Orbit	Perturbed
t=	100	x= 0.13299571833307644	0.13299571833726306 4
t=	5000	x= 0.37699928388910231 0	0.37699928387015657 6
t=	10000	x=-0.15909458335685522 4	-0.15909458334126030 9
t=	50000	x= 0.10199240073995576 0	0.10199240025396132 1
t=	100000	x=-0.38112053374651178 0	-0.38112053332725887 0
t=	100	x= 0.09027281773516783 5	0.09027282135576866 8
t=	200	x= 0.29503168748224928 3	0.29503188485862563 7
t=	300	x= 0.51522633010945018 1	0.51522544048069329 7
t=	400	x= 0.06344188934742586 7	0.06135955855100834 5
t=	500	x= 0.07835771929052352 8	-0.27081102267434109 5

Regular vs Chaotic orbits

Chaotic orbit

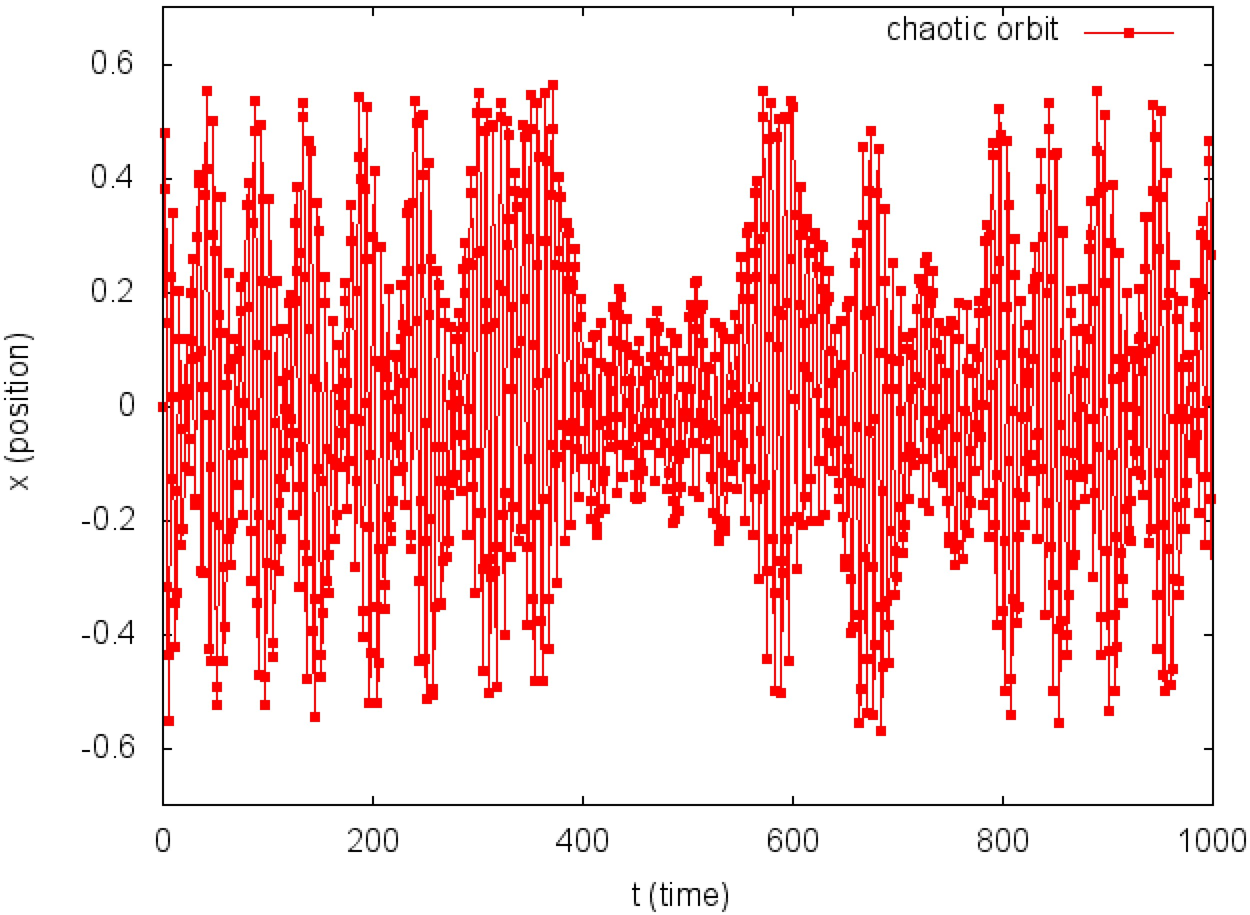

Regular vs Chaotic orbits

Chaotic orbit and its perturbation

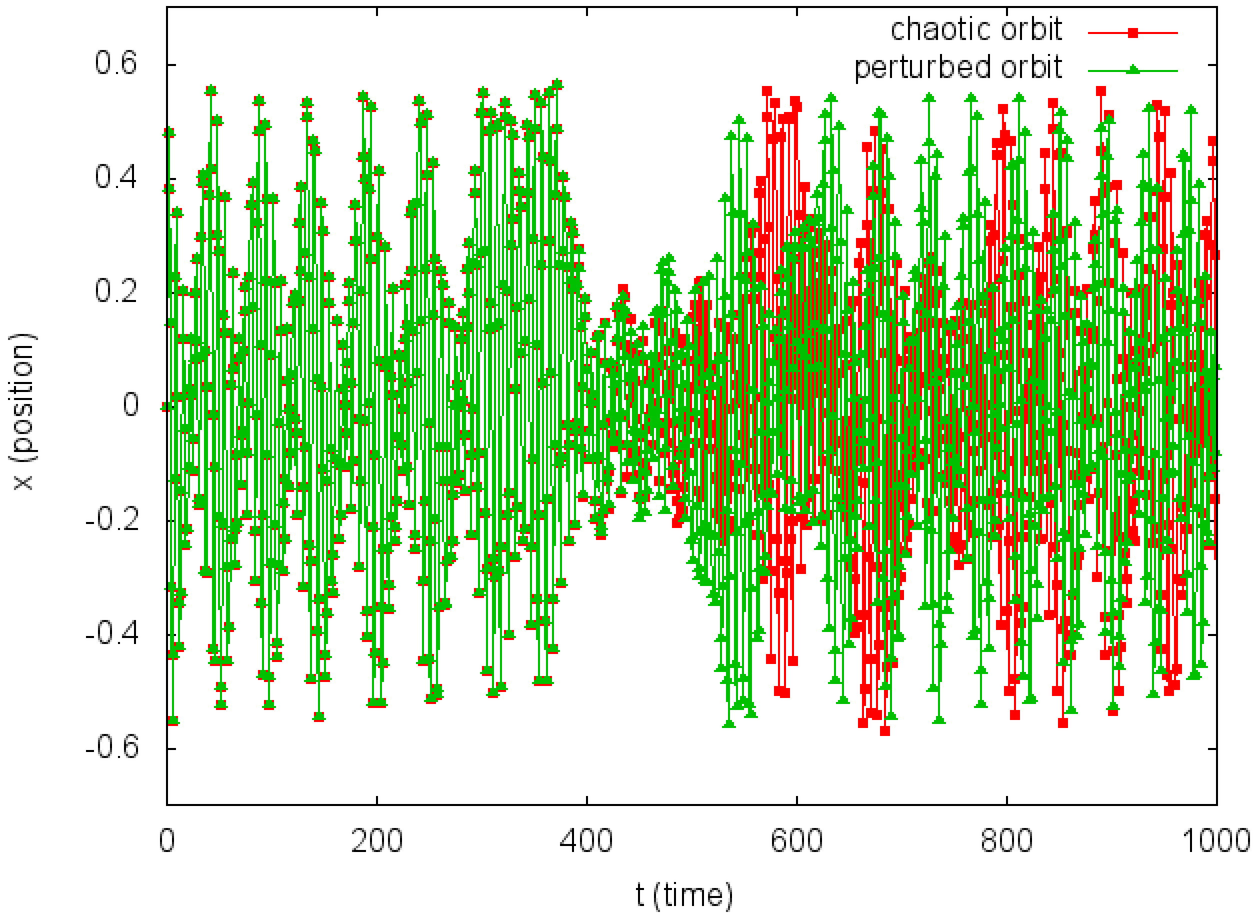

Regular vs Chaotic orbits

Regular orbit

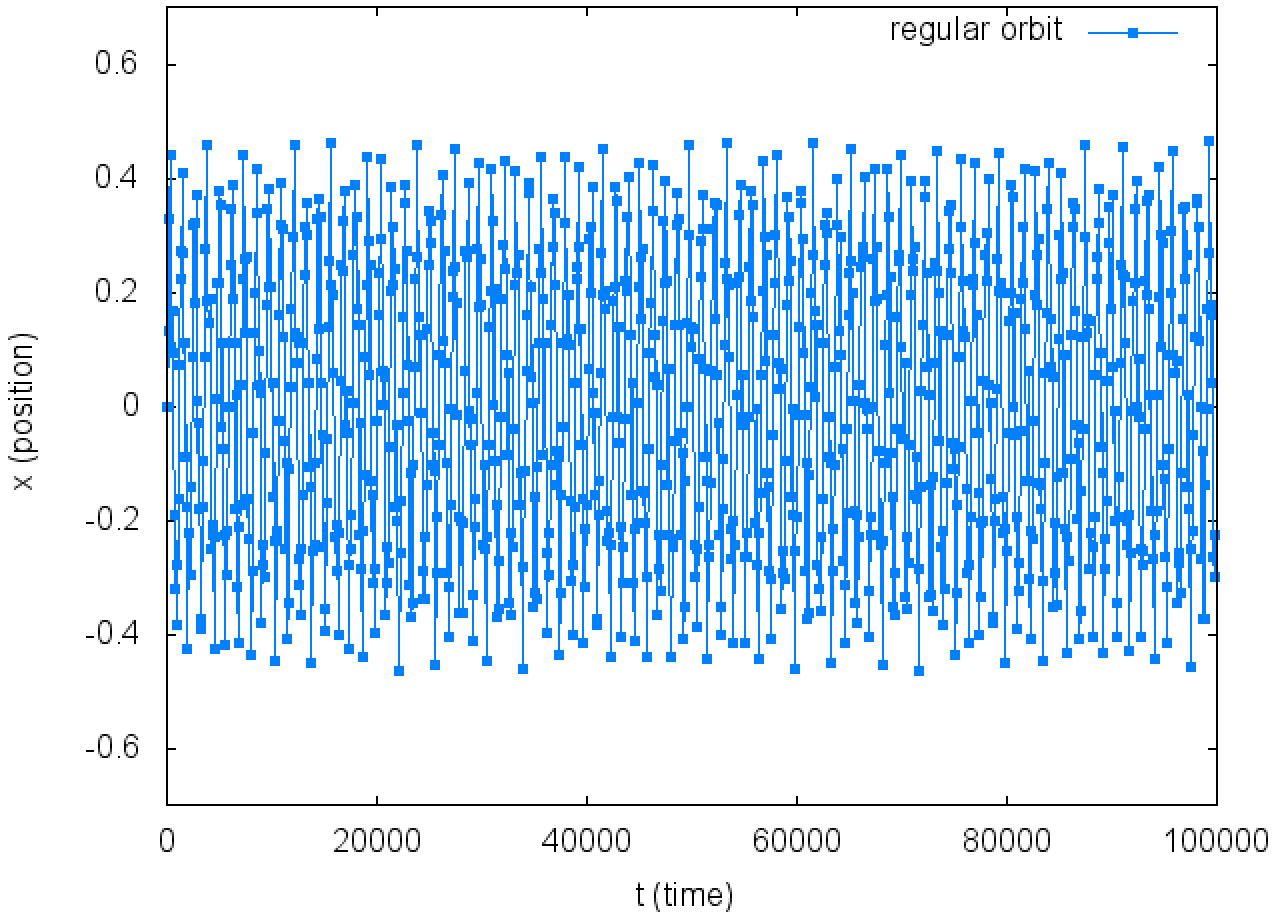

Regular vs Chaotic orbits

Regular orbit and its perturbation

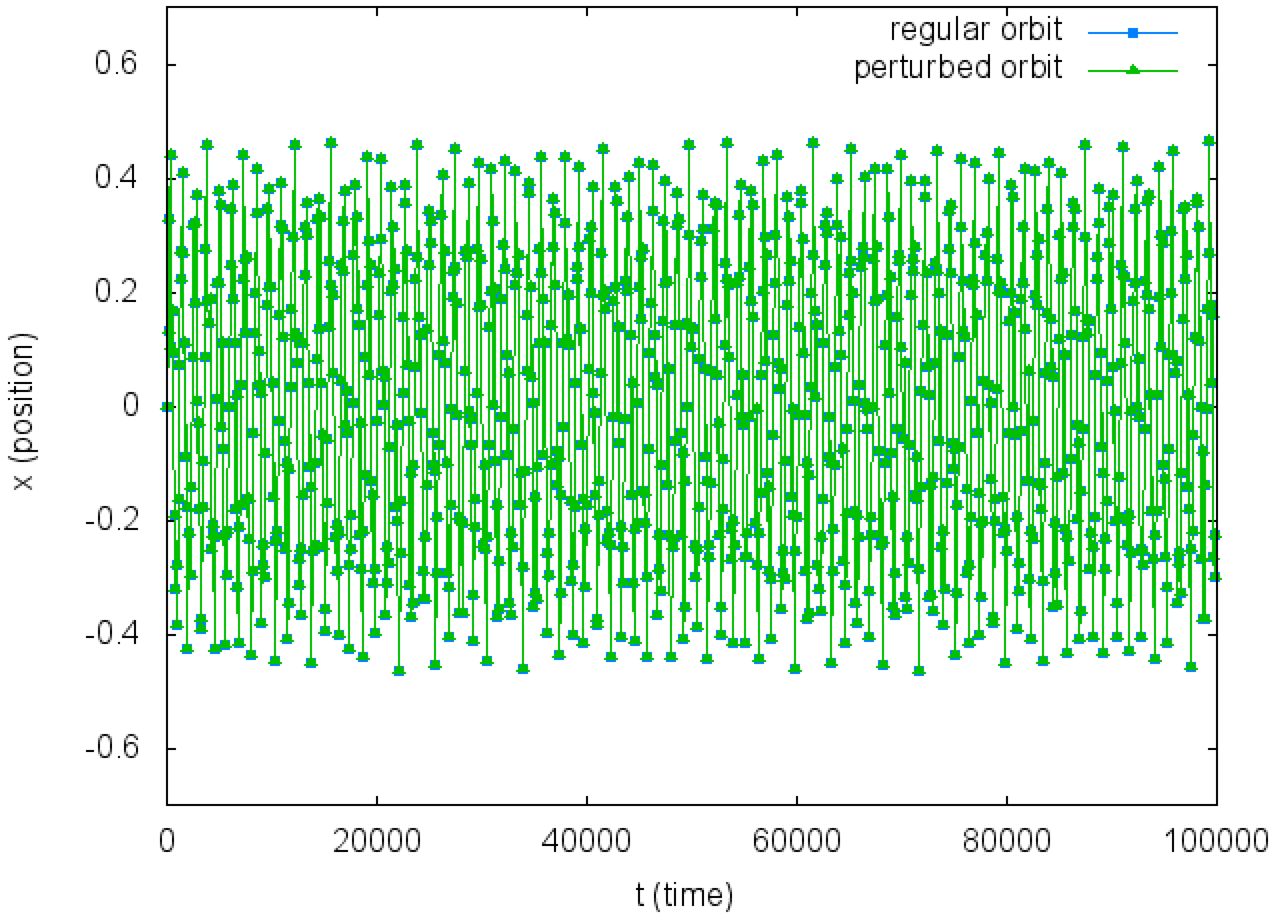

Regular vs Chaotic orbits

Chaotic orbit

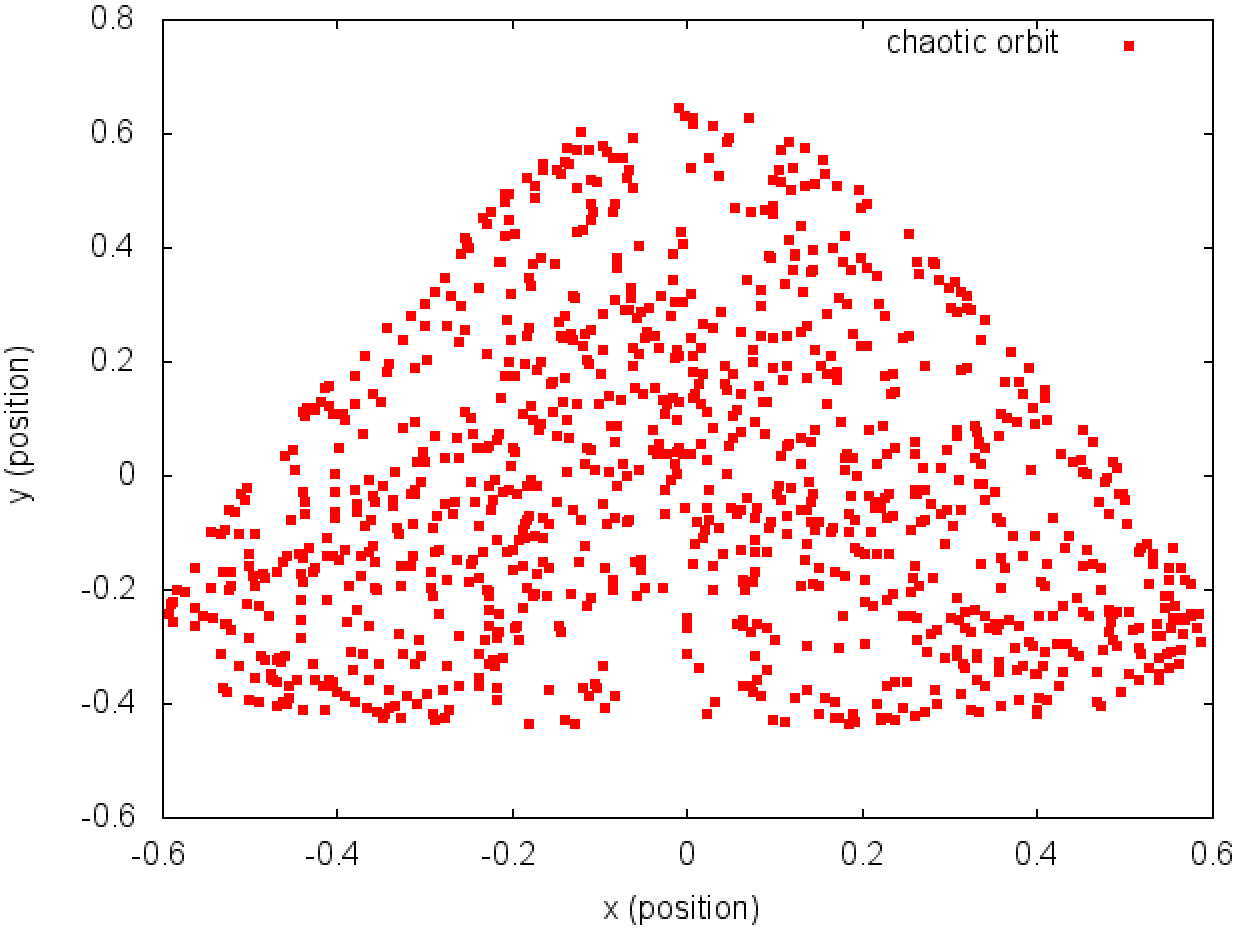

Results for $0 \leq t \leq 10^5$

Regular vs Chaotic orbits

Chaotic orbit and its perturbation

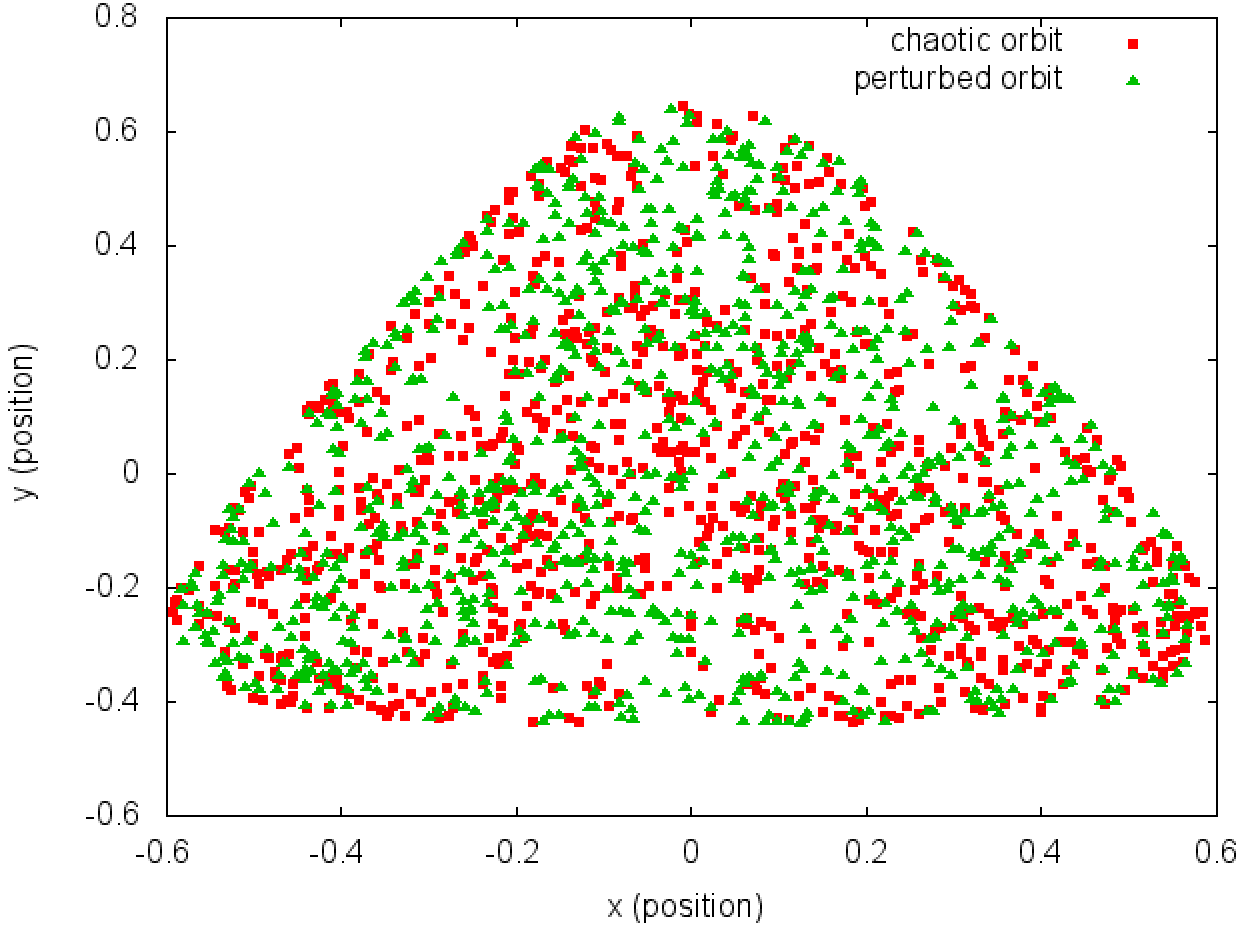

Results for $0 \le t \le 10^5$

Regular vs Chaotic orbits

Regular orbit

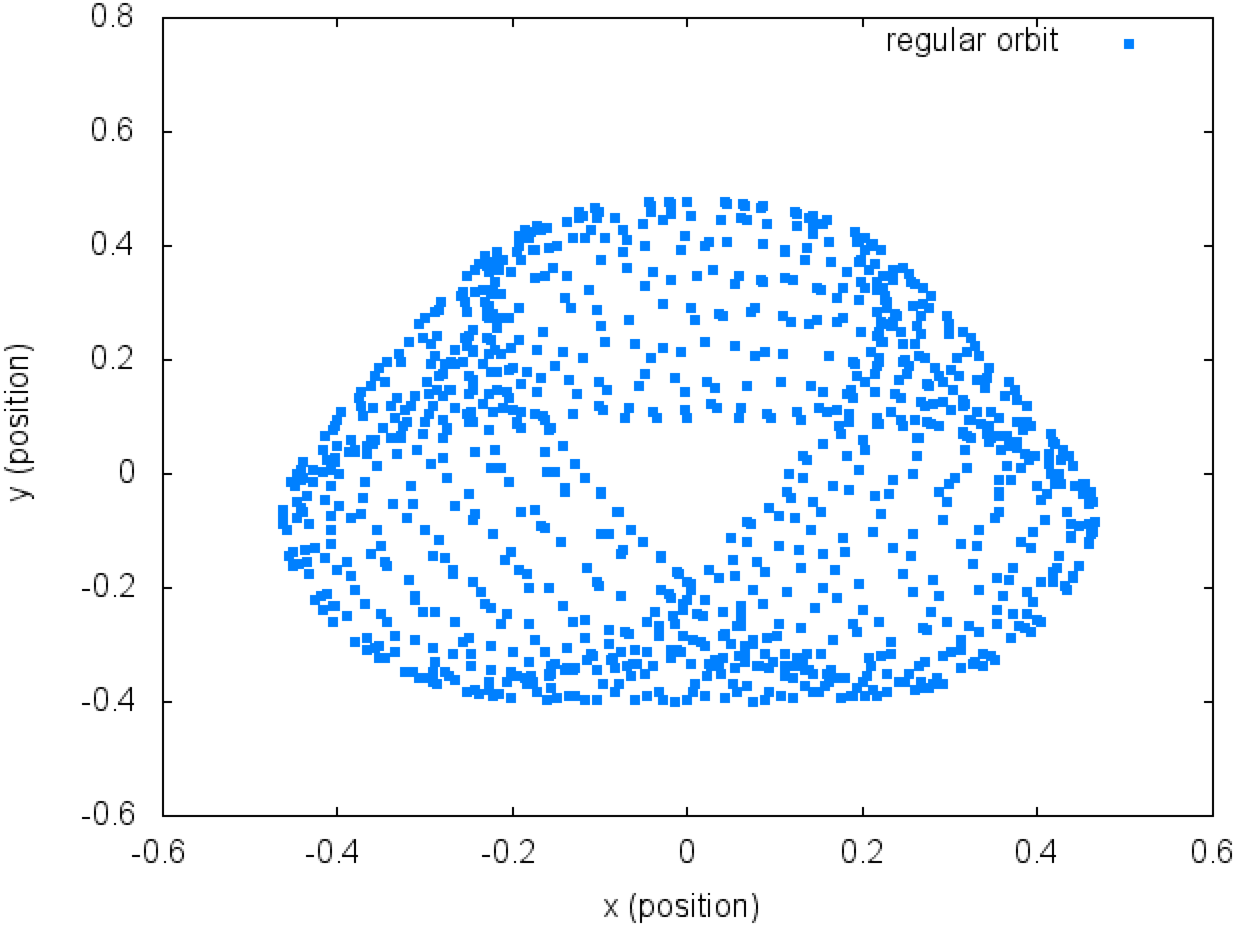

Results for $0 \leq t \leq 10^5$

Regular vs Chaotic orbits

Regular orbit and its perturbation

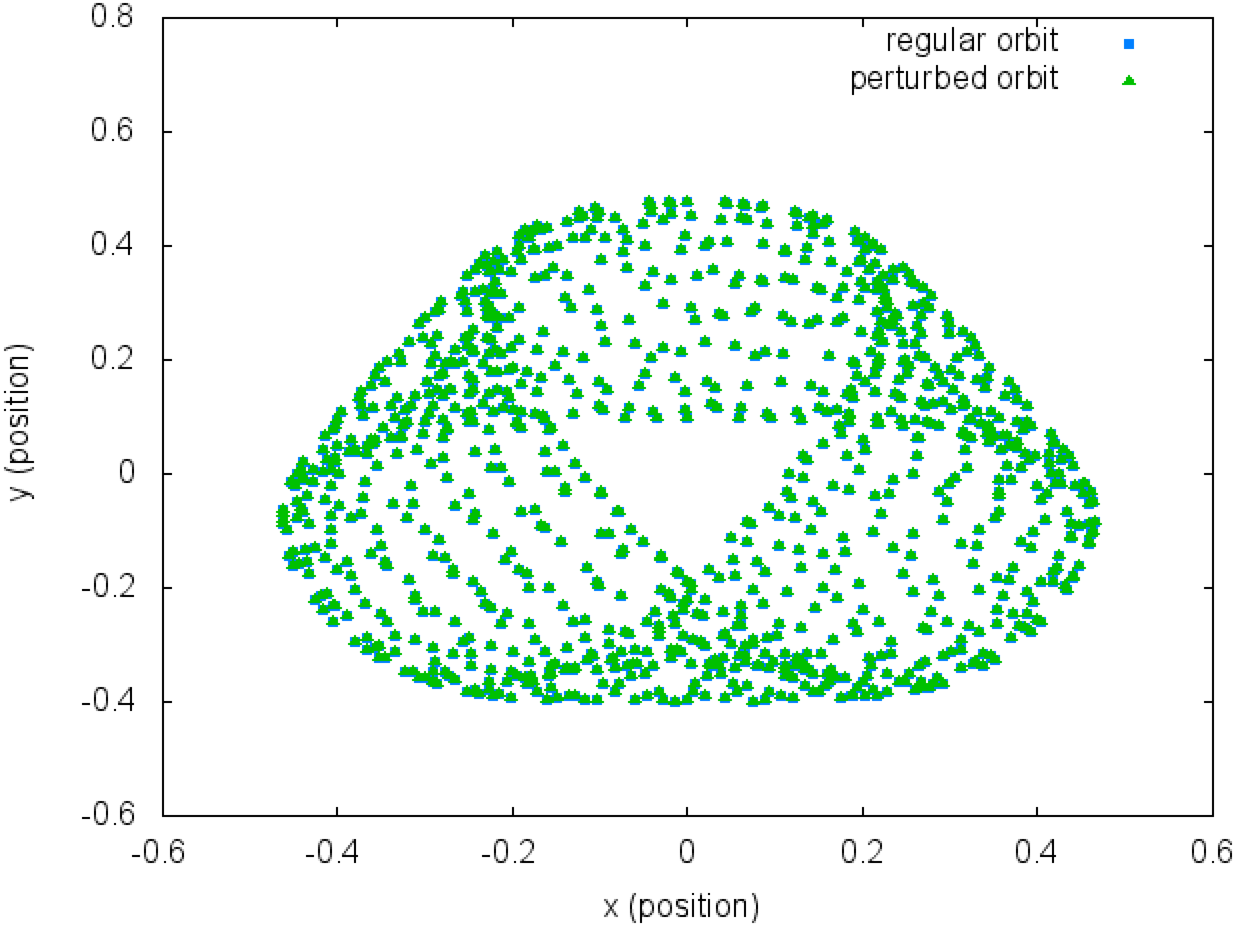

Results for $0 \leq t \leq 10^5$

Regular vs Chaotic orbits

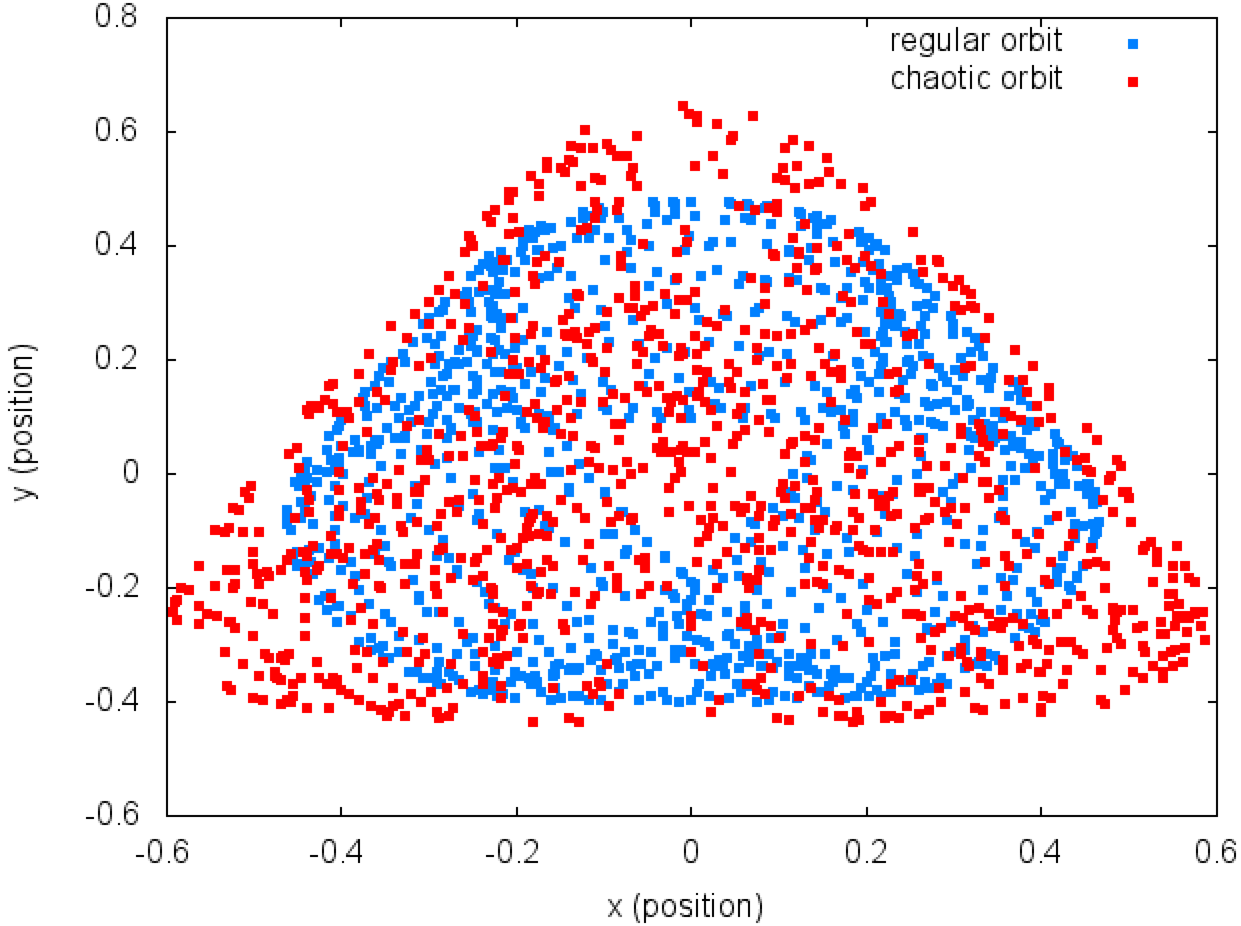

Results for $0 \leq t \leq 10^5$

Poincaré Surface of Section (PSS)

We can constrain the study of an N+1 degree of freedom Hamiltonian system to a **2N-dimensional subspace of the general phase space.**

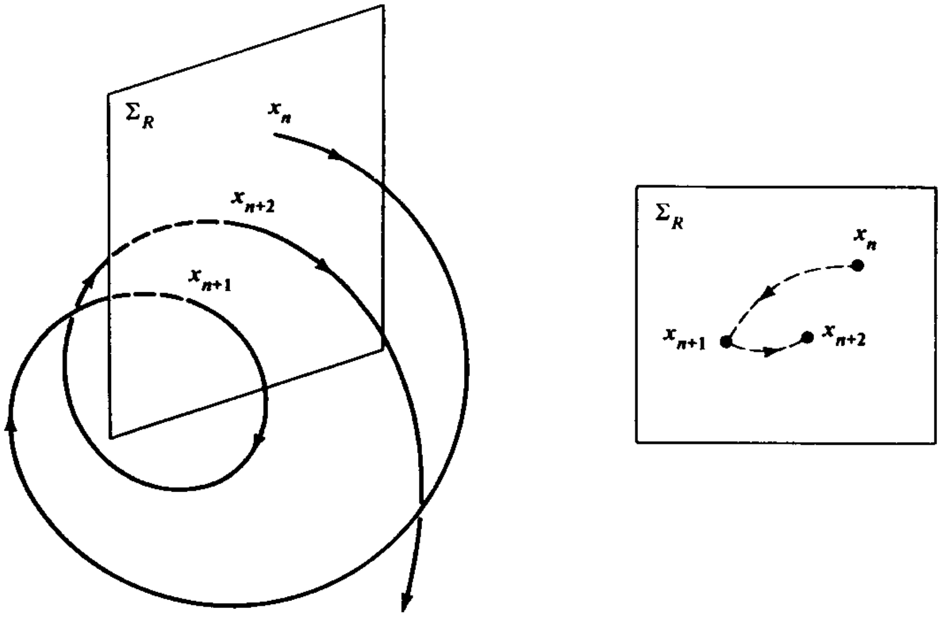

Lieberman & Lichtenberg, 1992, *Regular and Chaotic Dynamics*, Springer.

Poincaré Surface of Section (PSS)

We can constrain the study of an N+1 degree of freedom Hamiltonian system to a 2N-dimensional subspace of the general phase space.

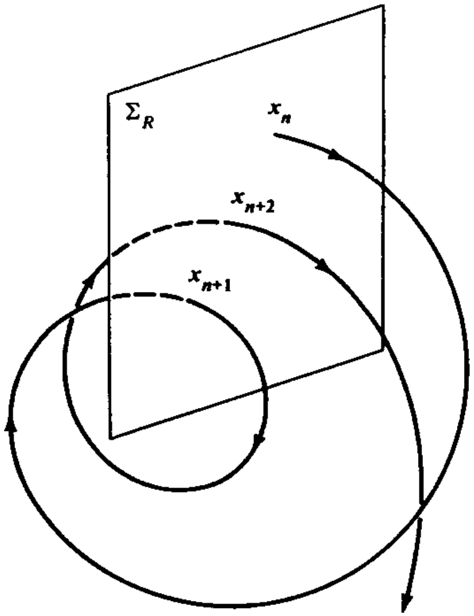

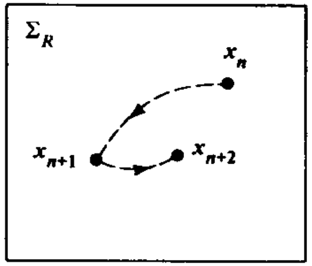

Lieberman & Lichtenberg, 1992, *Regular and Chaotic Dynamics*, Springer.

In general we can assume a PSS of the form q_{N+1}=constant. Then only variables $q_1,q_2,\ldots,q_N,p_1,p_2,\ldots,p_N$ are needed to describe the evolution of an orbit on the PSS, since p_{N+1} can be found from the Hamiltonian.

Poincaré Surface of Section (PSS)

We can constrain the study of an N+1 degree of freedom Hamiltonian system to a 2N-dimensional subspace of the general phase space.

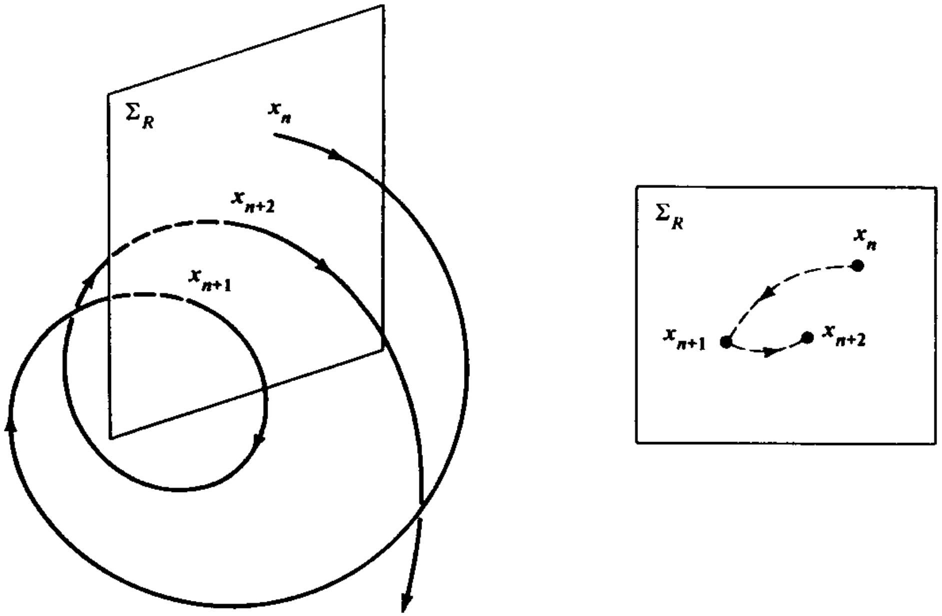

Lieberman & Lichtenberg, 1992, *Regular and Chaotic Dynamics*, Springer.

In general we can assume a PSS of the form q_{N+1}=constant. Then only variables $q_1,q_2,\ldots,q_N,p_1,p_2,\ldots,p_N$ are needed to describe the evolution of an orbit on the PSS, since p_{N+1} can be found from the Hamiltonian.

In this sense an N+1 degree of freedom Hamiltonian system corresponds to a 2N-dimensional map.

Hénon-Heiles system: PSS (x=0)

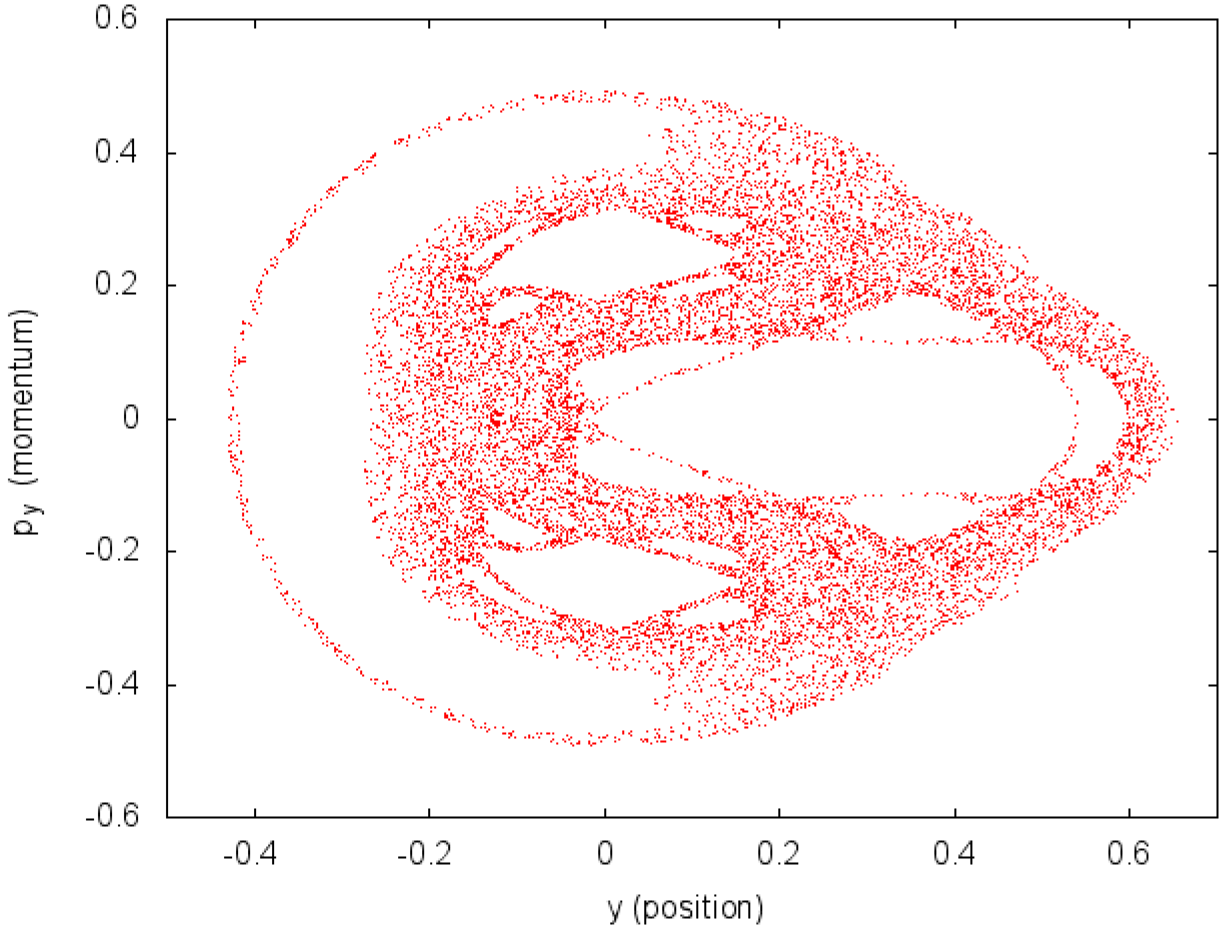

Chaotic orbit

Hénon-Heiles system: PSS (x=0)

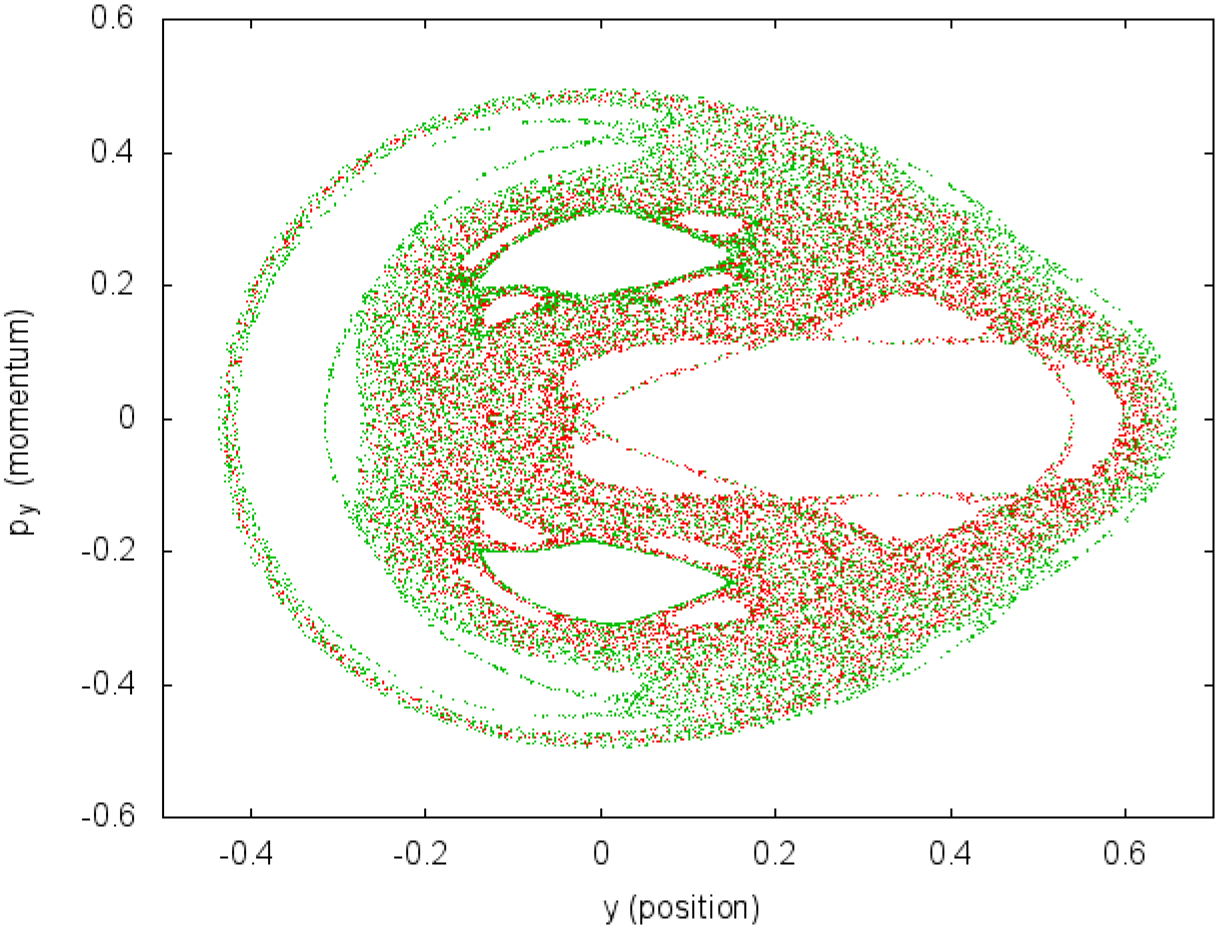

Chaotic orbit - Perturbed chaotic orbit

Hénon-Heiles system: PSS (x=0)

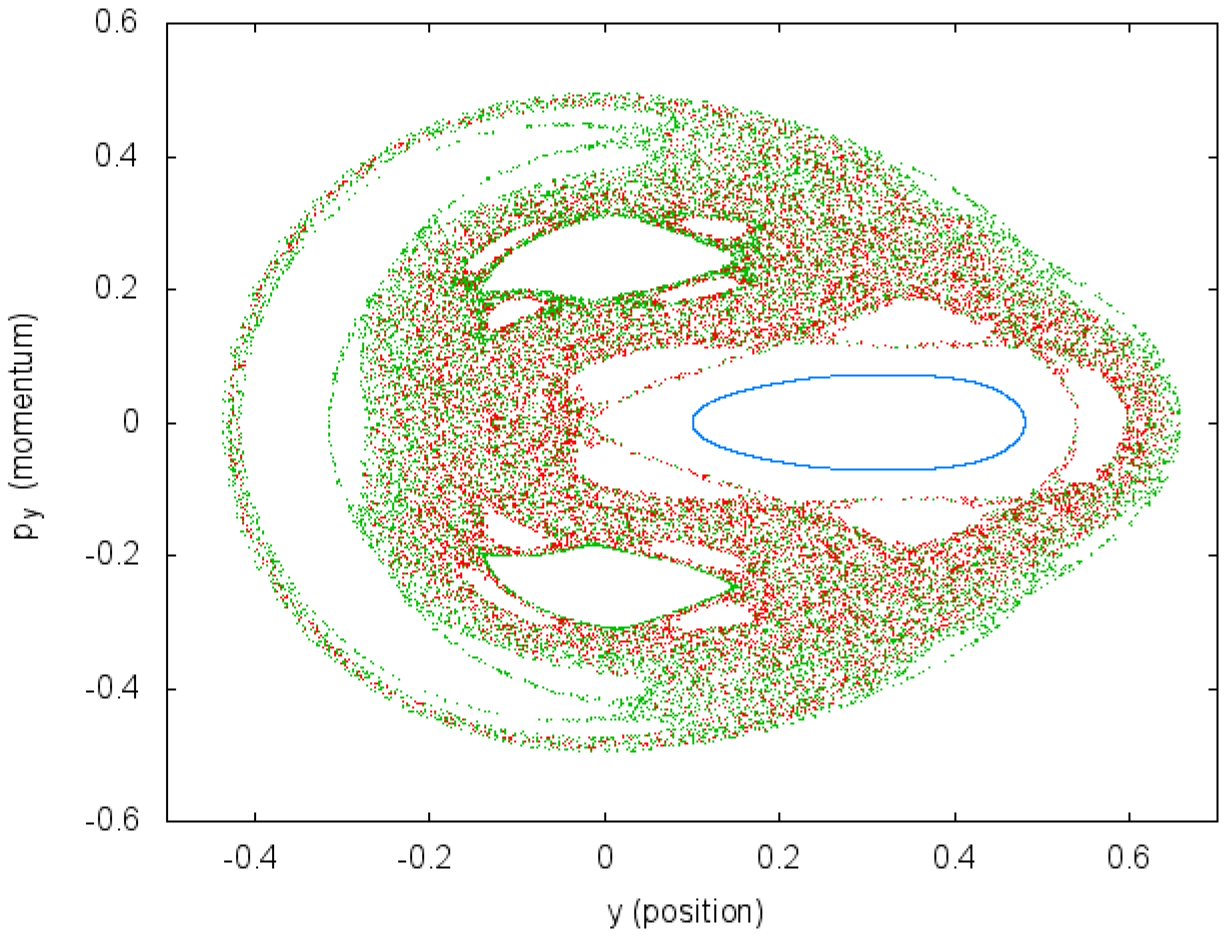

Chaotic orbit - Perturbed chaotic orbit

Regular orbit

Hénon-Heiles system: PSS (x=0)

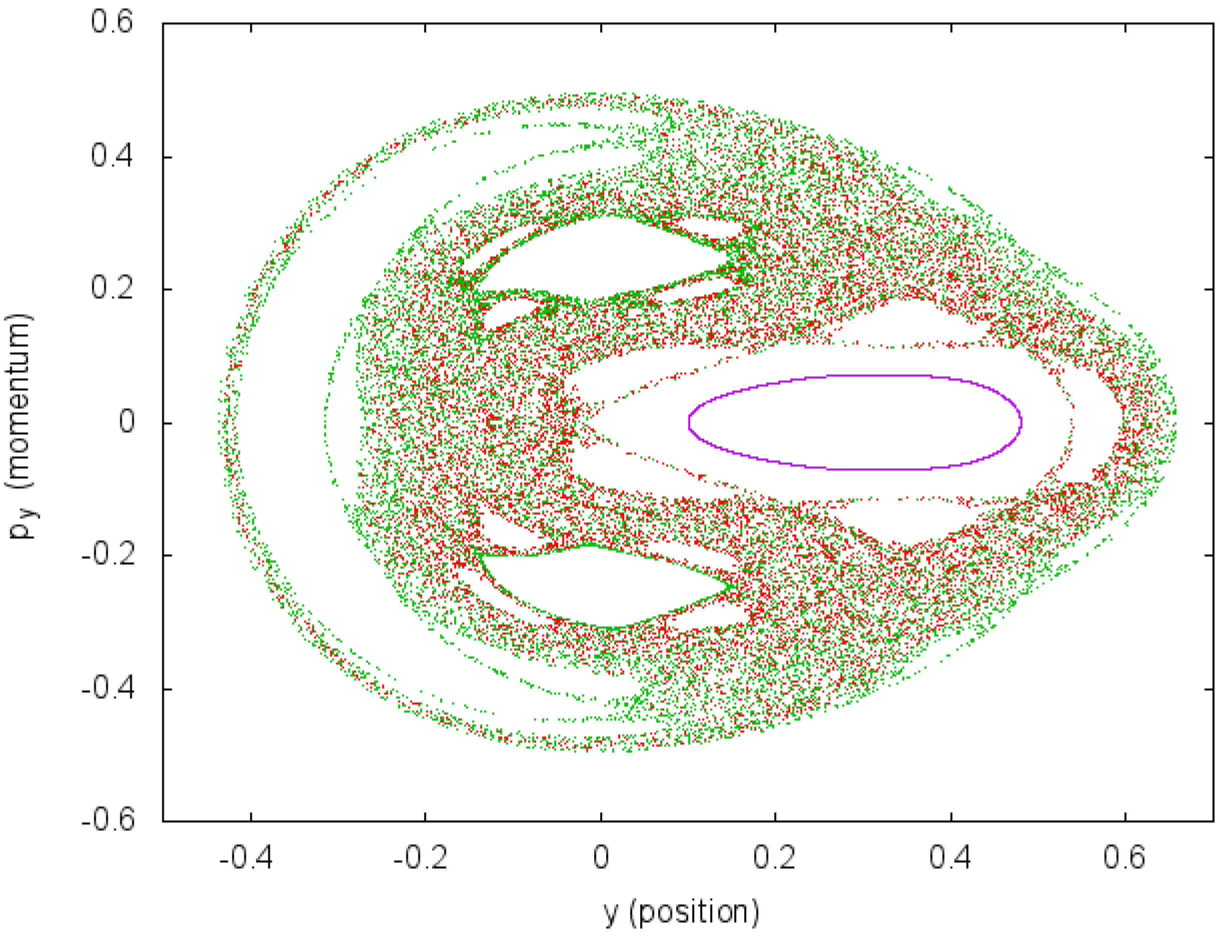

Chaotic orbit - Perturbed chaotic orbit

Regular orbit - Perturbed regular orbit

Hénon-Heiles system: PSS (x=0)

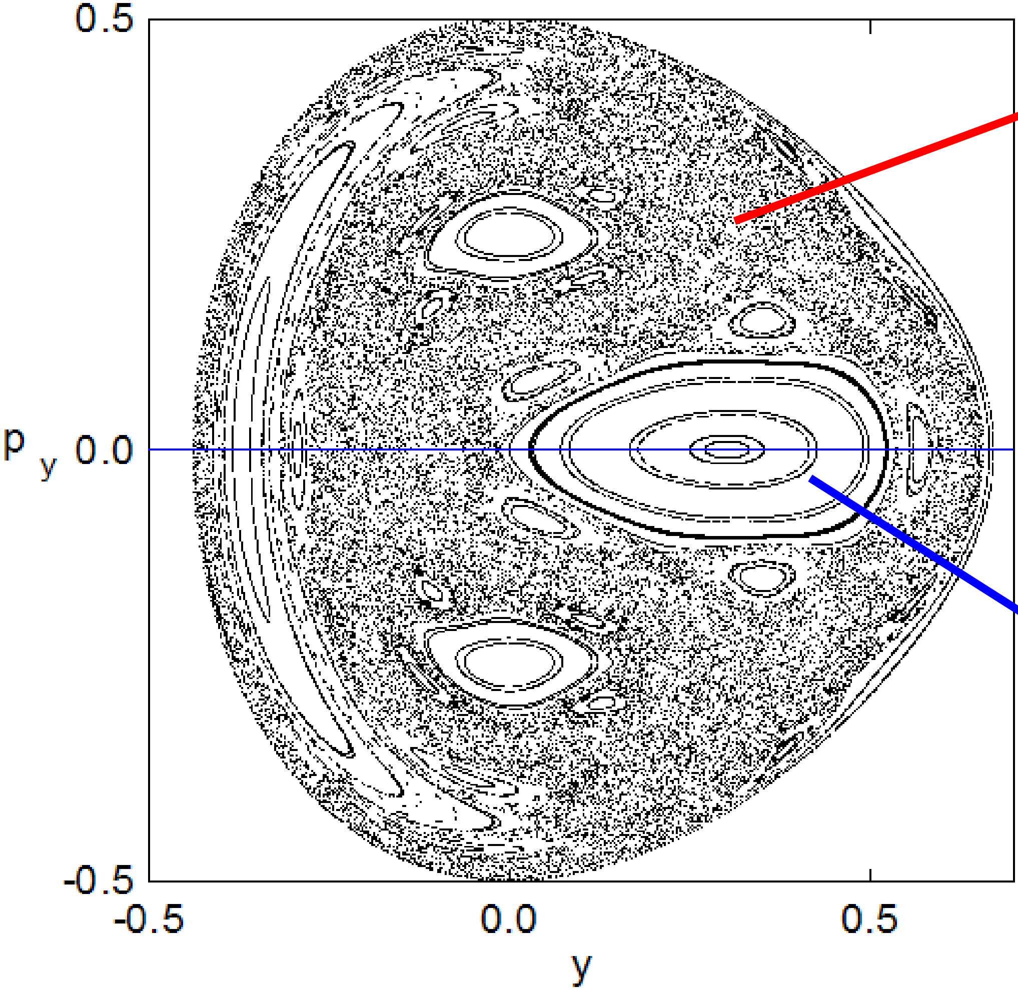

Chaotic motion
Chaotic sea

Regular motion
Island of stability

Chaos detection techniques

- **Based on the visualization of orbits**
  - ✓ **Poincaré Surface of Section (PSS)**
  - ✓ **the color and rotation (CR) method**
  - ✓ **the 3D phase space slices (3PSS) technique**

The color and rotation (CR) method

For 3 degree of freedom Hamiltonian systems and 4 dimensional symplectic maps:

We consider the 3D projection of the PSS and use color to indicate the 4th dimension.

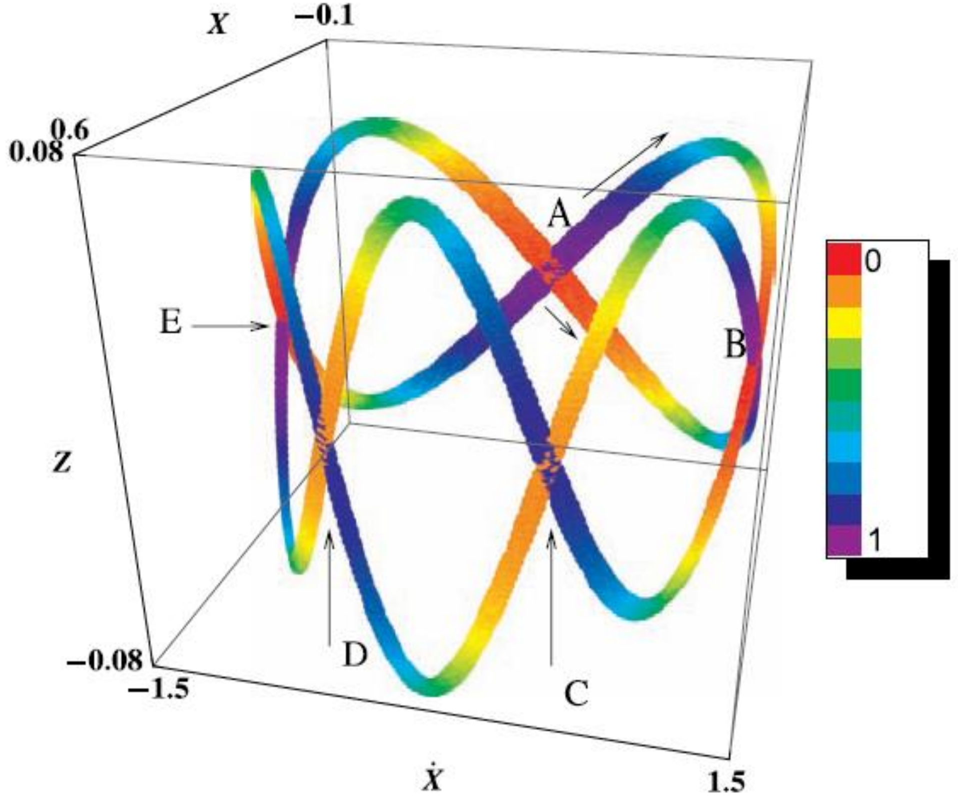

Katsanikas M and Patsis P A 2011 Int. J. Bif. Chaos 21 467

The 3D phase space slices (3PSS) technique

For 3 degree of freedom Hamiltonian systems and 4 dimensional symplectic maps:

We consider thin 3D phase space slices of the 4D phase space (e.g. $|p_2| \leq \varepsilon$) and present intersections of orbits with these slices.

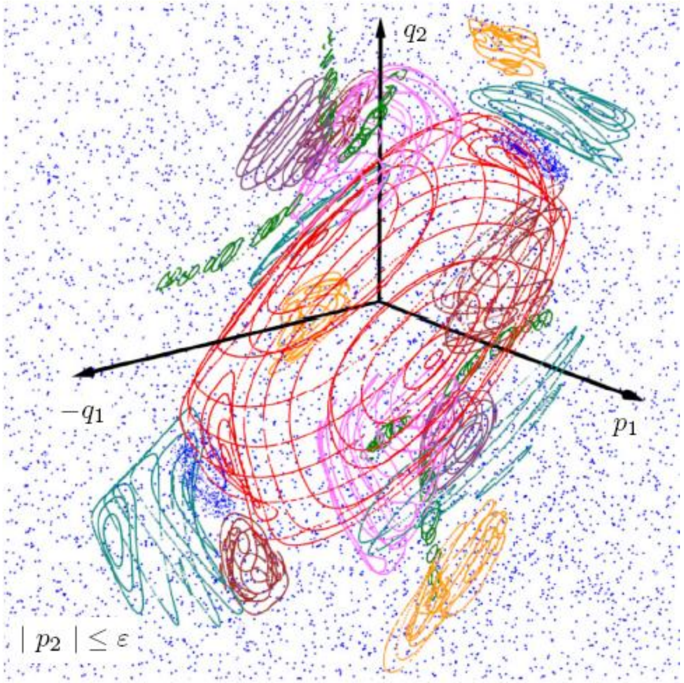

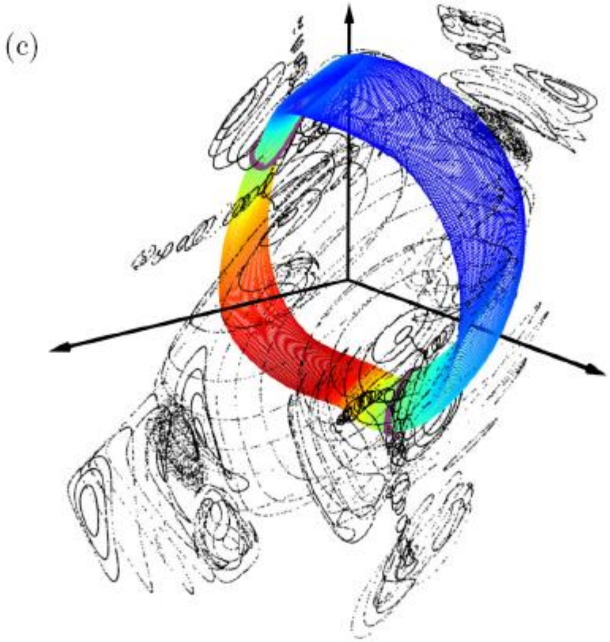

Richter et al. 2014 Phys. Rev. E 89 022902

Chaos detection techniques

- **Based on the visualization of orbits**
  - ✓ **Poincaré Surface of Section (PSS)**
  - ✓ **the color and rotation (CR) method**
  - ✓ **the 3D phase space slices (3PSS) technique**
- **Based on the numerical analysis of orbits**
  - ✓ **Frequency Map Analysis**
  - ✓ **0-1 test**

Frequency Map Analysis

Create **Frequency Maps** **by computing the fundamental frequencies of orbits.**

Regular motion: The computed frequencies do not vary in time

Chaotic motion: The computed frequencies vary in time

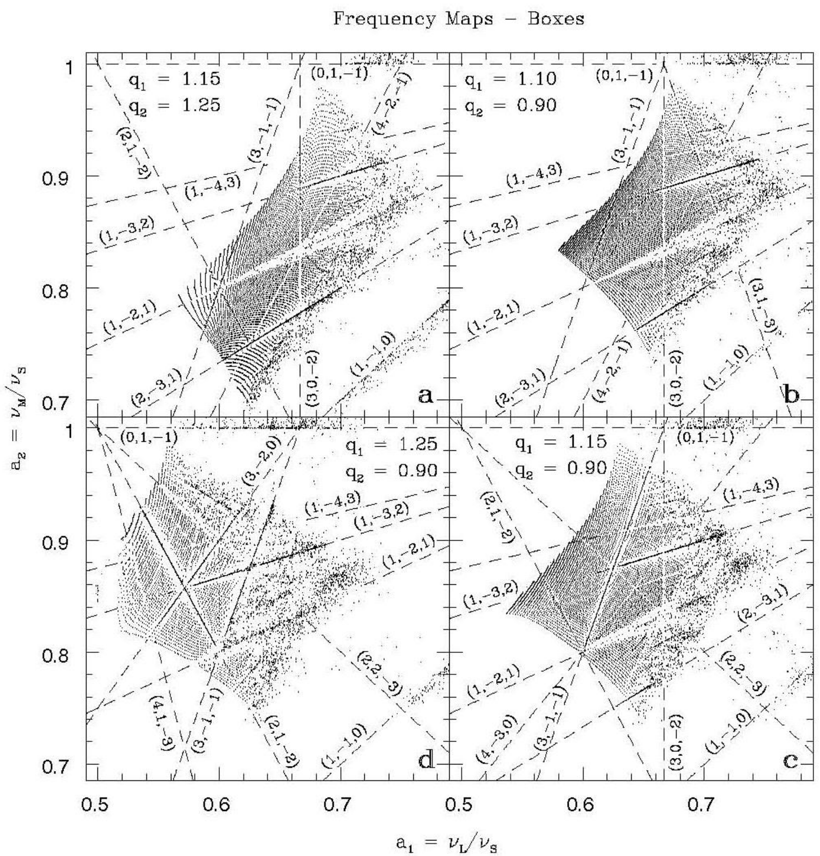

Papaphilippou Y and Laskar J 1998 Astron. Astrophys. 329 451

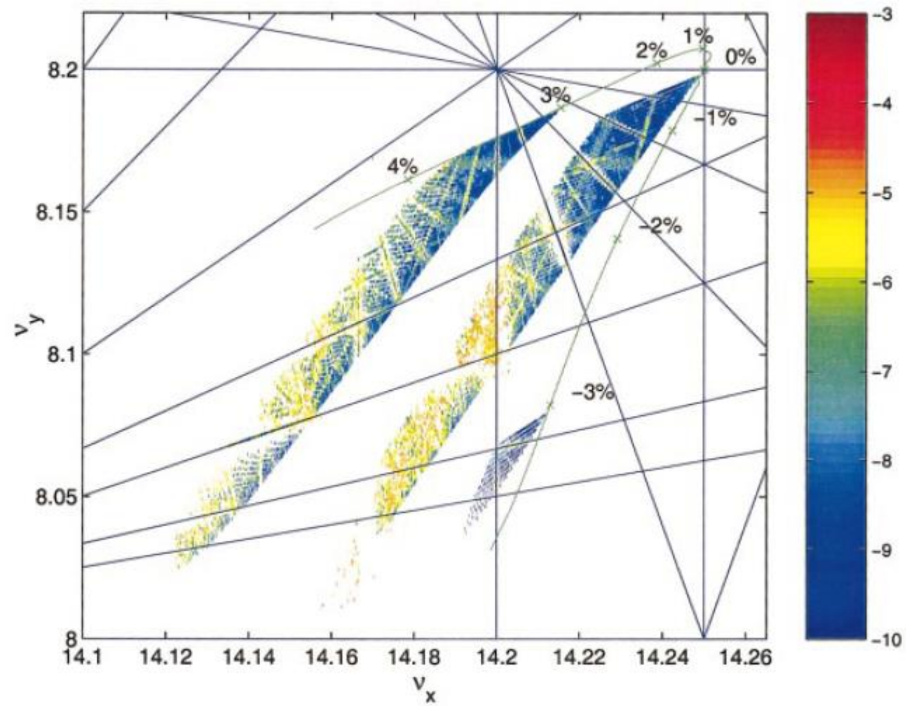

Steier C et al. 2002 Phys. Rev. E 65 056506

Chaos detection techniques

- **Based on the visualization of orbits**
  - ✓ **Poincaré Surface of Section (PSS)**
  - ✓ **the color and rotation (CR) method**
  - ✓ **the 3D phase space slices (3PSS) technique**
- **Based on the numerical analysis of orbits**
  - ✓ **Frequency Map Analysis**
  - ✓ **0-1 test**
- **Chaos indicators based on the evolution of deviation vectors from a given orbit**
  - ✓ **Maximum Lyapunov Exponent**
  - ✓ **Fast Lyapunov Indicator (FLI) and Orthogonal Fast Lyapunov Indicators (OFLI and OFLI2)**
  - ✓ **Mean Exponential Growth Factor of Nearby Orbits (MEGNO)**
  - ✓ **Relative Lyapunov Indicator (RLI)**
  - ✓ **Smaller ALignment Index – SALI**
  - ✓ **Generalized ALignment Index – GALI**

Variational Equations

We use the notation $\mathbf{x} = (q_1,q_2,\ldots,q_N,p_1,p_2,\ldots,p_N)^T$. The deviation vector from a given orbit is denoted by

$$\mathbf{v} = (\delta x_1, \delta x_2,\ldots,\delta x_n)^T \text{, with } n=2N$$

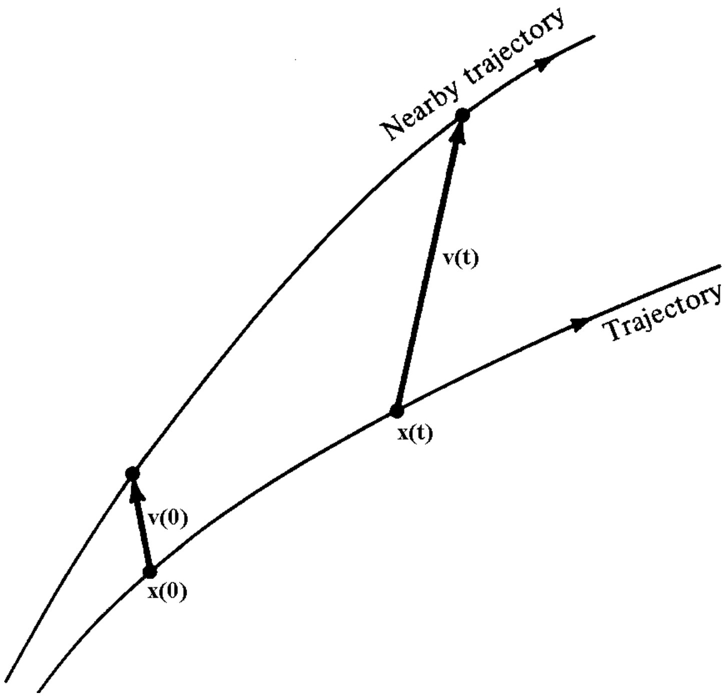

Benettin & Galgani, 1979, in Laval and Gressillon (eds.), op cit, 93

The time evolution of v is given by the so-called variational equations:

$$\frac{d\mathbf{v}}{dt} = -\mathbf{J} \cdot \mathbf{P} \cdot \mathbf{v}$$

where

$$\mathbf{J} = \begin{pmatrix} 0_N & -I_N \\ I_N & 0_N \end{pmatrix}, \quad P_{ij} = \frac{\partial^2 H}{\partial x_i \partial x_j} \quad i, j = 1, 2, \ldots, n$$

Example (Hénon-Heiles system)

$$H = \frac{1}{2}\left(p_x^2 + p_y^2\right) + \frac{1}{2}\left(x^2 + y^2\right) + x^2 y - \frac{1}{3} y^3$$

Hamilton's equations of motion:

$$\frac{dp_i}{dt} = -\frac{\partial H}{\partial q_i}, \quad \frac{dq_i}{dt} = \frac{\partial H}{\partial p_i} \Rightarrow \begin{cases} \dot{x} = p_x \\ \dot{y} = p_y \\ \dot{p}_x = -x - 2xy \\ \dot{p}_y = -y - x^2 + y^2 \end{cases}$$

Example (Hénon-Heiles system)

$$H = \frac{1}{2}\left(p_x^2 + p_y^2\right) + \frac{1}{2}\left(x^2 + y^2\right) + x^2 y - \frac{1}{3} y^3$$

Hamilton's equations of motion:

$$\frac{dp_i}{dt} = -\frac{\partial H}{\partial q_i}, \quad \frac{dq_i}{dt} = \frac{\partial H}{\partial p_i} \Rightarrow \begin{cases} \dot{x} = p_x \\ \dot{y} = p_y \\ \dot{p}_x = -x - 2xy \\ \dot{p}_y = -y - x^2 + y^2 \end{cases}$$

In order to get the variational equations we linearize the above equations by substituting x, y, px, py with $x+v_1$, $y+v_2$, p_x+v_3, p_y+v_4 where $v=(v_1,v_2,v_3,v_4)$ is the deviation vector. So we get:

$$\dot{p}_x + \dot{v}_3 = -x - v_1 - 2(x + v_1)(y + v_2) \Rightarrow$$

$$\dot{p}_x + \dot{v}_3 = -x - v_1 - 2xy - 2xv_2 - 2yv_1 - 2v_1 v_2 \Rightarrow$$

Example (Hénon-Heiles system)

$$H = \frac{1}{2}\left(p_x^2 + p_y^2\right) + \frac{1}{2}\left(x^2 + y^2\right) + x^2 y - \frac{1}{3}y^3$$

Hamilton's equations of motion:

$$\frac{dp_i}{dt} = -\frac{\partial H}{\partial q_i}, \quad \frac{dq_i}{dt} = \frac{\partial H}{\partial p_i} \Rightarrow \begin{cases} \dot{x} = p_x \\ \dot{y} = p_y \\ \boxed{\dot{p}_x = -x - 2xy} \\ \dot{p}_y = -y - x^2 + y^2 \end{cases}$$

In order to get the variational equations we linearize the above equations by substituting x, y, px, py with $x+v_1$, $y+v_2$, p_x+v_3, p_y+v_4 where $v=(v_1,v_2,v_3,v_4)$ is the deviation vector. So we get:

$$\dot{p}_x + \dot{v}_3 = -x - v_1 - 2(x + v_1)(y + v_2) \Rightarrow$$

$$\cancel{\dot{p}_x} + \dot{v}_3 = \cancel{-x} - v_1 - \cancel{2xy} - 2xv_2 - 2yv_1 - 2v_1v_2 \Rightarrow$$

Example (Hénon-Heiles system)

$$H = \frac{1}{2}\left(p_x^2 + p_y^2\right) + \frac{1}{2}\left(x^2 + y^2\right) + x^2 y - \frac{1}{3}y^3$$

Hamilton's equations of motion:

$$\frac{dp_i}{dt} = -\frac{\partial H}{\partial q_i}, \quad \frac{dq_i}{dt} = \frac{\partial H}{\partial p_i} \Rightarrow \begin{cases} \dot{x} = p_x \\ \dot{y} = p_y \\ \boxed{\dot{p}_x = -x - 2xy} \\ \dot{p}_y = -y - x^2 + y^2 \end{cases}$$

In order to get the variational equations we linearize the above equations by substituting x, y, px, py with $x+v_1, y+v_2, p_x+v_3, p_y+v_4$ where $v=(v_1,v_2,v_3,v_4)$ is the deviation vector. So we get:

$$\dot{p}_x + \dot{v}_3 = -x - v_1 - 2(x + v_1)(y + v_2) \Rightarrow$$

$$\dot{p}_x + \dot{v}_3 = -x - v_1 - 2xy - 2xv_2 - 2yv_1 - 2v_1v_2 \Rightarrow$$

Example (Hénon-Heiles system)

$$H = \frac{1}{2}\left(p_x^2 + p_y^2\right) + \frac{1}{2}\left(x^2 + y^2\right) + x^2 y - \frac{1}{3} y^3$$

Hamilton's equations of motion:

$$\frac{dp_i}{dt} = -\frac{\partial H}{\partial q_i}, \quad \frac{dq_i}{dt} = \frac{\partial H}{\partial p_i} \Rightarrow \begin{cases} \dot{x} = p_x \\ \dot{y} = p_y \\ \boxed{\dot{p}_x = -x - 2xy} \\ \dot{p}_y = -y - x^2 + y^2 \end{cases}$$

In order to get the variational equations we linearize the above equations by substituting x, y, px, py with $x+v_1$, $y+v_2$, p_x+v_3, p_y+v_4 where $v=(v_1,v_2,v_3,v_4)$ is the deviation vector. So we get:

$$\dot{p}_x + \dot{v}_3 = -x - v_1 - 2(x + v_1)(y + v_2) \Rightarrow$$

$$\cancel{\dot{p}_x} + \dot{v}_3 = \cancel{-x} - v_1 - \cancel{2xy} - 2xv_2 - 2yv_1 - \cancel{2v_1 v_2} \Rightarrow$$

$$\dot{v}_3 = -v_1 - 2yv_1 - 2xv_2$$

Example (Hénon-Heiles system)

Variational equations:

$$\frac{dv}{dt} = -J \cdot P \cdot v$$

Example (Hénon-Heiles system)

Variational equations:

$$\frac{d\mathbf{v}}{dt} = -\mathbf{J} \cdot \mathbf{P} \cdot \mathbf{v}$$

$$\begin{pmatrix} \dot{v}_1 \\ \dot{v}_2 \\ \dot{v}_3 \\ \dot{v}_4 \end{pmatrix}$$

Example (Hénon-Heiles system)

Variational equations: $\frac{d\mathbf{v}}{dt} = -\mathbf{J} \cdot \mathbf{P} \cdot \mathbf{v}$

$$\begin{pmatrix} \dot{v}_1 \\ \dot{v}_2 \\ \dot{v}_3 \\ \dot{v}_4 \end{pmatrix} = -\begin{pmatrix} 0 & 0 & -1 & 0 \\ 0 & 0 & 0 & -1 \\ 1 & 0 & 0 & 0 \\ 0 & 1 & 0 & 0 \end{pmatrix}$$

Example (Hénon-Heiles system)

Variational equations: $$\frac{\mathbf{dv}}{\mathbf{dt}} = -\mathbf{J} \cdot \mathbf{P} \cdot \mathbf{v}$$

$$\begin{pmatrix} \dot{v}_1 \\ \dot{v}_2 \\ \dot{v}_3 \\ \dot{v}_4 \end{pmatrix} = -\begin{pmatrix} 0 & 0 & -1 & 0 \\ 0 & 0 & 0 & -1 \\ 1 & 0 & 0 & 0 \\ 0 & 1 & 0 & 0 \end{pmatrix} \begin{pmatrix} 1+2y & 2x & 0 & 0 \\ 2x & 1-2y & 0 & 0 \\ 0 & 0 & 1 & 0 \\ 0 & 0 & 0 & 1 \end{pmatrix}$$

Example (Hénon-Heiles system)

Variational equations: $$\frac{d\mathbf{v}}{dt} = -\mathbf{J}\cdot\mathbf{P}\cdot\mathbf{v}$$

$$\begin{pmatrix} \dot{v}_1 \\ \dot{v}_2 \\ \dot{v}_3 \\ \dot{v}_4 \end{pmatrix} = -\begin{pmatrix} 0 & 0 & -1 & 0 \\ 0 & 0 & 0 & -1 \\ 1 & 0 & 0 & 0 \\ 0 & 1 & 0 & 0 \end{pmatrix} \begin{pmatrix} 1+2y & 2x & 0 & 0 \\ 2x & 1-2y & 0 & 0 \\ 0 & 0 & 1 & 0 \\ 0 & 0 & 0 & 1 \end{pmatrix} \begin{pmatrix} v_1 \\ v_2 \\ v_3 \\ v_4 \end{pmatrix}$$

Example (Hénon-Heiles system)

Variational equations: $\frac{d\mathbf{v}}{dt} = -\mathbf{J} \cdot \mathbf{P} \cdot \mathbf{v}$

$$\begin{pmatrix} \dot{v}_1 \\ \dot{v}_2 \\ \dot{v}_3 \\ \dot{v}_4 \end{pmatrix} = -\begin{pmatrix} 0 & 0 & -1 & 0 \\ 0 & 0 & 0 & -1 \\ 1 & 0 & 0 & 0 \\ 0 & 1 & 0 & 0 \end{pmatrix} \begin{pmatrix} 1+2y & 2x & 0 & 0 \\ 2x & 1-2y & 0 & 0 \\ 0 & 0 & 1 & 0 \\ 0 & 0 & 0 & 1 \end{pmatrix} \begin{pmatrix} v_1 \\ v_2 \\ v_3 \\ v_4 \end{pmatrix}$$

$$\dot{v}_1 = v_3$$

$$\dot{v}_2 = v_4$$

$$\dot{v}_3 = -v_1 - 2xv_2 - 2yv_1$$

$$\dot{v}_4 = -v_2 - 2xv_1 + 2yv_2$$

Example (Hénon-Heiles system)

Variational equations: $\frac{dv}{dt} = -J \cdot P \cdot v$

$$\begin{pmatrix} \dot{v}_1 \\ \dot{v}_2 \\ \dot{v}_3 \\ \dot{v}_4 \end{pmatrix} = -\begin{pmatrix} 0 & 0 & -1 & 0 \\ 0 & 0 & 0 & -1 \\ 1 & 0 & 0 & 0 \\ 0 & 1 & 0 & 0 \end{pmatrix} \begin{pmatrix} 1+2y & 2x & 0 & 0 \\ 2x & 1-2y & 0 & 0 \\ 0 & 0 & 1 & 0 \\ 0 & 0 & 0 & 1 \end{pmatrix} \begin{pmatrix} v_1 \\ v_2 \\ v_3 \\ v_4 \end{pmatrix}$$

$$\dot{v}_1 = v_3$$

$$\dot{v}_2 = v_4$$

$$\boxed{\dot{v}_3 = -v_1 - 2xv_2 - 2yv_1}$$

$$\dot{v}_4 = -v_2 - 2xv_1 + 2yv_2$$

Example (Hénon-Heiles system)

Variational equations: $\frac{dv}{dt} = -J \cdot P \cdot v$

$$\begin{pmatrix} \dot{v}_1 \\ \dot{v}_2 \\ \dot{v}_3 \\ \dot{v}_4 \end{pmatrix} = -\begin{pmatrix} 0 & 0 & -1 & 0 \\ 0 & 0 & 0 & -1 \\ 1 & 0 & 0 & 0 \\ 0 & 1 & 0 & 0 \end{pmatrix} \begin{pmatrix} 1+2y & 2x & 0 & 0 \\ 2x & 1-2y & 0 & 0 \\ 0 & 0 & 1 & 0 \\ 0 & 0 & 0 & 1 \end{pmatrix} \begin{pmatrix} v_1 \\ v_2 \\ v_3 \\ v_4 \end{pmatrix}$$

$$\begin{aligned} \dot{v}_1 &= v_3 \\ \dot{v}_2 &= v_4 \\ \dot{v}_3 &= -v_1 - 2xv_2 - 2yv_1 \\ \dot{v}_4 &= -v_2 - 2xv_1 + 2yv_2 \end{aligned} \quad + \quad \begin{aligned} \dot{x} &= p_x \\ \dot{y} &= p_y \\ \dot{p}_x &= -x - 2xy \\ \dot{p}_y &= -y - x^2 + y^2 \end{aligned}$$

Complete set of equations

Symplectic Maps

Consider an 2N-dimensional symplectic map T. In this case we have discrete time.

This is an area-preserving map whose Jacobian matrix

$$\mathbf{M} = \frac{\partial \mathbf{T}}{\partial \mathbf{x}} = \begin{bmatrix} \frac{\partial T_1}{\partial x_1} & \frac{\partial T_1}{\partial x_2} & \cdots & \frac{\partial T_1}{\partial x_{2N}} \\ \frac{\partial T_2}{\partial x_1} & \frac{\partial T_2}{\partial x_2} & \cdots & \frac{\partial T_2}{\partial x_{2N}} \\ \vdots & \vdots & & \vdots \\ \frac{\partial T_{2N}}{\partial x_1} & \frac{\partial T_{2N}}{\partial x_2} & \cdots & \frac{\partial T_{2N}}{\partial x_{2N}} \end{bmatrix}$$

satisfies

$$M^T \cdot J_{2N} \cdot M = J_{2N}$$

Symplectic Maps

Consider an 2N-dimensional symplectic map T. In this case we have discrete time.

The evolution of an orbit with initial condition

$$P(0)=(x_1(0), x_2(0),\ldots,x_{2N}(0))$$

is governed by the equations of map T

$$P(i+1)=T\,P(i)\ ,\ i=0,1,2,\ldots$$

The evolution of an initial deviation vector

$$v(0) = (\delta x_1(0), \delta x_2(0),\ldots, \delta x_{2N}(0))$$

is given by the corresponding tangent map

$$v(i+1) = \left.\frac{\partial T}{\partial P}\right|_i \cdot v(i)\ ,\ i = 0, 1, 2, \ldots$$

Example – 2D map

Equations of the map:

$$\begin{pmatrix} x_1' \\ x_2' \end{pmatrix} = T\begin{pmatrix} x_1 \\ x_2 \end{pmatrix} \Rightarrow \begin{aligned} x_1' &= x_1 + x_2 \\ x_2' &= x_2 - \nu \sin(x_1 + x_2) \end{aligned} \qquad (\mathrm{mod}\ 2\pi)$$

Example – 2D map

Equations of the map:

$$\begin{pmatrix} x_1' \\ x_2' \end{pmatrix} = T\begin{pmatrix} x_1 \\ x_2 \end{pmatrix} \Rightarrow \begin{aligned} x_1' &= x_1 + x_2 \\ x_2' &= x_2 - \nu \sin(x_1 + x_2) \end{aligned} \qquad (\mathrm{mod}\ 2\pi)$$

Tangent map:

$$v(i+1) = \left.\frac{\partial T}{\partial P}\right|_i \cdot v(i)$$

Example – 2D map

Equations of the map:

$$\begin{pmatrix} x_1' \\ x_2' \end{pmatrix} = T\begin{pmatrix} x_1 \\ x_2 \end{pmatrix} \Rightarrow \begin{aligned} x_1' &= x_1 + x_2 \\ x_2' &= x_2 - \nu \sin(x_1 + x_2) \end{aligned} \qquad (\mathrm{mod}\ 2\pi)$$

Tangent map:

$$v(i+1) = \left.\frac{\partial T}{\partial P}\right|_i \cdot v(i)$$

$$\begin{pmatrix} dx_1' \\ dx_2' \end{pmatrix}$$

Example – 2D map

Equations of the map:

$$\begin{pmatrix} x'_1 \\ x'_2 \end{pmatrix} = T\begin{pmatrix} x_1 \\ x_2 \end{pmatrix} \Rightarrow \begin{array}{rcl} x'_1 & = & x_1 + x_2 \\ x'_2 & = & x_2 - v\sin(x_1 + x_2) \end{array} \qquad (\mathrm{mod}\ 2\pi)$$

Tangent map:

$$v(i+1) = \left.\frac{\partial T}{\partial P}\right|_i \cdot v(i)$$

$$\begin{pmatrix} dx'_1 \\ dx'_2 \end{pmatrix} = \begin{pmatrix} 1 & 1 \\ -v\cos(x_1 + x_2) & 1 - v\cos(x_1 + x_2) \end{pmatrix}$$

Example – 2D map

Equations of the map:

$$\begin{pmatrix} x'_1 \\ x'_2 \end{pmatrix} = T\begin{pmatrix} x_1 \\ x_2 \end{pmatrix} \Rightarrow \begin{array}{lcl} x'_1 & = & x_1 + x_2 \\ x'_2 & = & x_2 - \nu \sin(x_1 + x_2) \end{array} \qquad (\mathrm{mod}\ 2\pi)$$

Tangent map:

$$v(i+1) = \left.\frac{\partial T}{\partial P}\right|_i \cdot v(i)$$

$$\begin{pmatrix} dx'_1 \\ dx'_2 \end{pmatrix} = \begin{pmatrix} 1 & 1 \\ -\nu\cos(x_1 + x_2) & 1 - \nu\cos(x_1 + x_2) \end{pmatrix} \begin{pmatrix} dx_1 \\ dx_2 \end{pmatrix}$$

Lyapunov Exponents

Roughly speaking, the Lyapunov exponents of a given orbit characterize the mean exponential rate of divergence of trajectories surrounding it.

Consider an orbit in the 2N-dimensional phase space with initial condition x(0) and an initial deviation vector from it v(0). Then the mean exponential rate of divergence is:

$$\sigma(x(0), v(0)) = \lim_{t\to\infty} \frac{1}{t} \ln \frac{\|v(t)\|}{\|v(0)\|}$$

We commonly use the Euclidian norm and set d(0)=||v(0)||=1

Lyapunov Exponents

There exists an M-dimensional basis $\{\hat{e}_i\}$ of v such that for any v, σ takes one of the M (possibly nondistinct) values

$$\sigma_i(x(0)) = \sigma(x(0), \hat{e}_i)$$

which are the Lyapunov exponents.

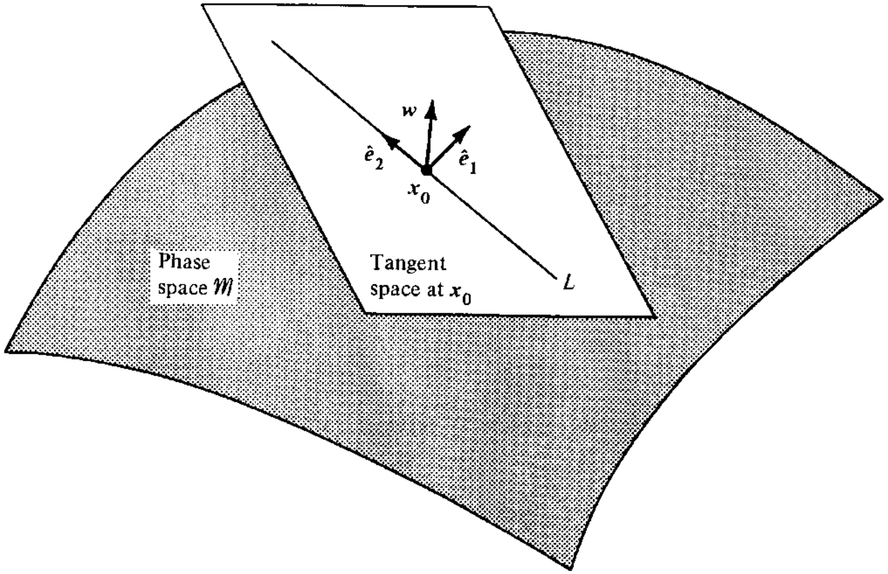

Benettin & Galgani, 1979, in Laval and Gressillon (eds.), op cit, 93

In autonomous Hamiltonian systems the M exponents are ordered in pairs of opposite sign numbers and two of them are 0.

Computation of the Maximum Lyapunov Exponent

Due to the exponential growth of v(t) (and of d(t)=||v(t)||) we renormalize v(t) from time to time.

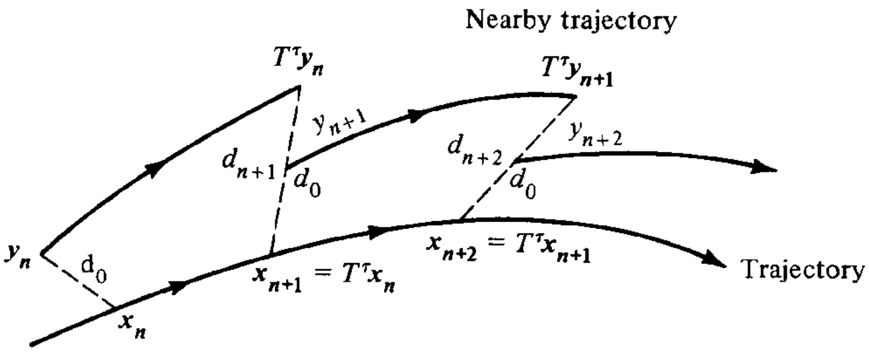

Figure 5.6. Numerical calculation of the maximal Liapunov characteristic exponent. Here $y = x + v$ and τ is a finite interval of time (after Benettin *et al.*, 1976).

Then the Maximum Lyapunov exponent is computed as

$$\sigma_1 = \lim_{n \to \infty} \frac{1}{n\tau} \sum_{i=1}^{n} \ln d_i$$

Maximum Lyapunov Exponent

σ_1=0: Regular motion

$\sigma_1 \neq$0: Chaotic motion

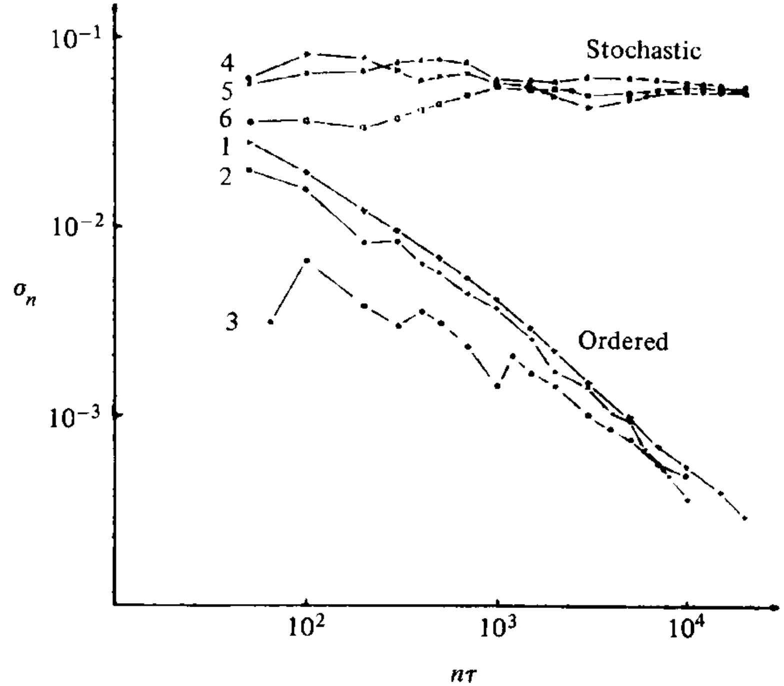

Figure 5.7. Behavior of σ_n at the intermediate energy $E = 0.125$ for initial points taken in the ordered (curves 1–3) or stochastic (curves 4–6) regions (after Benettin *et al*., 1976).

If we start with more than one linearly independent deviation vectors they will align to the direction defined by the largest Lyapunov exponent for chaotic orbits.

Maximum Lyapunov Exponent

Hénon-Heiles system: Chaotic orbit

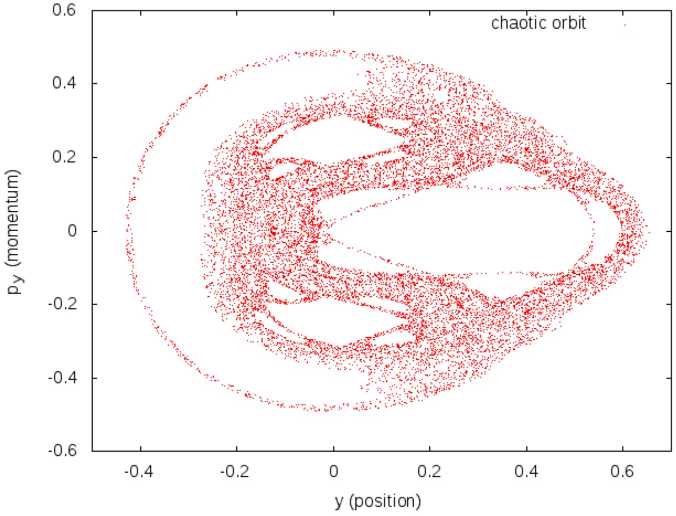

Maximum Lyapunov Exponent

Hénon-Heiles system: Chaotic orbit

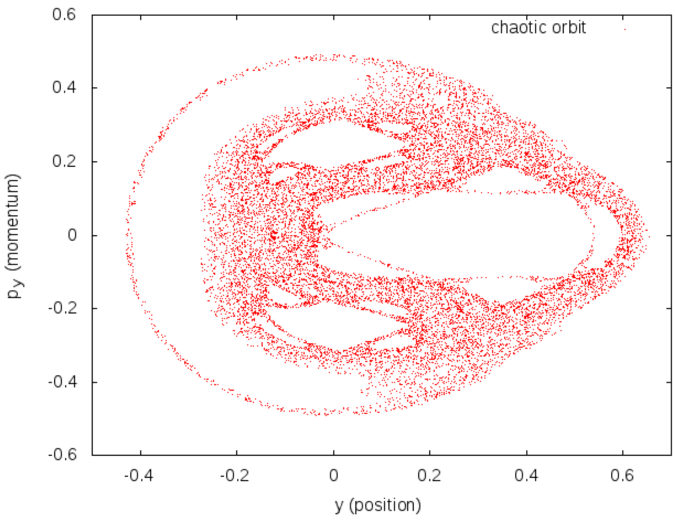

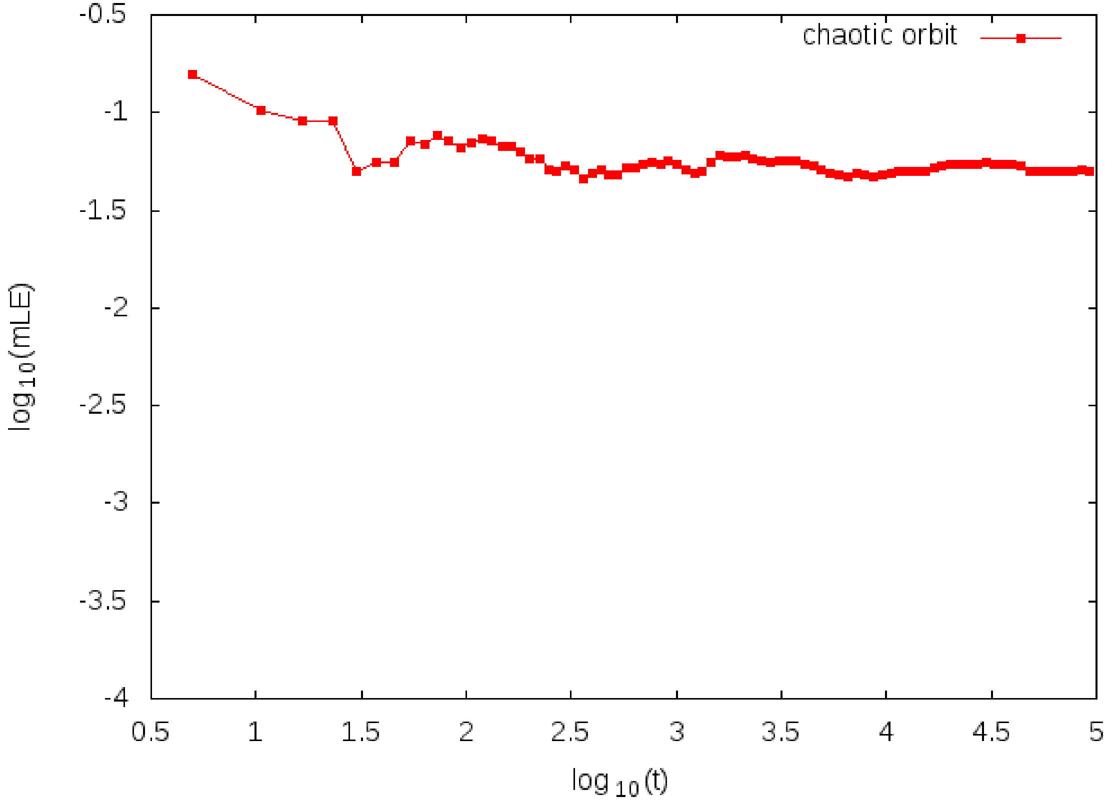

Maximum Lyapunov Exponent

Hénon-Heiles system: Chaotic orbit and Regular orbit

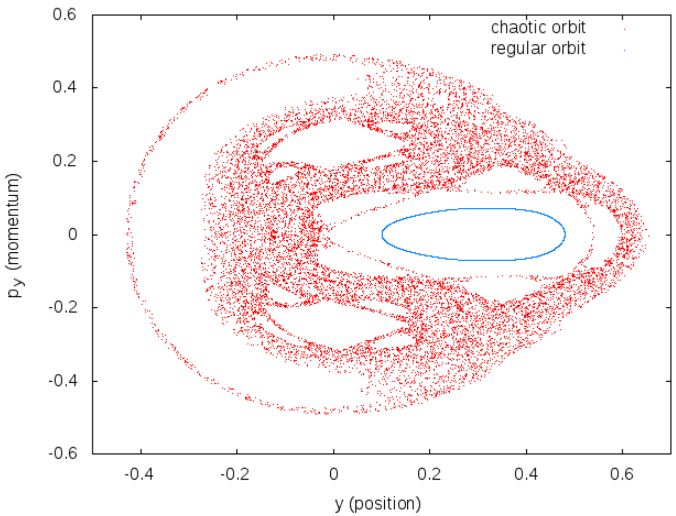

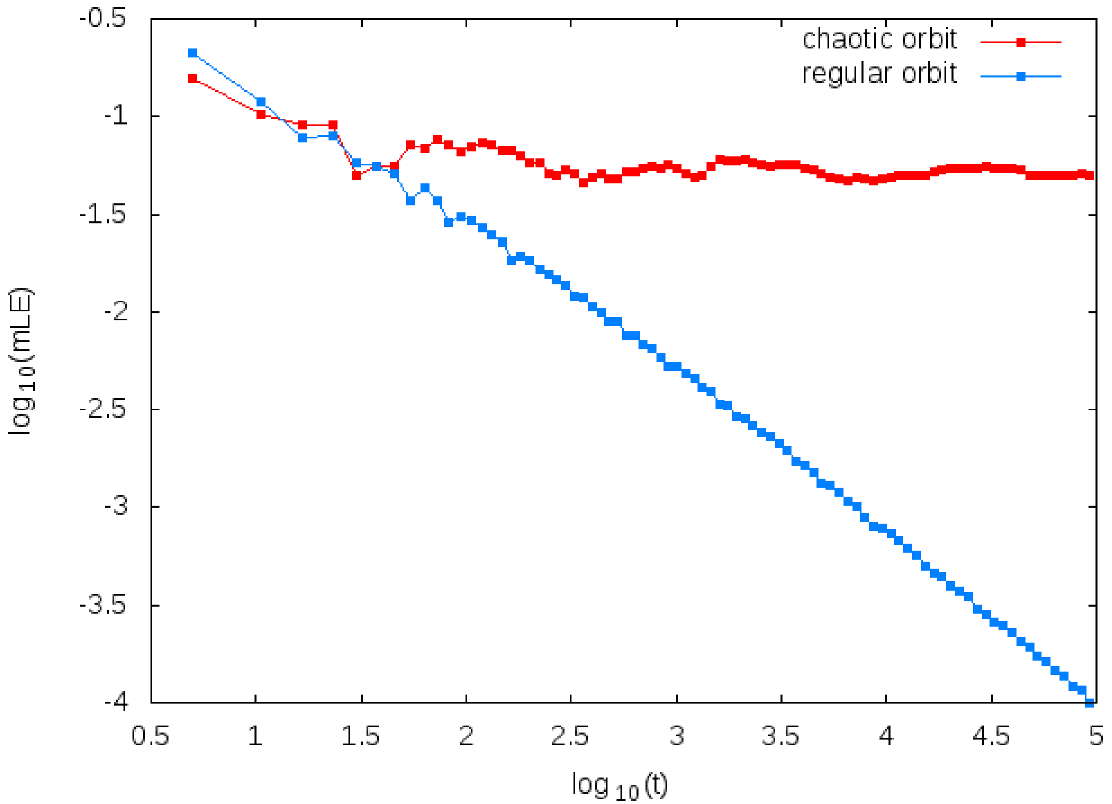

The
Smaller ALignment Index
(SALI)
method

Definition of the SALI

We follow the evolution in time of two different initial deviation vectors ($v_1(0)$, $v_2(0)$), and define the SALI (Ch.S. 2001, J. Phys. A) as:

$$SALI(t) = \min\left\{ \left\| \hat{v}_1(t) + \hat{v}_2(t) \right\|, \left\| \hat{v}_1(t) - \hat{v}_2(t) \right\| \right\}$$

where

$$\hat{v}_1(t) = \frac{v_1(t)}{\left\| v_1(t) \right\|}$$

When the two vectors become collinear

$$SALI(t) \rightarrow 0$$

Behavior of the SALI for chaotic motion

For chaotic orbits the two initially different deviation vectors tend to coincide with the direction defined by the maximum Lyapunov exponent.

Behavior of the SALI for chaotic motion

For chaotic orbits the two initially different deviation vectors tend to coincide with the direction defined by the maximum Lyapunov exponent.

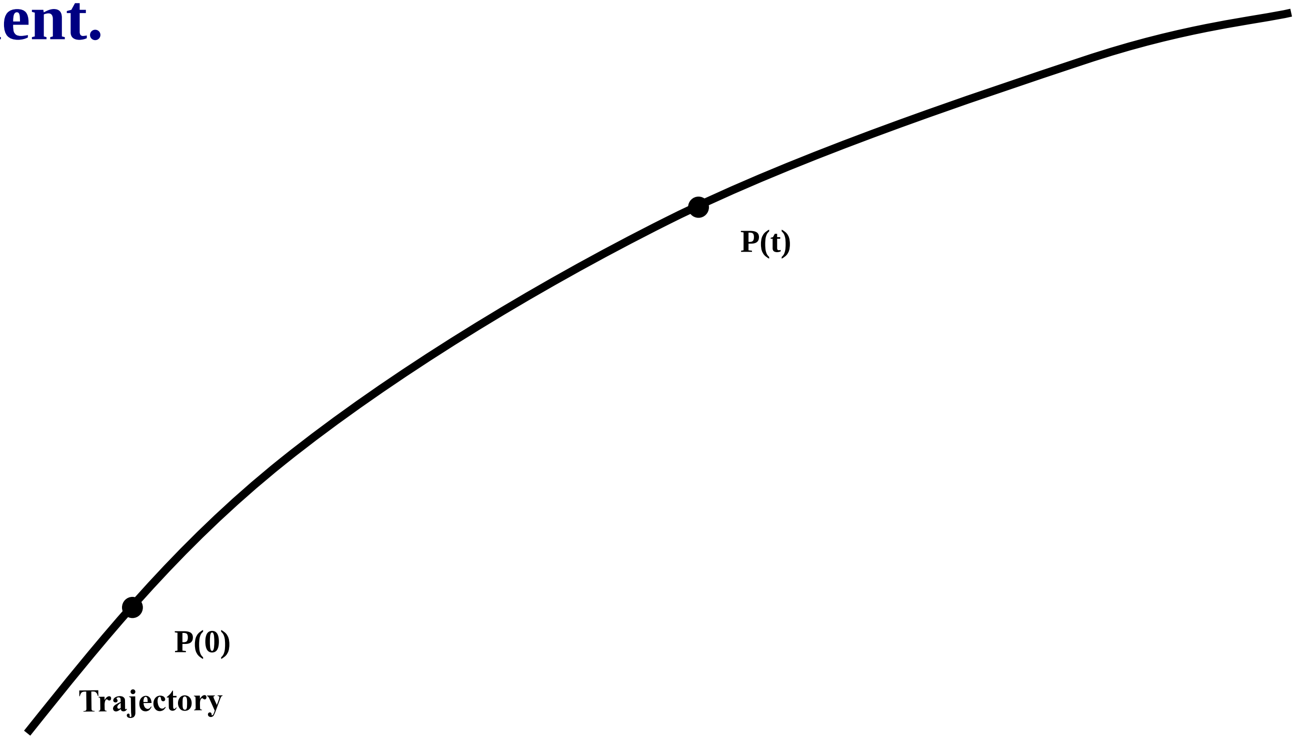

Behavior of the SALI for chaotic motion

For chaotic orbits the two initially different deviation vectors tend to coincide with the direction defined by the maximum Lyapunov exponent.

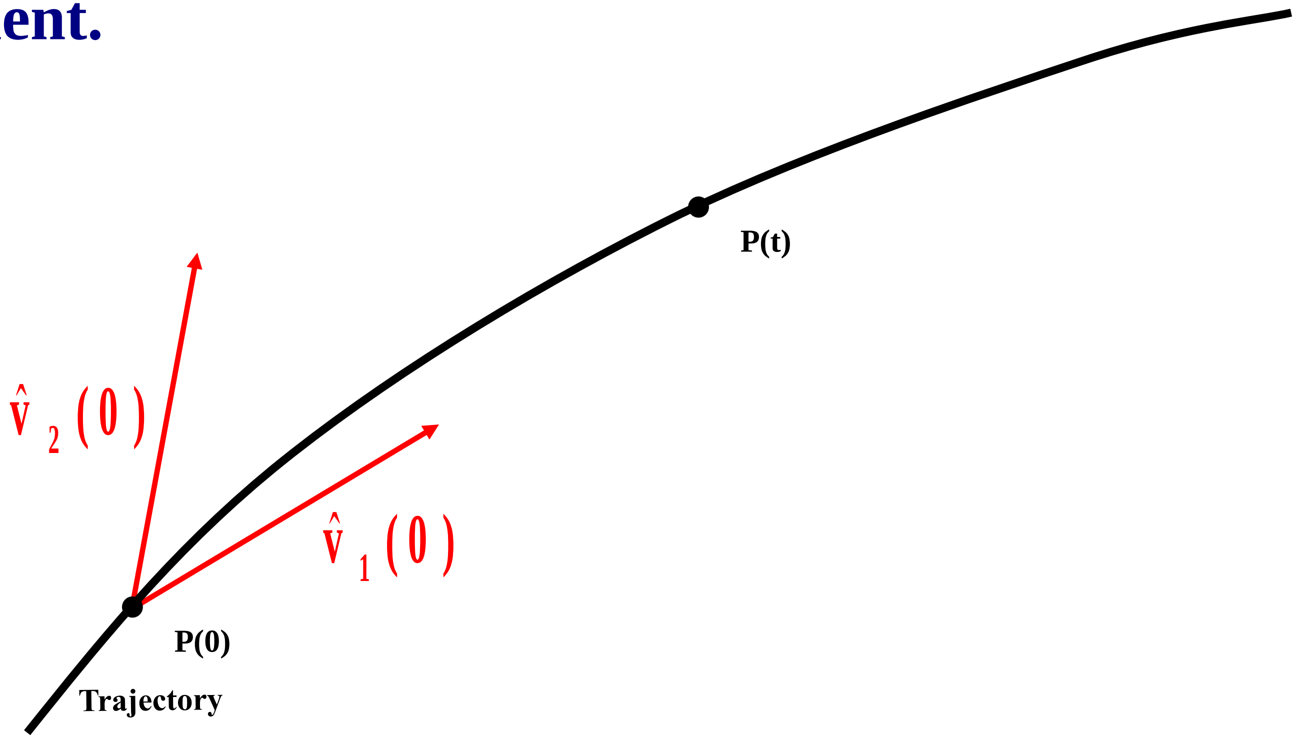

Behavior of the SALI for chaotic motion

For chaotic orbits the two initially different deviation vectors tend to coincide with the direction defined by the maximum Lyapunov exponent.

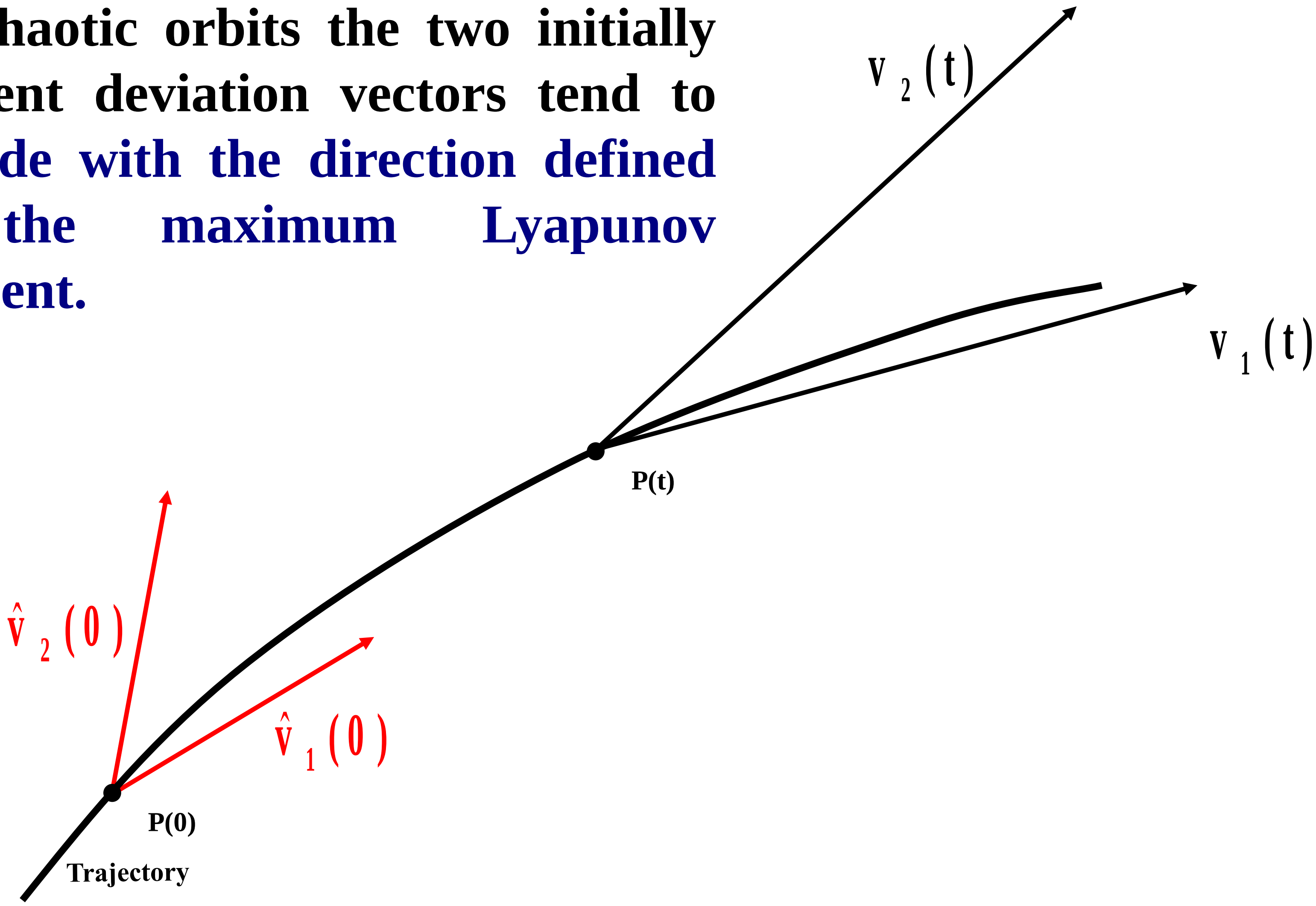

Behavior of the SALI for chaotic motion

For chaotic orbits the two initially different deviation vectors tend to coincide with the direction defined by the maximum Lyapunov exponent.

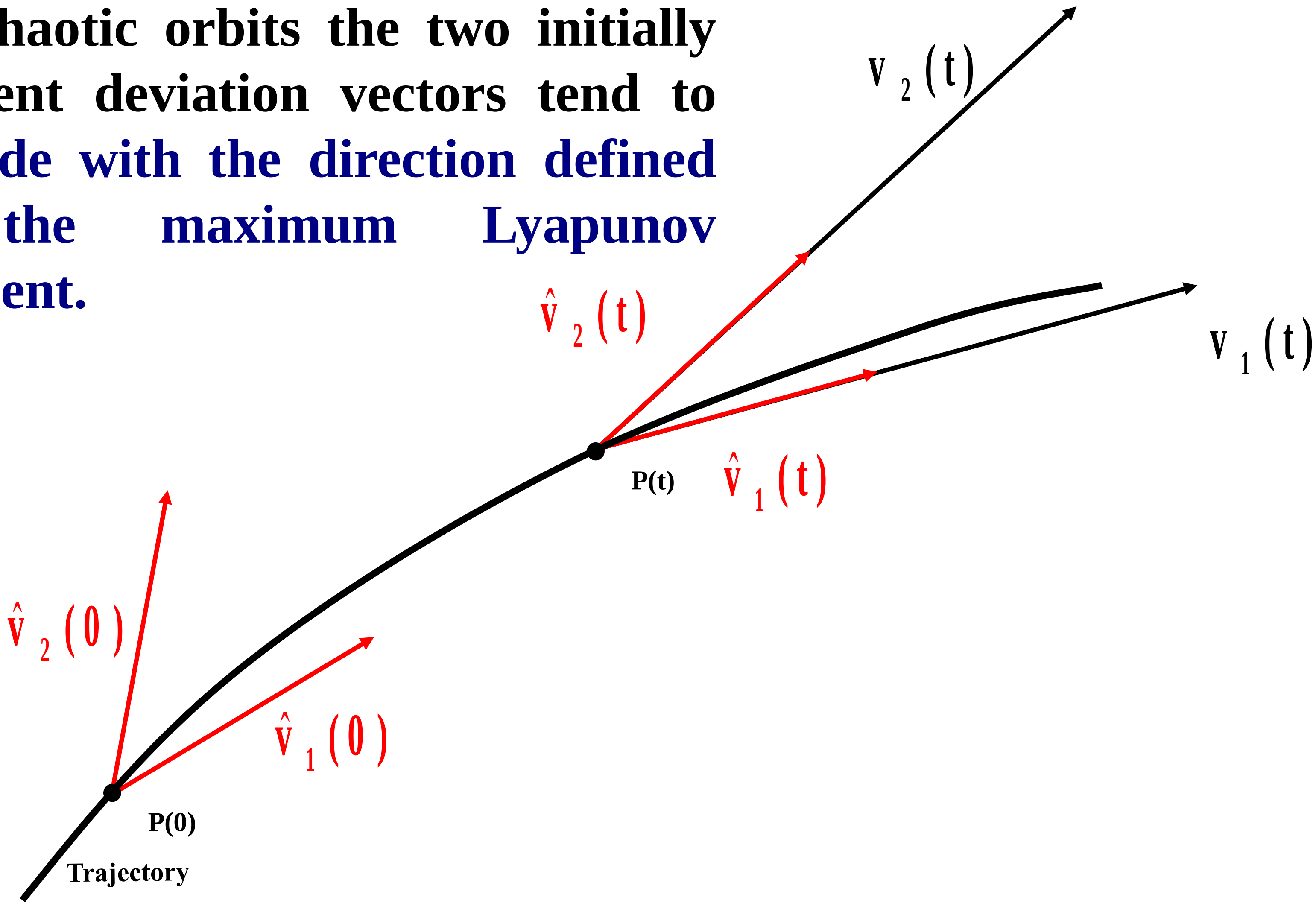

Behavior of the SALI for chaotic motion

For chaotic orbits the two initially different deviation vectors tend to coincide with the direction defined by the maximum Lyapunov exponent.

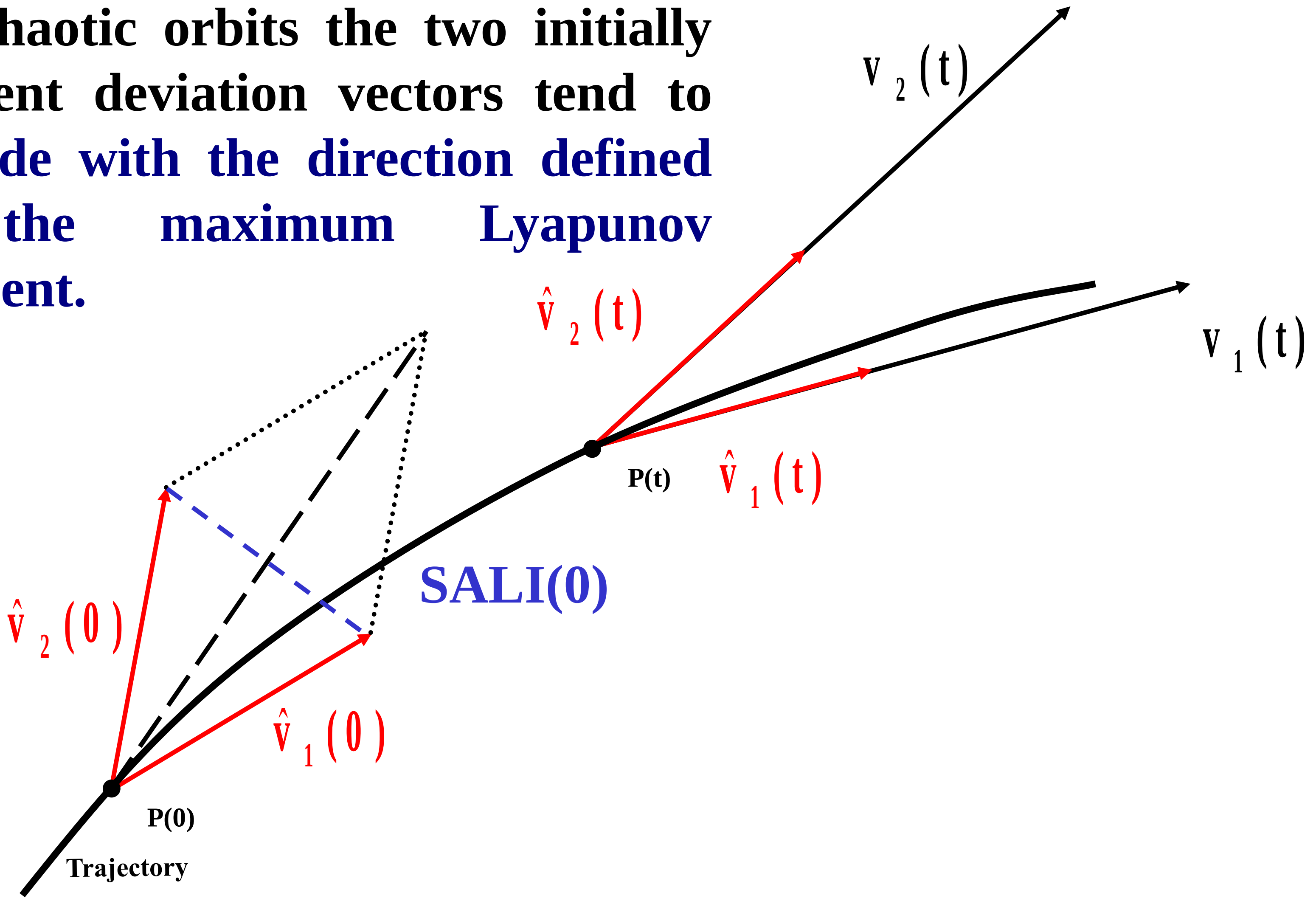

Behavior of the SALI for chaotic motion

For chaotic orbits the two initially different deviation vectors tend to **coincide with the direction defined by the maximum Lyapunov exponent.**

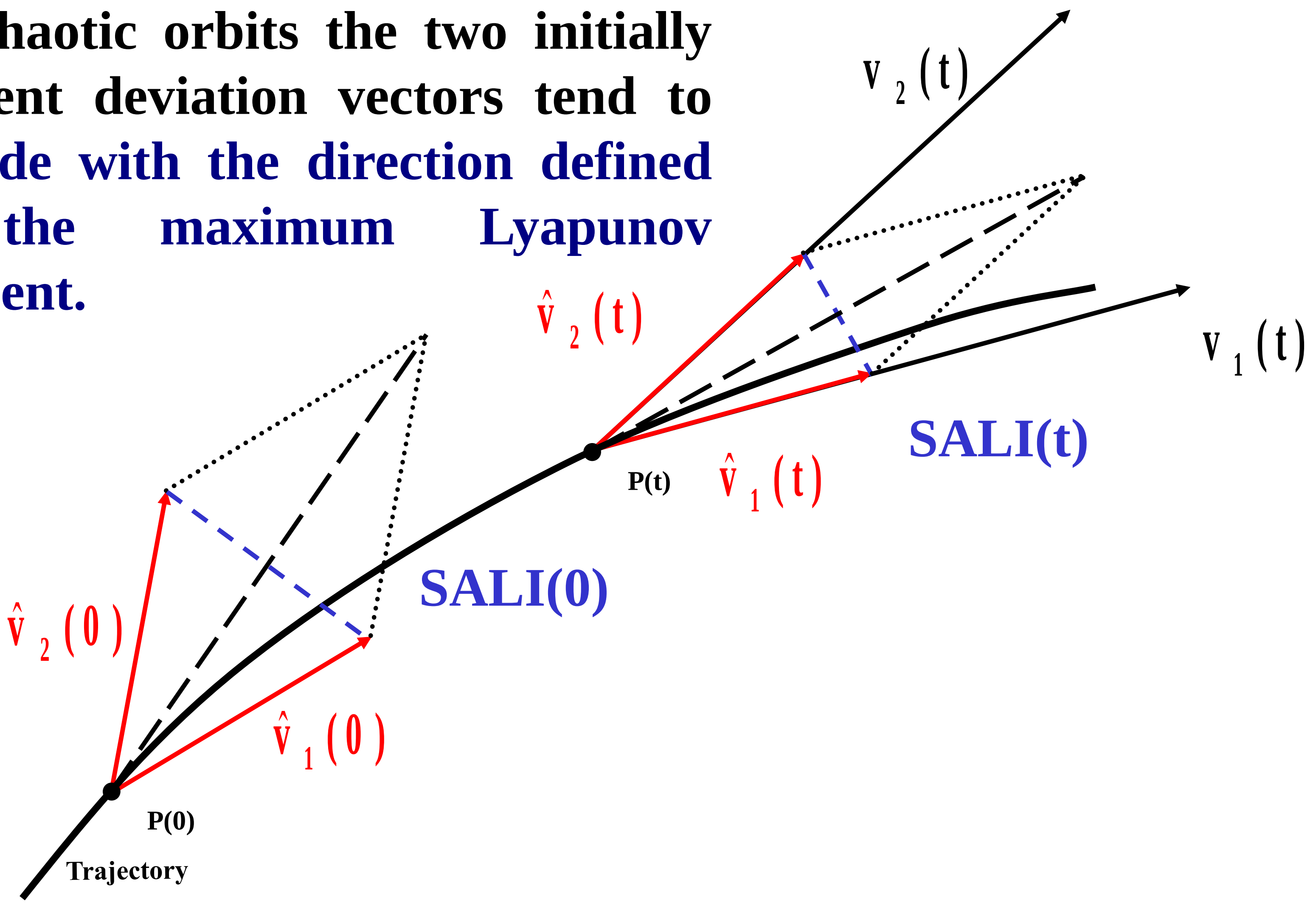

Behavior of the SALI for chaotic motion

We test the validity of the approximation $SALI \sim e^{-(\sigma_1-\sigma_2)t}$ (Ch.S., Antonopoulos, Bountis, Vrahatis, 2004, J. Phys. A) for a chaotic orbit of the 3D Hamiltonian

$$H = \sum_{i=1}^{3} \frac{\omega_i}{2}(q_i^2 + p_i^2) + q_1^2 q_2 + q_1^2 q_3$$

with $\omega_1=1$, $\omega_2=1.4142$, $\omega_3=1.7321$, $H=0.09$

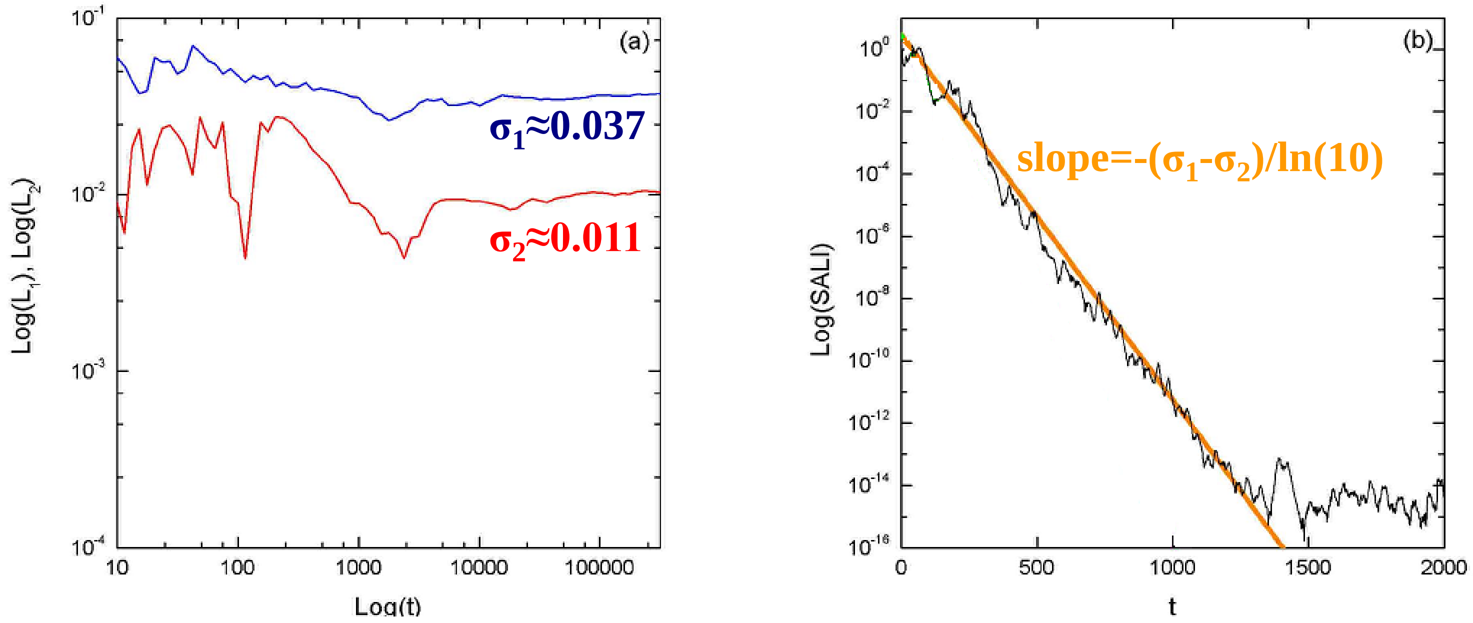

Behavior of the SALI for regular motion

Regular motion occurs on a torus and two different initial deviation vectors become tangent to the torus, generally having different directions.

Behavior of the SALI for regular motion

Regular motion occurs on a torus and two different initial deviation vectors become tangent to the torus, generally having different directions.

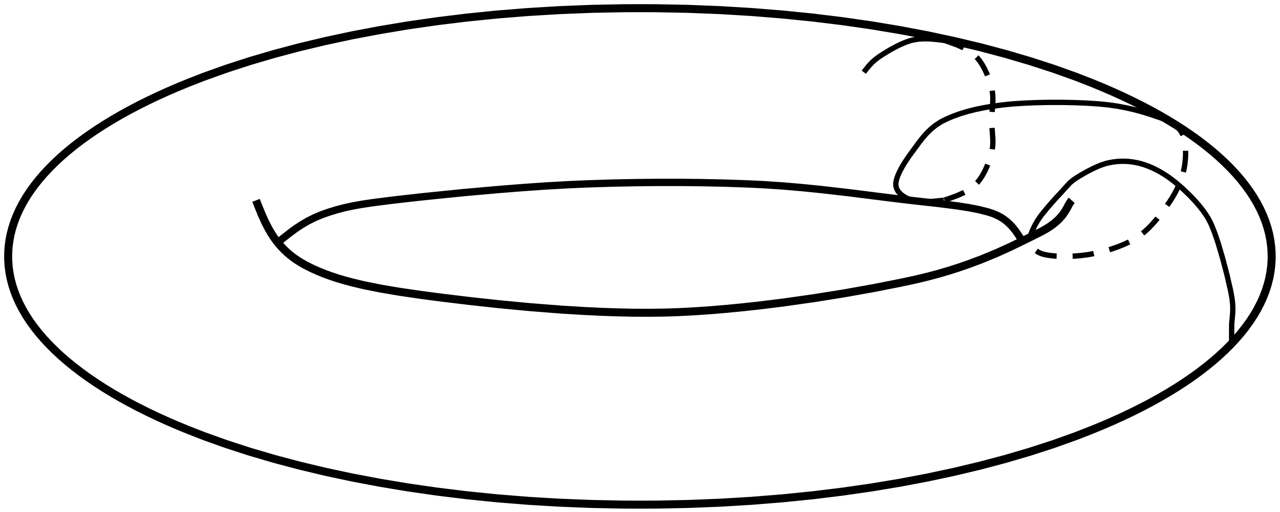

Behavior of the SALI for regular motion

Regular motion occurs on a torus and two different initial deviation vectors become tangent to the torus, generally having different directions.

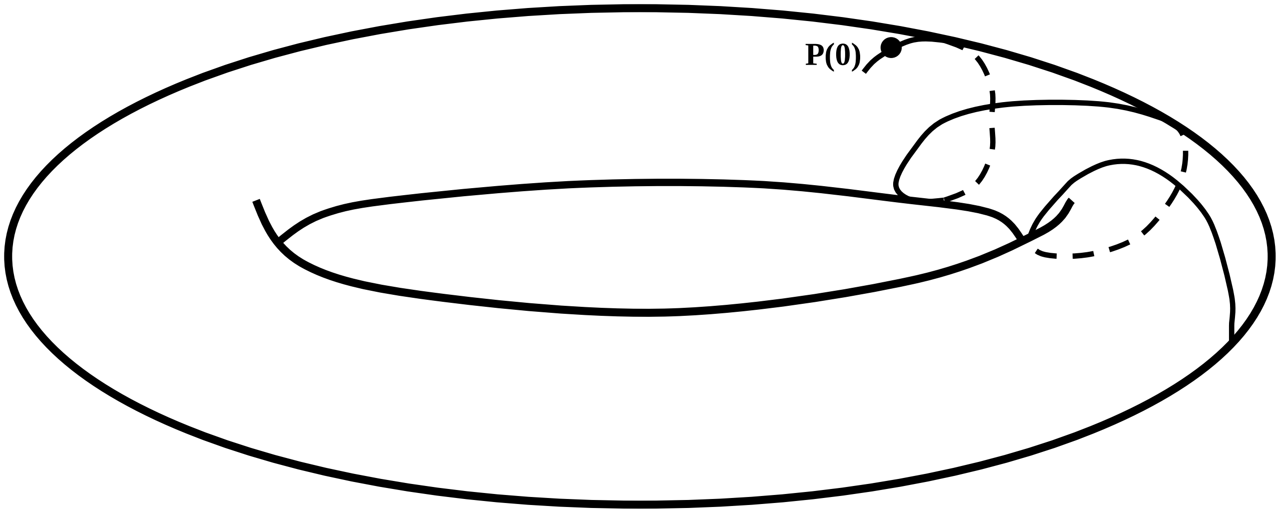

Behavior of the SALI for regular motion

Regular motion occurs on a torus and two different initial deviation vectors become tangent to the torus, generally having different directions.

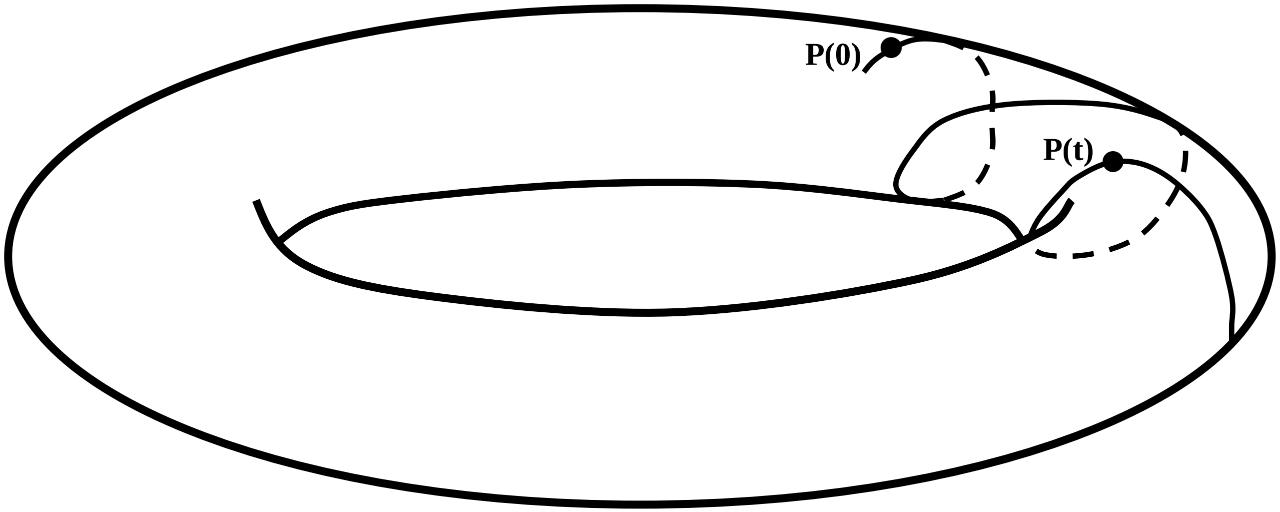

Behavior of the SALI for regular motion

Regular motion occurs on a torus and two different initial deviation vectors become tangent to the torus, generally having different directions.

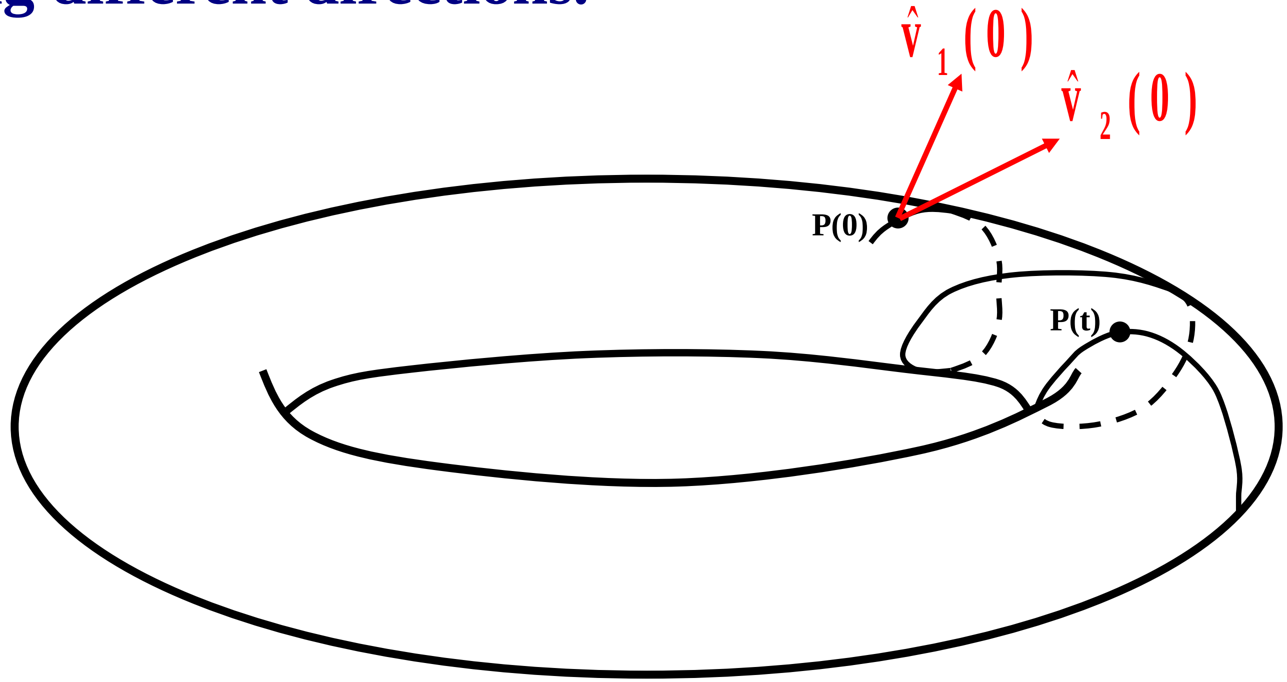

Behavior of the SALI for regular motion

Regular motion occurs on a torus and two different initial deviation vectors become tangent to the torus, generally having different directions.

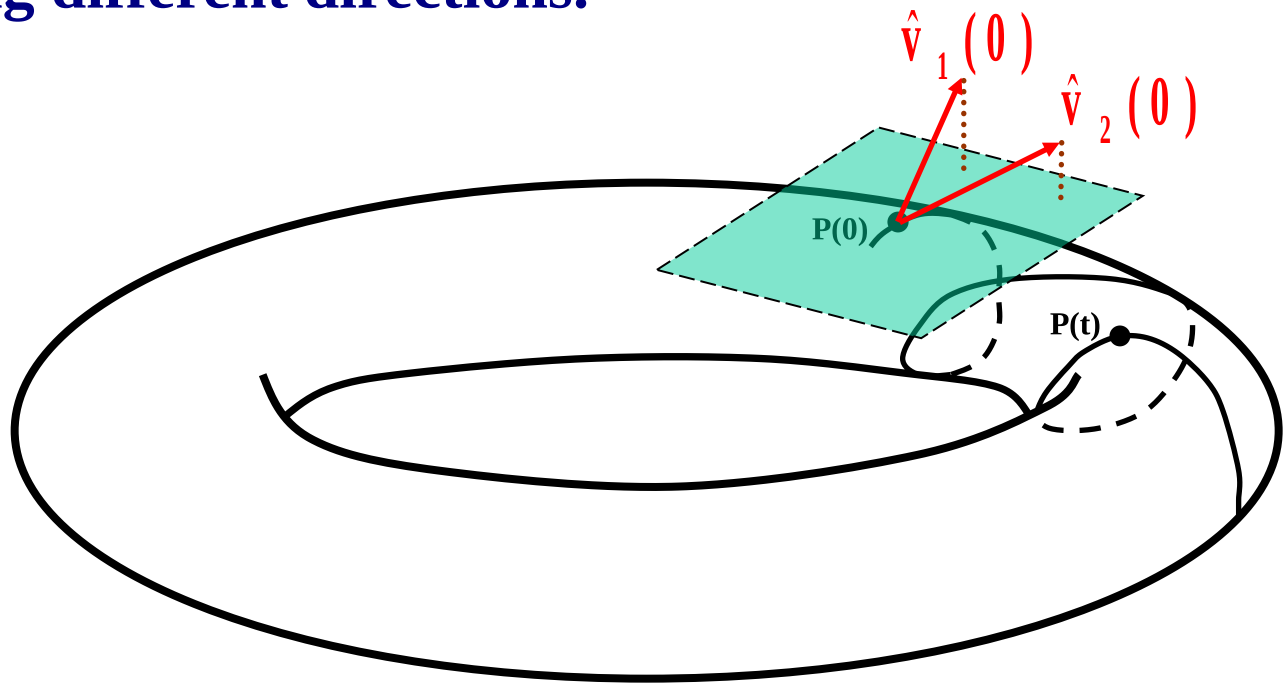

Behavior of the SALI for regular motion

Regular motion occurs on a torus and two different initial deviation vectors become tangent to the torus, generally having different directions.

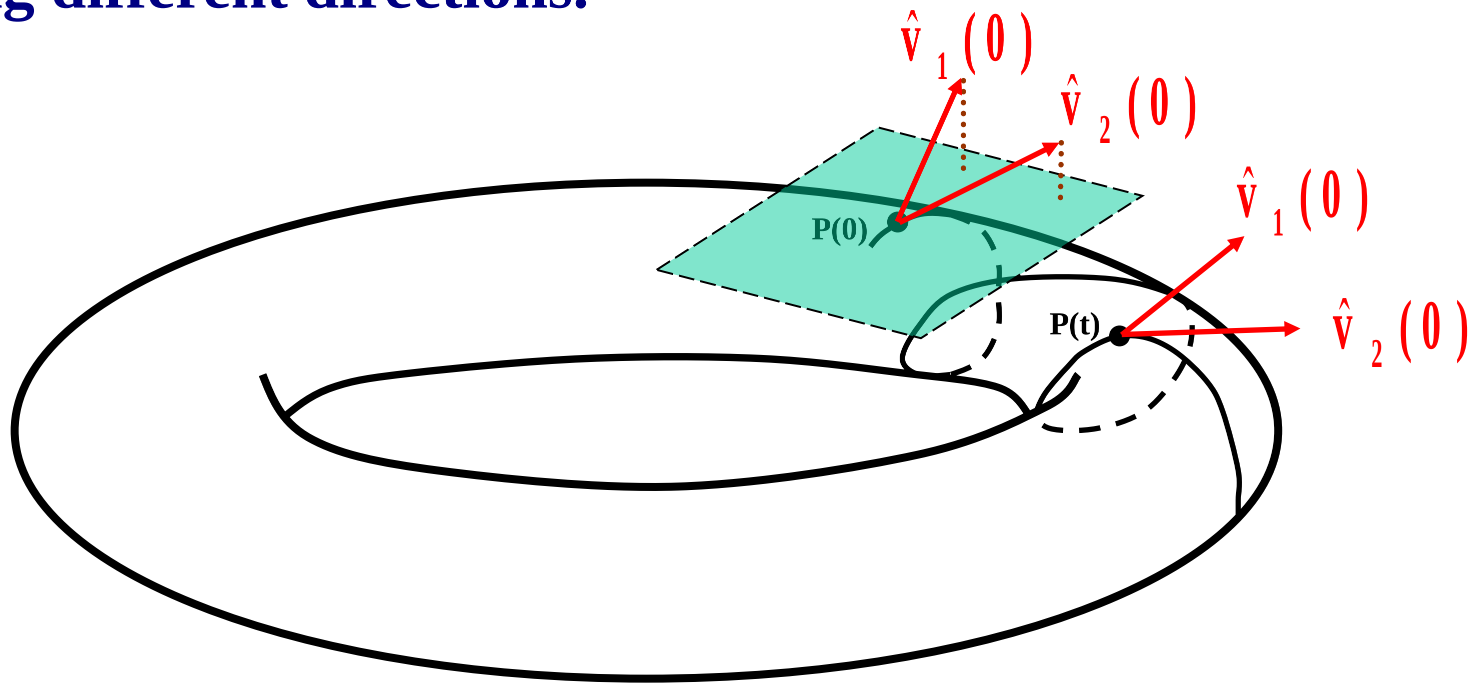

Behavior of the SALI for regular motion

Regular motion occurs on a torus and two different initial deviation vectors become tangent to the torus, generally having different directions.

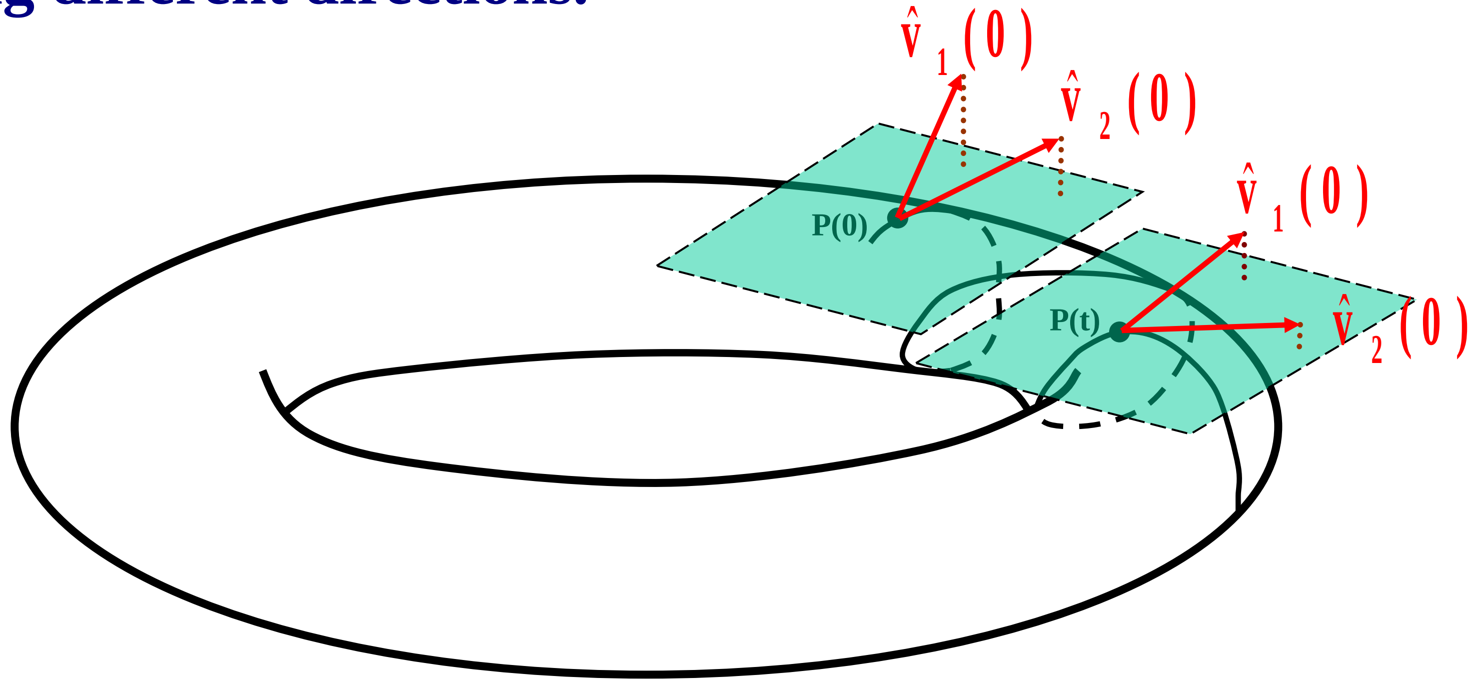

Applications – Hénon-Heiles system

As an example, we consider the 2D Hénon-Heiles system:

$$H_2 = \frac{1}{2}(p_x^2 + p_y^2) + \frac{1}{2}(x^2 + y^2) + x^2 y - \frac{1}{3}y^3$$

For E=1/8 we consider the orbits with initial conditions:
Regular orbit, x=0, y=0.55, p_x=0.2417, p_y=0
Chaotic orbit, x=0, y=-0.016, p_x=0.49974, p_y=0
Chaotic orbit, x=0, y=-0.01344, p_x=0.49982, p_y=0

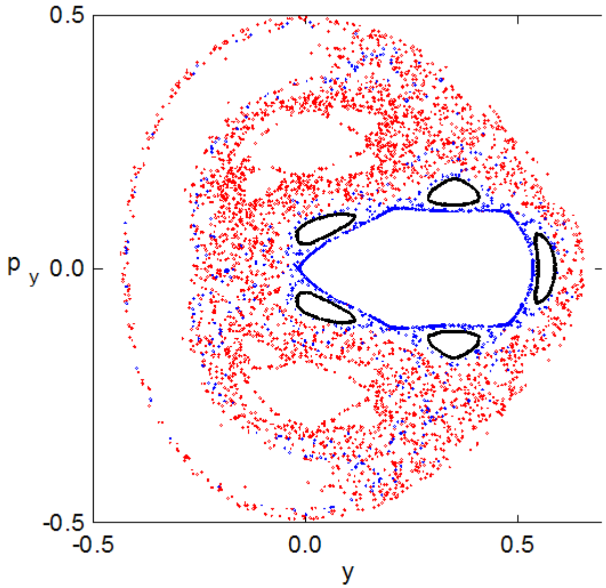

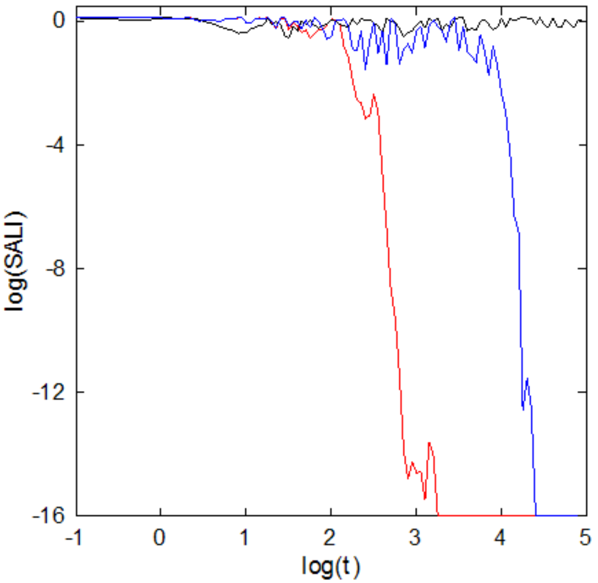

Applications – Hénon-Heiles system

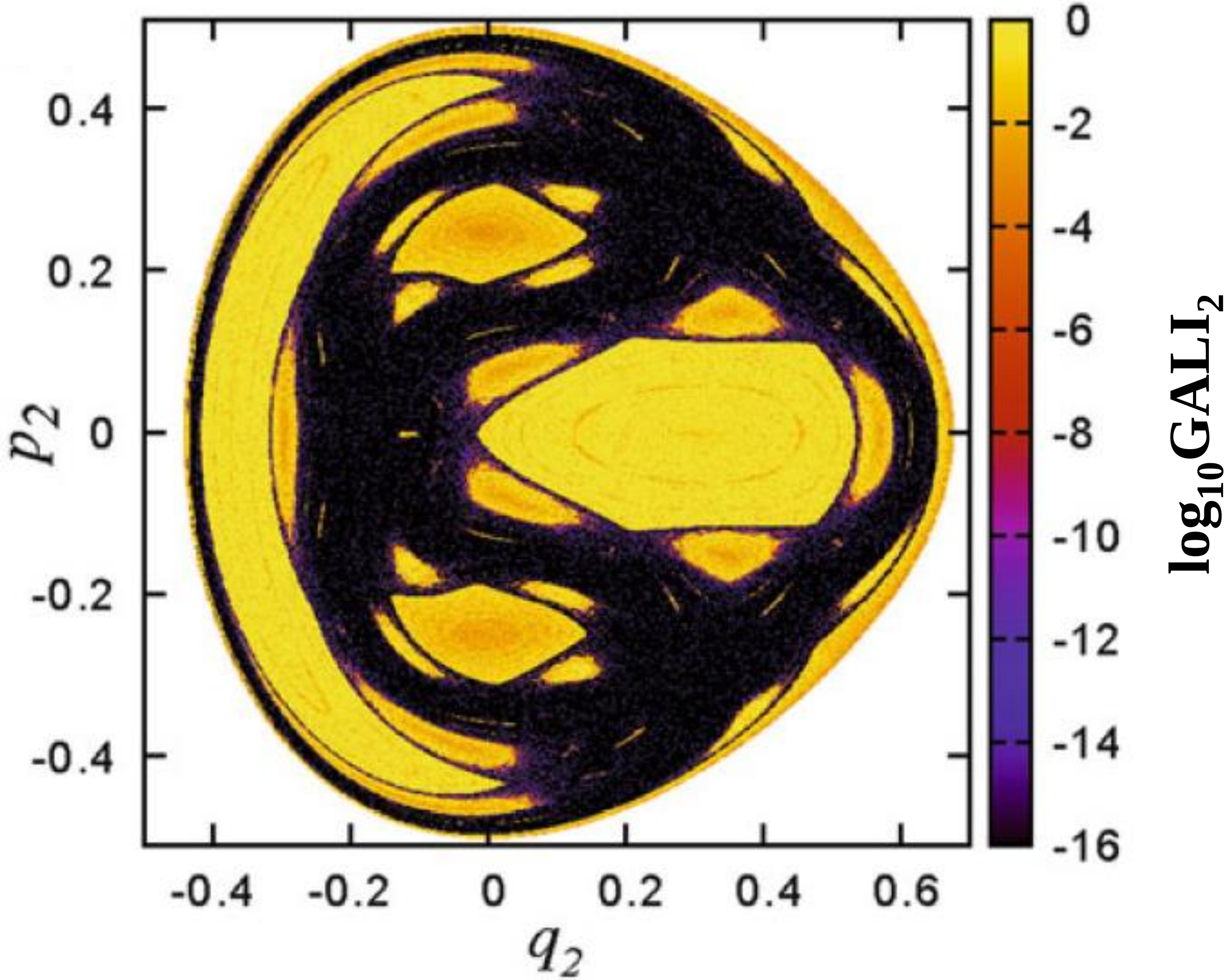

Applications – 4D map

$$\begin{aligned} x_1' &= x_1 + x_2 \\ x_2' &= x_2 - \nu \sin(x_1 + x_2) - \mu [1 - \cos(x_1 + x_2 + x_3 + x_4)] \\ x_3' &= x_3 + x_4 \\ x_4' &= x_4 - \kappa \sin(x_3 + x_4) - \mu [1 - \cos(x_1 + x_2 + x_3 + x_4)] \end{aligned} \quad (\mathrm{mod}\ 2\pi)$$

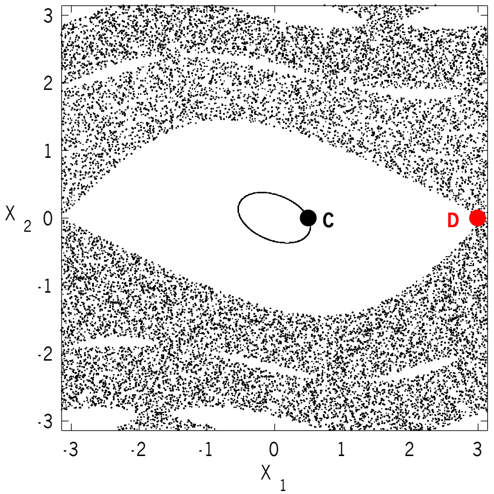

For ν=0.5, κ=0.1, μ=0.1 we consider the orbits:

regular orbit C *with initial conditions* $x_1=0.5$, $x_2=0$, $x_3=0.5$, $x_4=0$.

chaotic orbit D *with initial conditions* $x_1=3$, $x_2=0$, $x_3=0.5$, $x_4=0$.

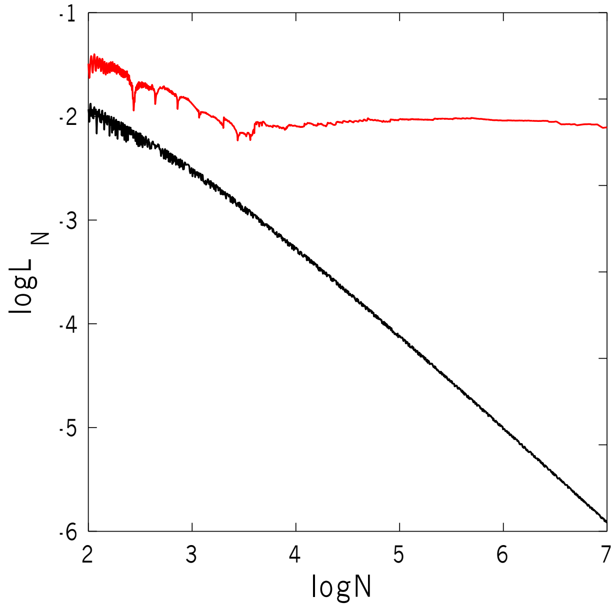

Applications – 4D map

$$\begin{aligned} x_1' &= x_1 + x_2 \\ x_2' &= x_2 - \nu \sin(x_1 + x_2) - \mu[1 - \cos(x_1 + x_2 + x_3 + x_4)] \\ x_3' &= x_3 + x_4 \\ x_4' &= x_4 - \kappa \sin(x_3 + x_4) - \mu[1 - \cos(x_1 + x_2 + x_3 + x_4)] \end{aligned} \quad (\text{mod } 2\pi)$$

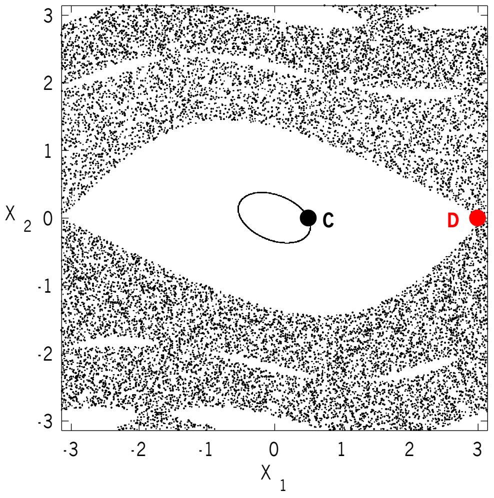

For ν=0.5, κ=0.1, μ=0.1 we consider the orbits:

regular orbit C *with initial conditions x_1=0.5, x_2=0, x_3=0.5, x_4=0.*

chaotic orbit D *with initial conditions x_1=3, x_2=0, x_3=0.5, x_4=0.*

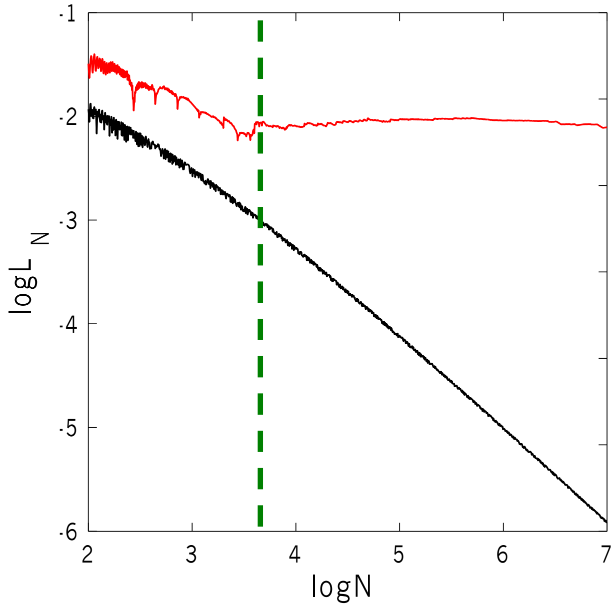

Applications – 4D map

$$\begin{aligned} x_1' &= x_1 + x_2 \\ x_2' &= x_2 - \nu \sin(x_1 + x_2) - \mu [1 - \cos(x_1 + x_2 + x_3 + x_4)] \\ x_3' &= x_3 + x_4 \\ x_4' &= x_4 - \kappa \sin(x_3 + x_4) - \mu [1 - \cos(x_1 + x_2 + x_3 + x_4)] \end{aligned} \quad (\text{mod } 2\pi)$$

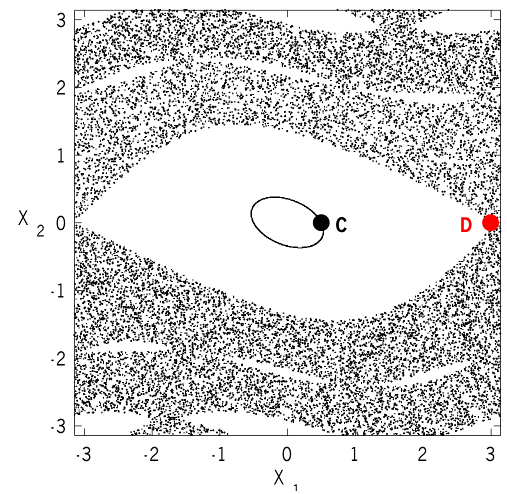

For ν=0.5, κ=0.1, μ=0.1 we consider the orbits:

***regular orbit C** with initial conditions x_1=0.5, x_2=0, x_3=0.5, x_4=0.*

***chaotic orbit D** with initial conditions x_1=3, x_2=0, x_3=0.5, x_4=0.*

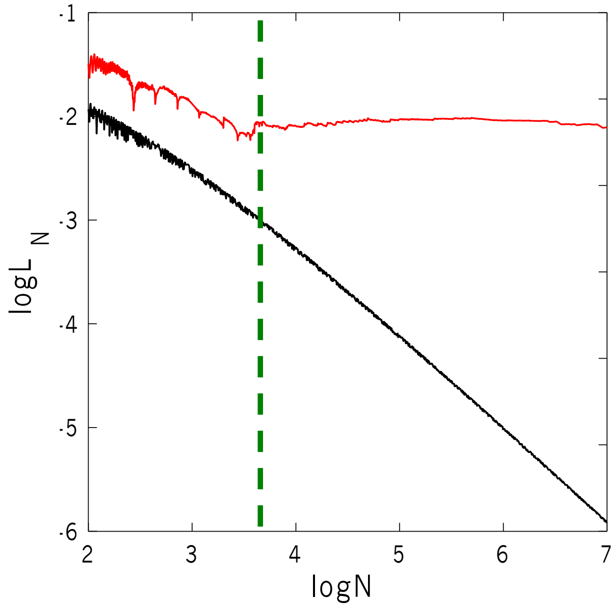

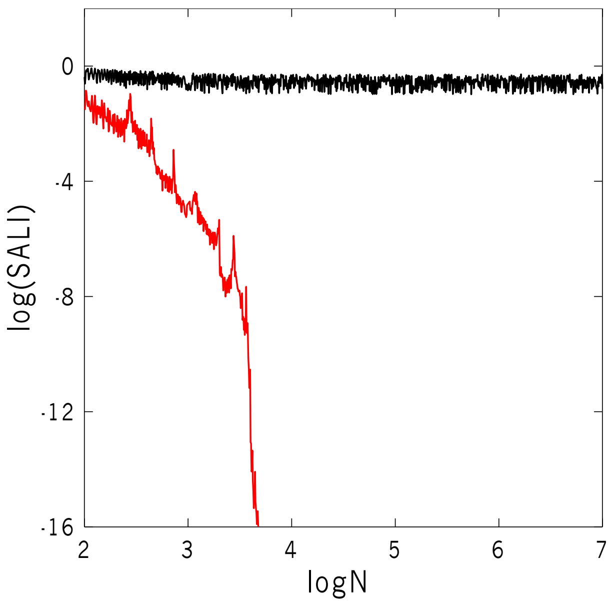

Applications – 4D map

$$
\begin{aligned}
x_1' &= x_1 + x_2 \\
x_2' &= x_2 - \nu \sin(x_1 + x_2) - \mu[1 - \cos(x_1 + x_2 + x_3 + x_4)] \\
x_3' &= x_3 + x_4 \\
x_4' &= x_4 - \kappa \sin(x_3 + x_4) - \mu[1 - \cos(x_1 + x_2 + x_3 + x_4)]
\end{aligned}
\pmod{2\pi}
$$

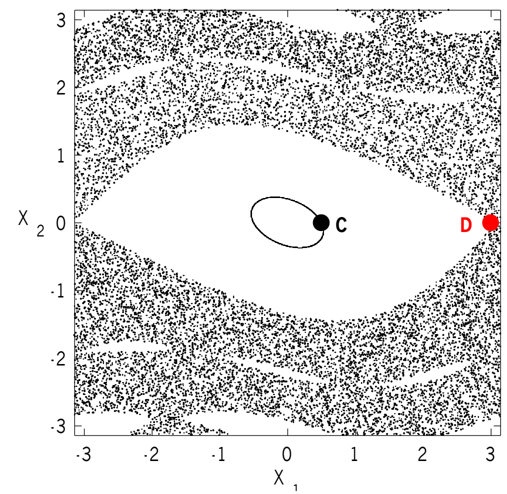

For ν=0.5, κ=0.1, μ=0.1 we consider the orbits:

regular orbit C *with initial conditions* $x_1=0.5, x_2=0, x_3=0.5, x_4=0.$

chaotic orbit D *with initial conditions* $x_1=3, x_2=0, x_3=0.5, x_4=0.$

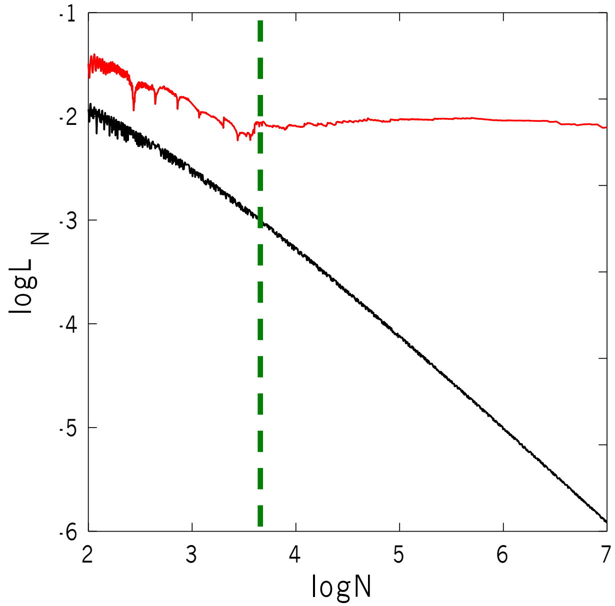

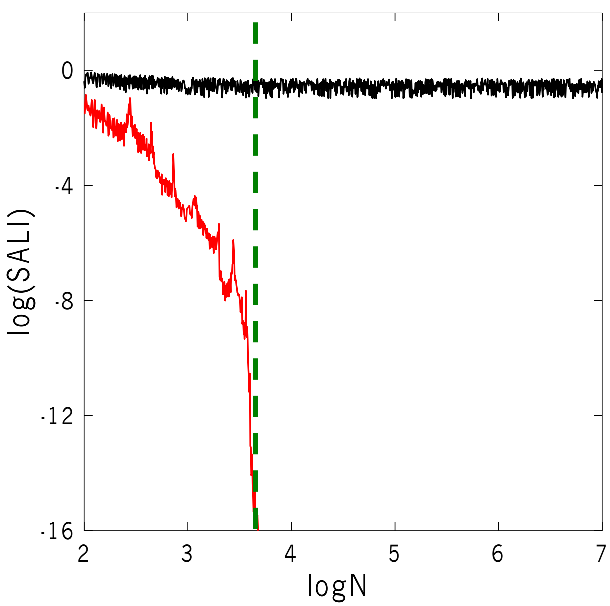

The
Generalized ALignment Indices
(GALIs)
method

Definition of the Generalized Alignment Index (GALI)

SALI effectively measures the 'area' of the parallelogram formed by the two deviation vectors.

Definition of the Generalized Alignment Index (GALI)

SALI effectively measures the 'area' of the parallelogram formed by the two deviation vectors.

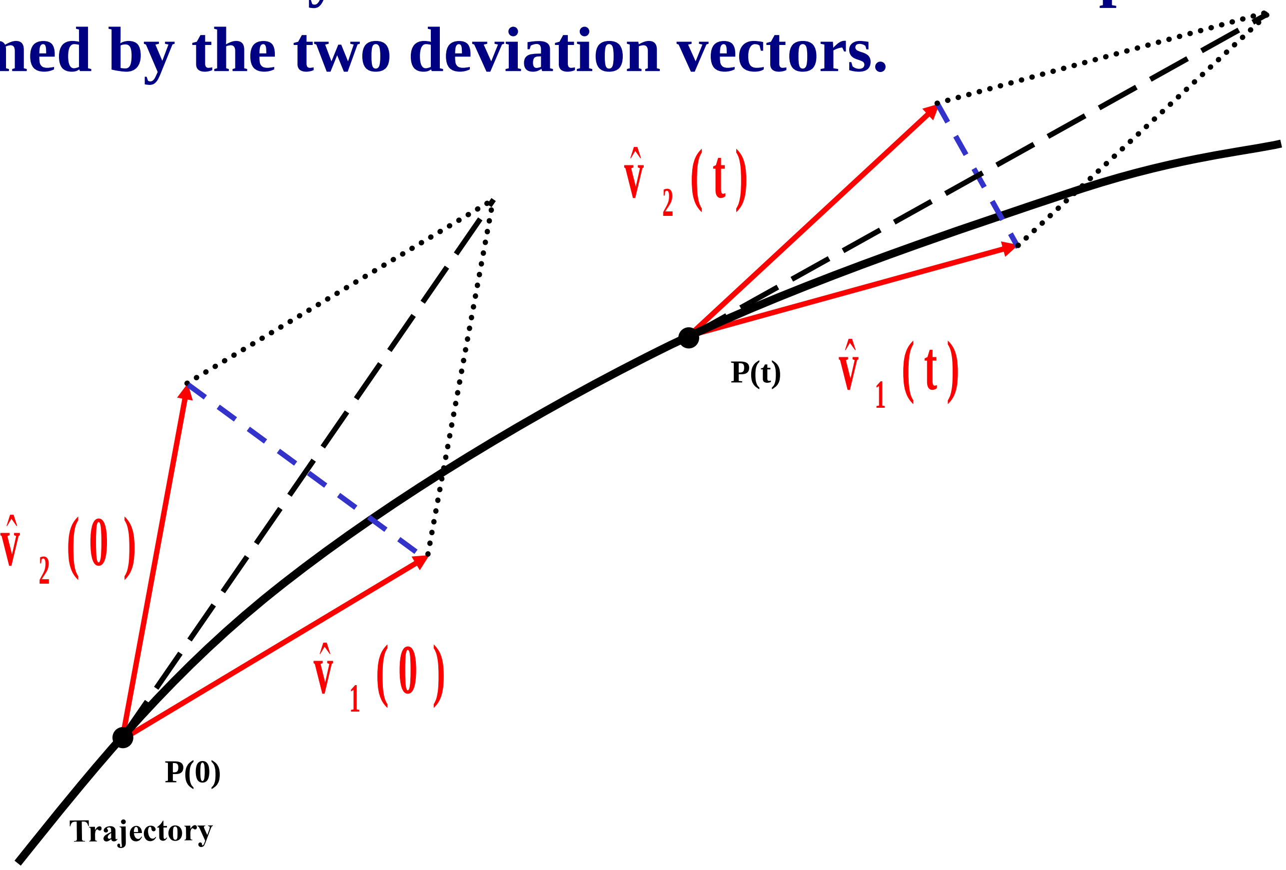

Definition of the Generalized Alignment Index (GALI)

SALI effectively measures the 'area' of the parallelogram formed by the two deviation vectors.

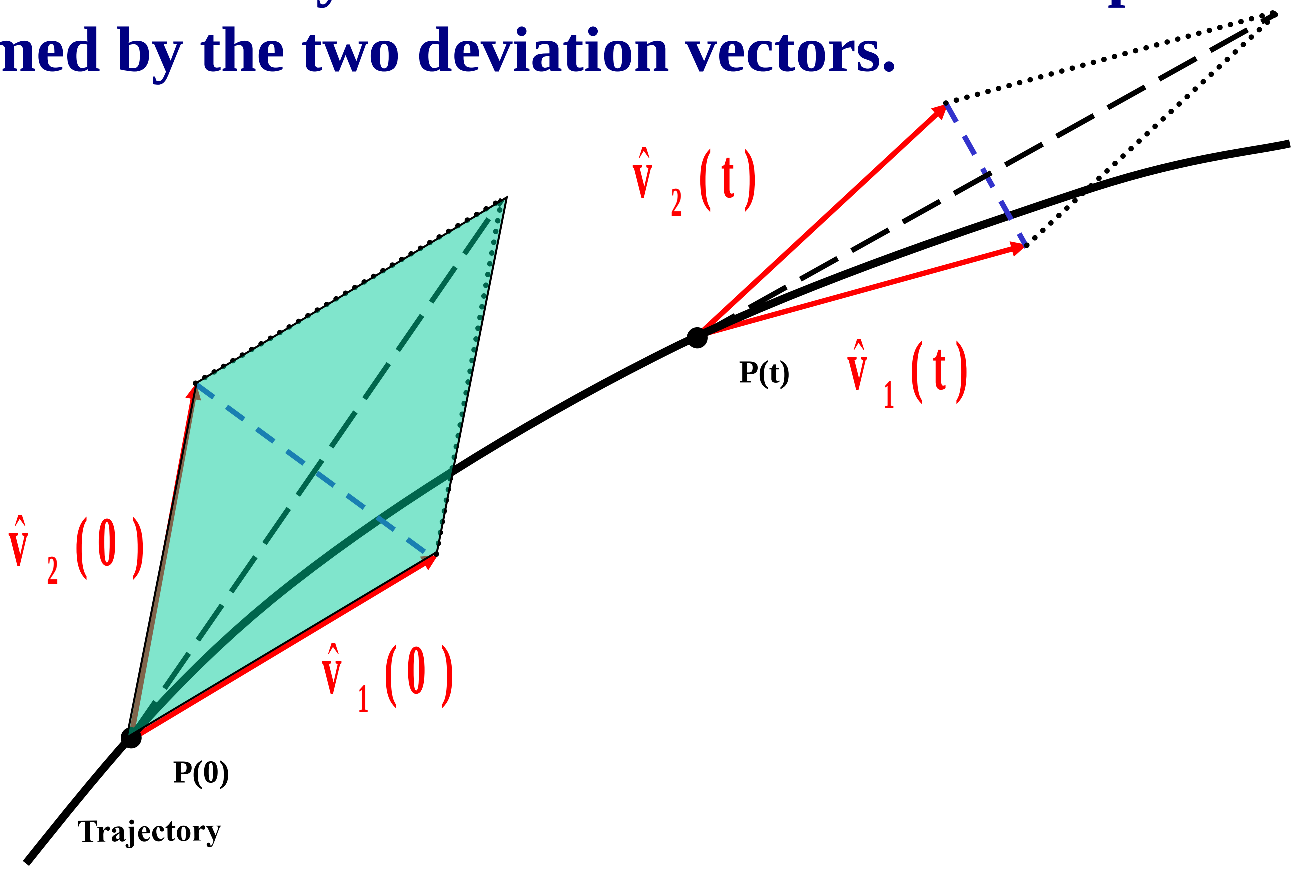

Definition of the Generalized Alignment Index (GALI)

SALI effectively measures the 'area' of the parallelogram formed by the two deviation vectors.

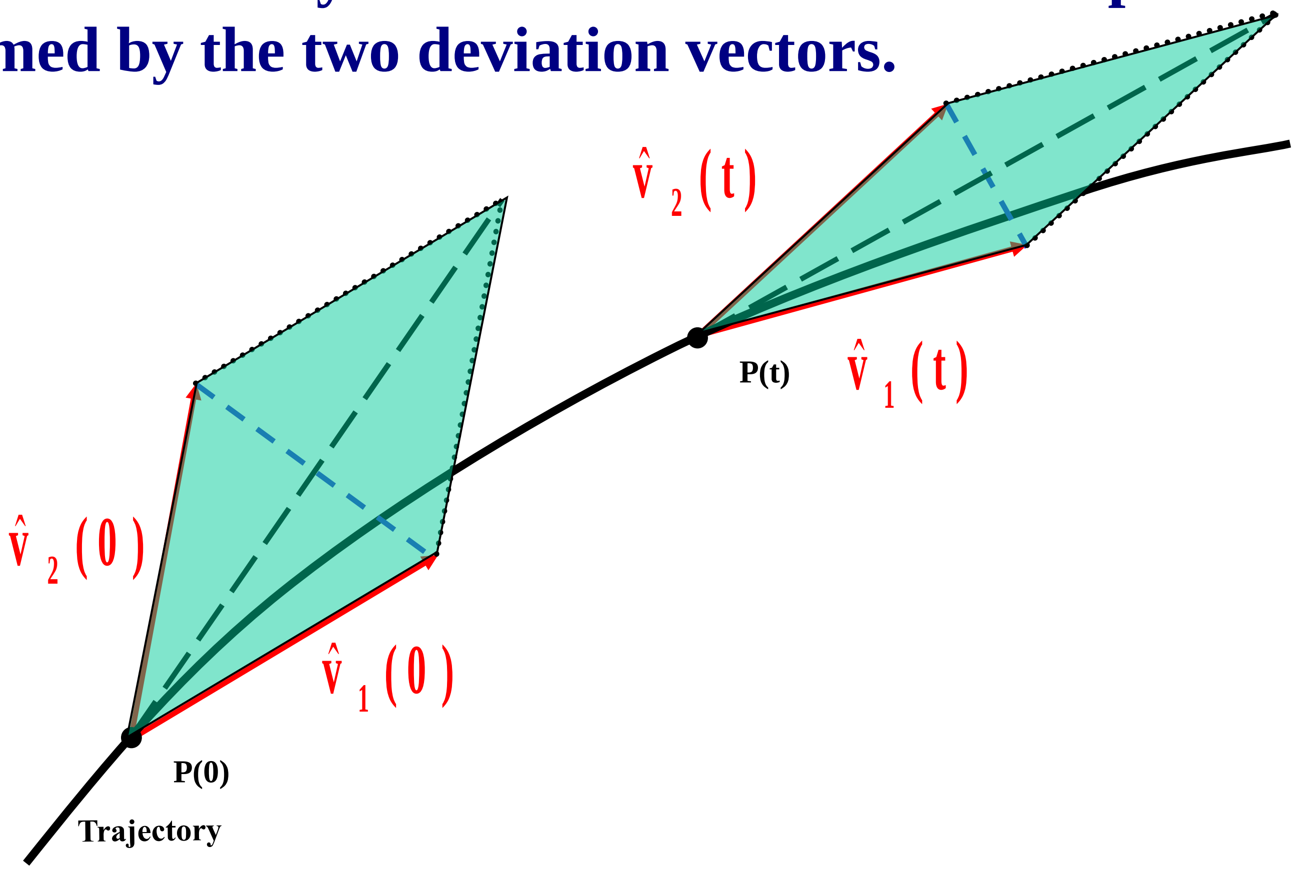

Definition of the Generalized Alignment Index (GALI)

SALI effectively measures the 'area' of the parallelogram formed by the two deviation vectors.

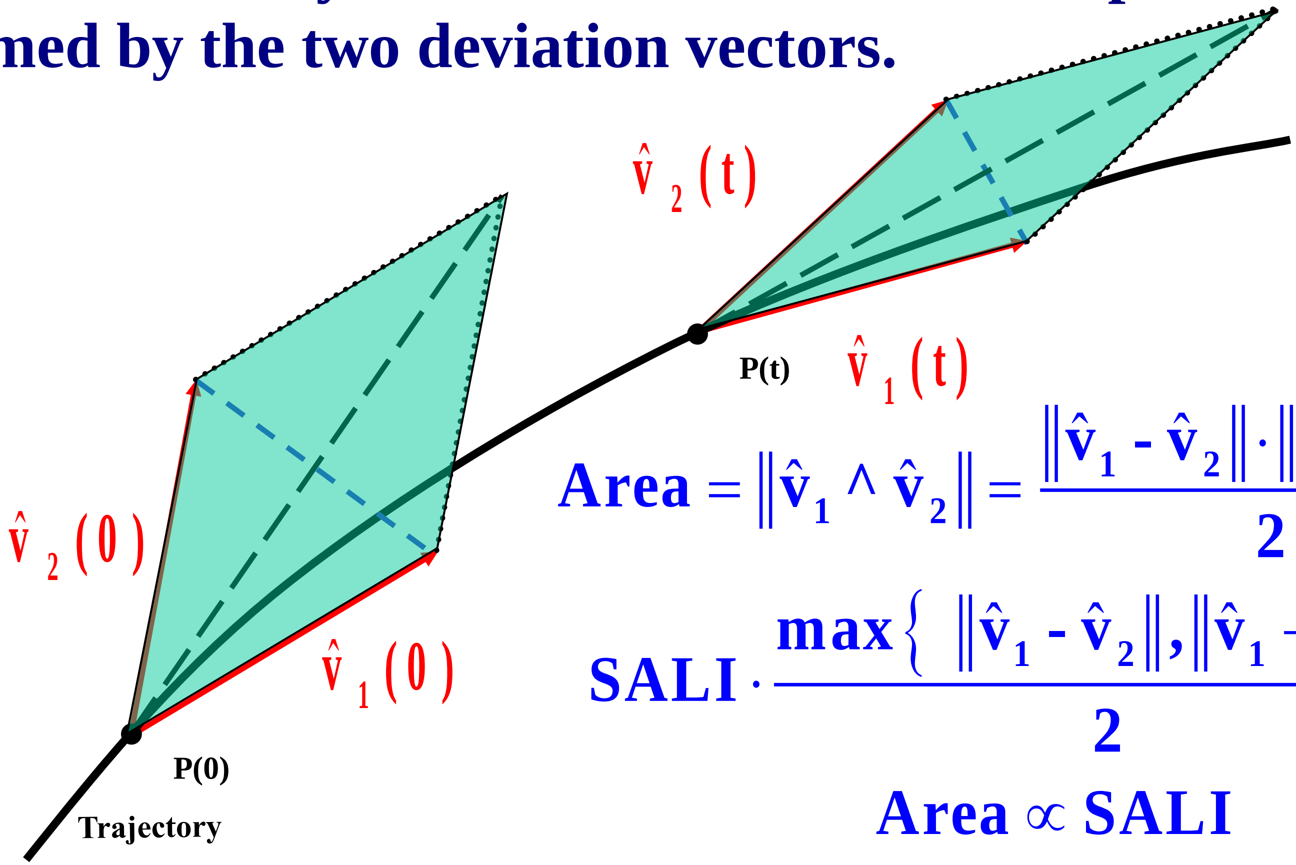

$$\text{Area} = \left\|\hat{\mathbf{v}}_1 \wedge \hat{\mathbf{v}}_2\right\| = \frac{\left\|\hat{\mathbf{v}}_1 - \hat{\mathbf{v}}_2\right\| \cdot \left\|\hat{\mathbf{v}}_1 + \hat{\mathbf{v}}_2\right\|}{2} =$$

$$\text{SALI} \cdot \frac{\max\left\{\left\|\hat{\mathbf{v}}_1 - \hat{\mathbf{v}}_2\right\|, \left\|\hat{\mathbf{v}}_1 + \hat{\mathbf{v}}_2\right\|\right\}}{2} \Rightarrow$$

$$\text{Area} \propto \text{SALI}$$

Definition of the GALI

In the case of an N degree of freedom Hamiltonian system or a 2N symplectic map we follow the evolution of

k deviation vectors with 2≤k≤2N,

and define (Ch.S., Bountis, Antonopoulos, 2007, Physica D) the Generalized Alignment Index (GALI) of order k :

$$GALI_k(t) = \left\| \hat{v}_1(t) \wedge \hat{v}_2(t) \wedge \ldots \wedge \hat{v}_k(t) \right\|$$

where

$$\hat{v}_1(t) = \frac{v_1(t)}{\left\| v_1(t) \right\|}$$

Behavior of the $GALI_k$ for chaotic motion

$GALI_k$ ($2 \leq k \leq 2N$) tends exponentially to zero with exponents that involve the values of the first k largest Lyapunov exponents $\sigma_1, \sigma_2, \ldots, \sigma_k$:

$$GALI_k(t) \propto e^{-\left[(\sigma_1-\sigma_2)+(\sigma_1-\sigma_3)+\ldots+(\sigma_1-\sigma_k)\right]t}$$

The above relation is valid even if some Lyapunov exponents are equal, or very close to each other.

Behavior of the $GALI_k$ for chaotic motion

N particles Fermi-Pasta-Ulam (FPU) system:

$$H = \frac{1}{2}\sum_{i=1}^{N} p_i^2 + \sum_{i=0}^{N}\left[\frac{1}{2}(q_{i+1} - q_i)^2 + \frac{\beta}{4}(q_{i+1} - q_i)^4\right]$$

with fixed boundary conditions, N=8 and β=1.5.

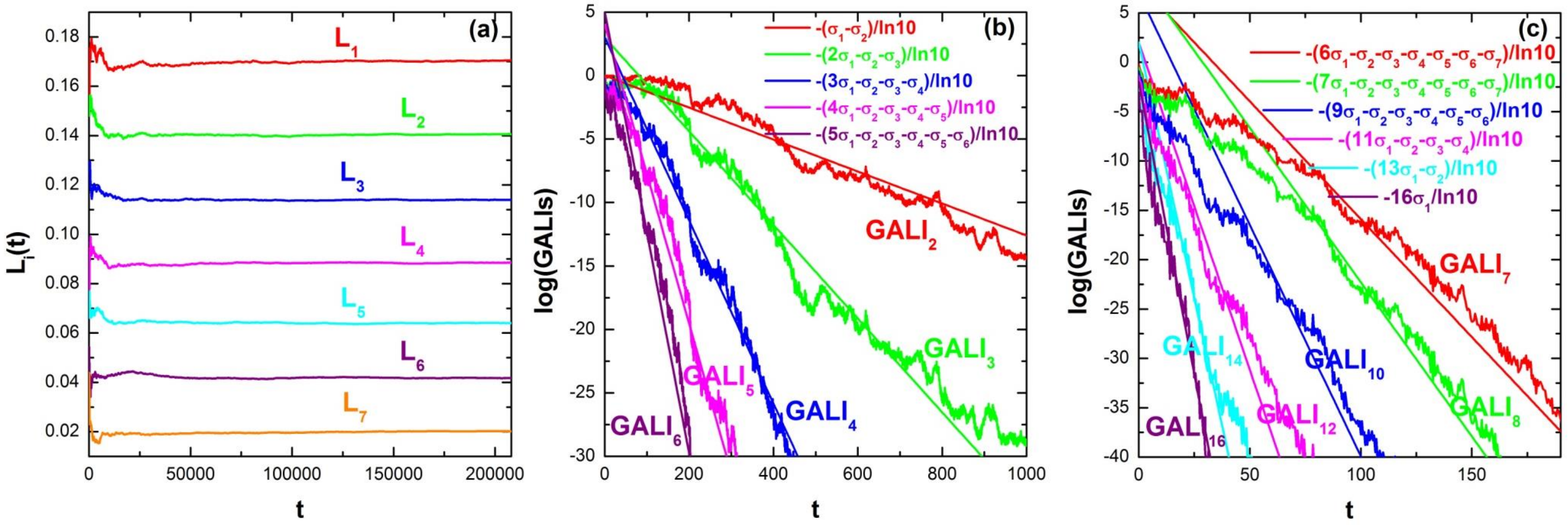

Behavior of the $GALI_k$ for regular motion

If the motion occurs on an s-dimensional torus with s≤N then the behavior of $GALI_k$ is given by (Ch.S., Bountis, Antonopoulos, 2008, Eur. Phys. J. Sp. Top.):

$$GALI_k(t) \propto \begin{cases} \text{constant} & \text{if} \quad 2 \le k \le s \\ \dfrac{1}{t^{k-s}} & \text{if} \quad s < k \le 2N - s \\ \dfrac{1}{t^{2(k-N)}} & \text{if} \quad 2N - s < k \le 2N \end{cases}$$

while in the common case with s=N we have :

$$GALI_k(t) \propto \begin{cases} \text{constant} & \text{if} \quad 2 \le k \le N \\ \dfrac{1}{t^{2(k-N)}} & \text{if} \quad N < k \le 2N \end{cases}$$

Behavior of the $GALI_k$ for regular motion

N=8 FPU system

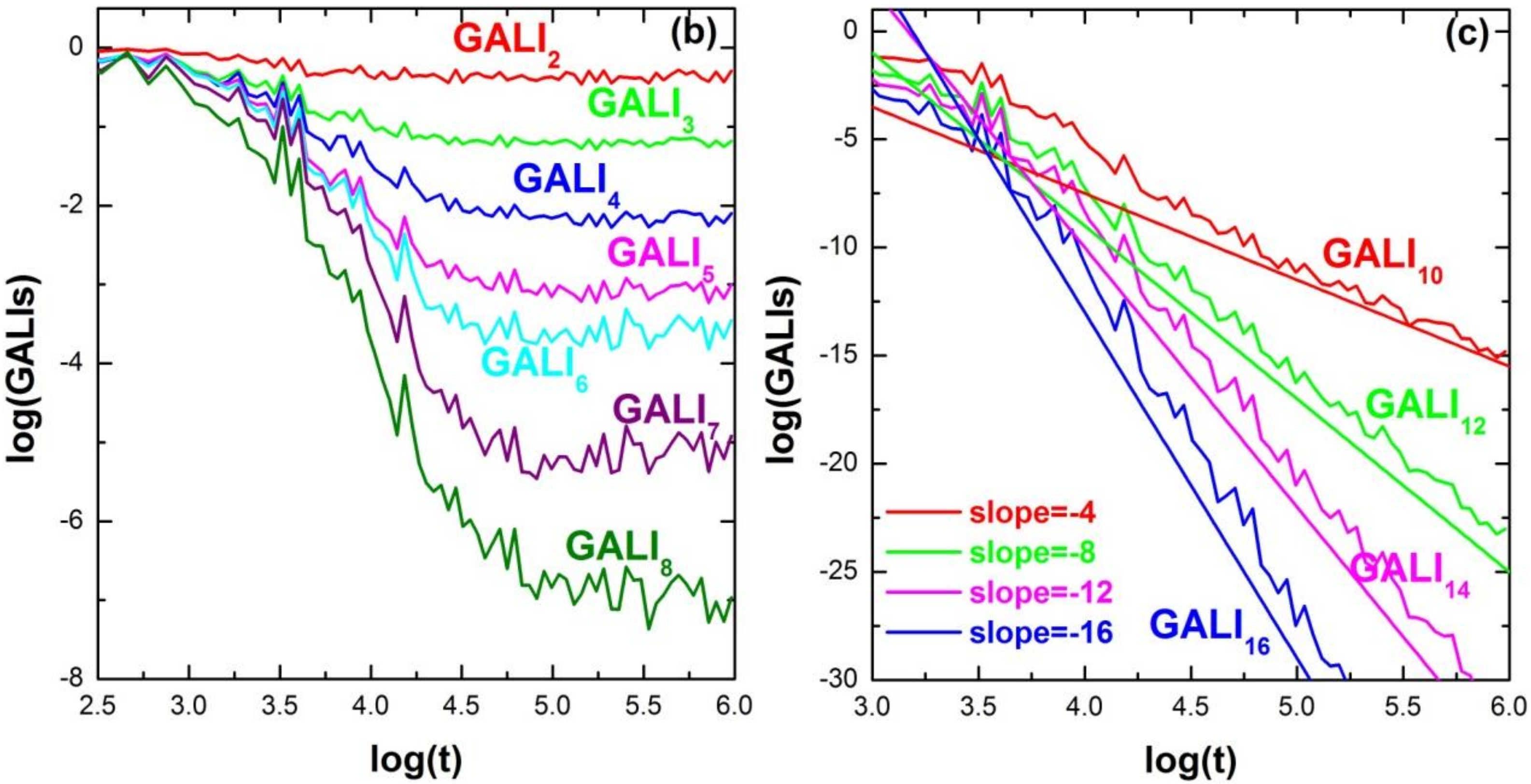

A time-dependent Hamiltonian system

Barred galaxies

NGC 1433

NGC 2217

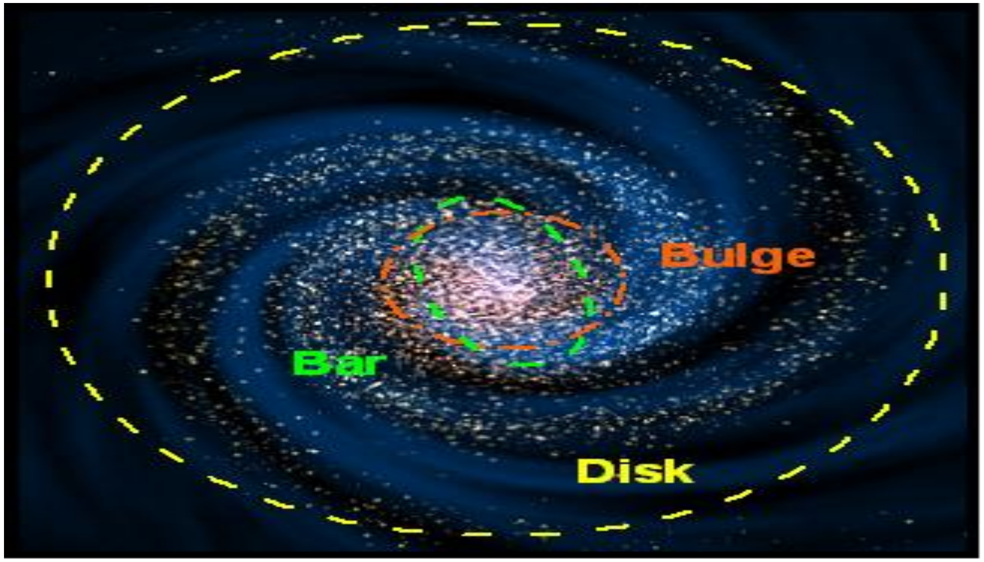

Barred galaxy model

The 3D bar rotates around its short *z*-axis (*x*: long axis and *y*: intermediate). The Hamiltonian that describes the motion for this model is:

$$H = \frac{1}{2}(p_x^2 + p_y^2 + p_z^2) + V(x,y,z) - \Omega_b(xp_y - yp_x) \equiv Energy$$

This model consists of the superposition of potentials describing an axisymmetric part and a bar component of the galaxy (Manos, Bountis, Ch.S., 2013, J. Phys. A).

a) Axisymmetric component:

i) Plummer sphere:

$$V_{sphere}(x,y,z) = -\frac{GM_S}{\sqrt{x^2 + y^2 + z^2 + \varepsilon_s^2}}$$

ii) Miyamoto–Nagai disc:

$$V_{disc}(x,y,z) = -\frac{GM_D}{\sqrt{x^2 + y^2 + (A + \sqrt{B^2 + z^2})^2}}$$

b) Bar component: $V_{bar}(x,y,z) = -\pi Gabc\frac{\rho_c}{n+1}\int_\lambda^\infty \frac{du}{\Delta(u)}(1 - m^2(u))^{n+1},$

(Ferrers bar)

$$\rho_c = \frac{105}{32\pi}\frac{GM_B}{abc}$$

where $m^2(u) = \frac{x^2}{a^2+u} + \frac{y^2}{b^2+u} + \frac{z^2}{c^2+u}, \; \Delta^2(u) = (a^2+u)(b^2+u)(c^2+u),$

n: positive integer ($n = 2$ for our model), λ: the unique positive solution of $m^2(\lambda) = 1$

Its density is:

$$\rho = \begin{cases} \rho_c(1 - m^2)^n, & \text{for } m \le 1 \\ 0, & \text{for } m > 1 \end{cases}, \; \text{where } m^2 = \frac{x^2}{a^2} + \frac{y^2}{b^2} + \frac{z^2}{c^2}, \; a > b > c \text{ and } n = 2.$$

Time-dependent barred galaxy model

The 3D bar rotates around its short *z*-axis (*x*: long axis and *y*: intermediate). The Hamiltonian that describes the motion for this model is:

$$H = \frac{1}{2}(p_x^2 + p_y^2 + p_z^2) + V(x,y,z,t) - \Omega_b(xp_y - yp_x) \equiv Energy$$

This model consists of the superposition of potentials describing an axisymmetric part and a bar component of the galaxy (Manos, Bountis, Ch.S., 2013, J. Phys. A).

a) Axisymmetric component:

$$M_S + M_B(t) + M_D(t) = 1, \quad \text{with} \quad M_B(t) = M_B(0) + \alpha t$$

i) Plummer sphere:

$$V_{sphere}(x,y,z) = -\frac{GM_S}{\sqrt{x^2 + y^2 + z^2 + \varepsilon_s^2}}$$

ii) Miyamoto–Nagai disc:

$$V_{disc}(x,y,z) = -\frac{GM_D(t)}{\sqrt{x^2 + y^2 + (A + \sqrt{B^2 + z^2})^2}}$$

b) Bar component: $V_{bar}(x,y,z) = -\pi Gabc \frac{\rho_c}{n+1} \int_\lambda^\infty \frac{du}{\Delta(u)} (1 - m^2(u))^{n+1},$

(Ferrers bar)

$$\rho_c = \frac{105}{32\pi} \frac{GM_B(t)}{abc}$$

where $m^2(u) = \frac{x^2}{a^2+u} + \frac{y^2}{b^2+u} + \frac{z^2}{c^2+u}, \quad \Delta^2(u) = (a^2+u)(b^2+u)(c^2+u),$

n: positive integer ($n = 2$ for our model), λ: the unique positive solution of $m^2(\lambda) = 1$

Its density is:

$$\rho = \begin{cases} \rho_c (1 - m^2)^n, & \text{for } m \le 1 \\ 0, & \text{for } m > 1 \end{cases}, \quad \text{where } m^2 = \frac{x^2}{a^2} + \frac{y^2}{b^2} + \frac{z^2}{c^2}, \quad a > b > c \text{ and } n = 2.$$

Time-dependent 2D barred galaxy model

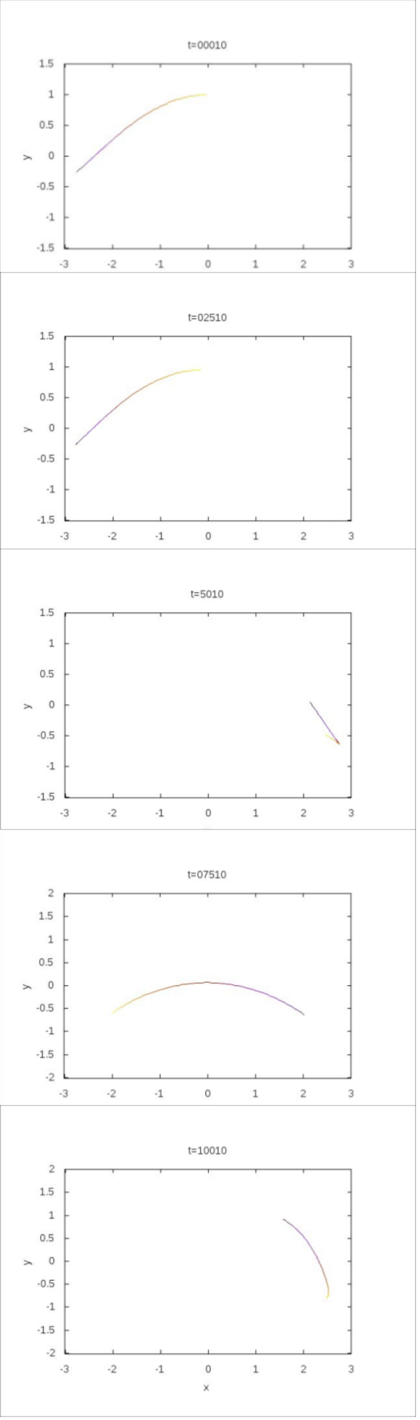

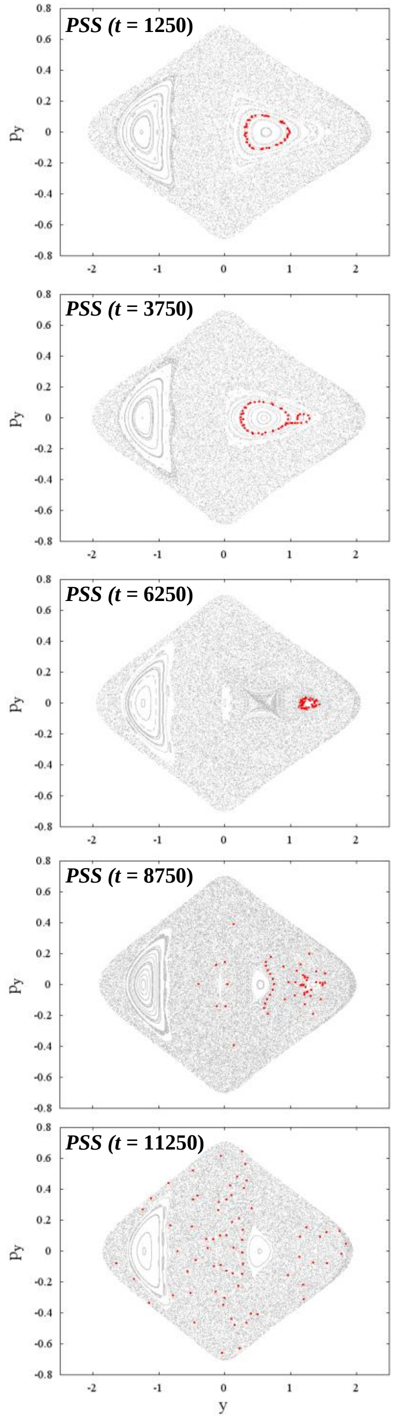

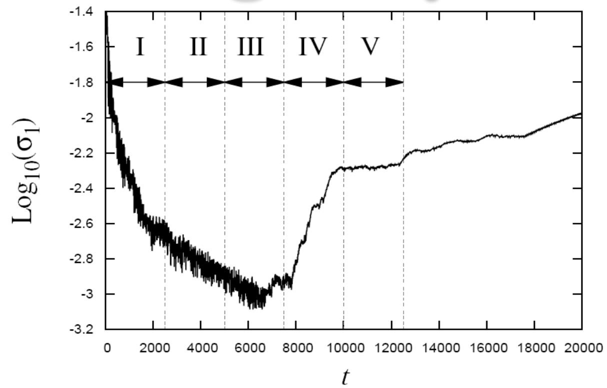

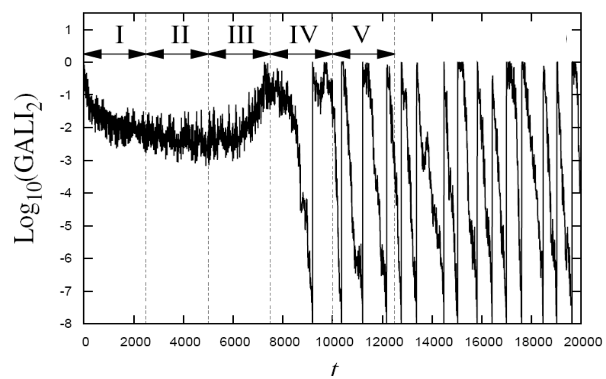

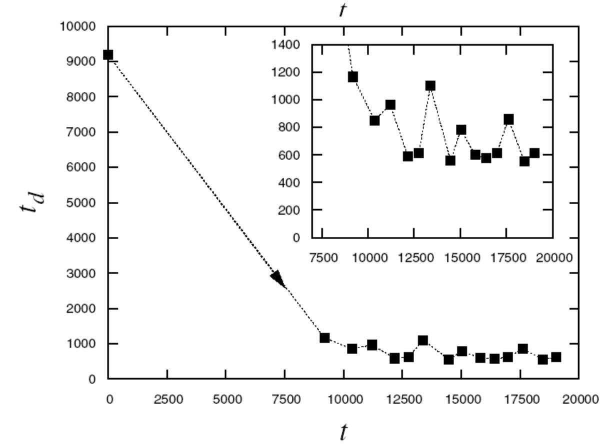

Time-dependent 3D barred galaxy model

Interplay between chaotic and regular motion

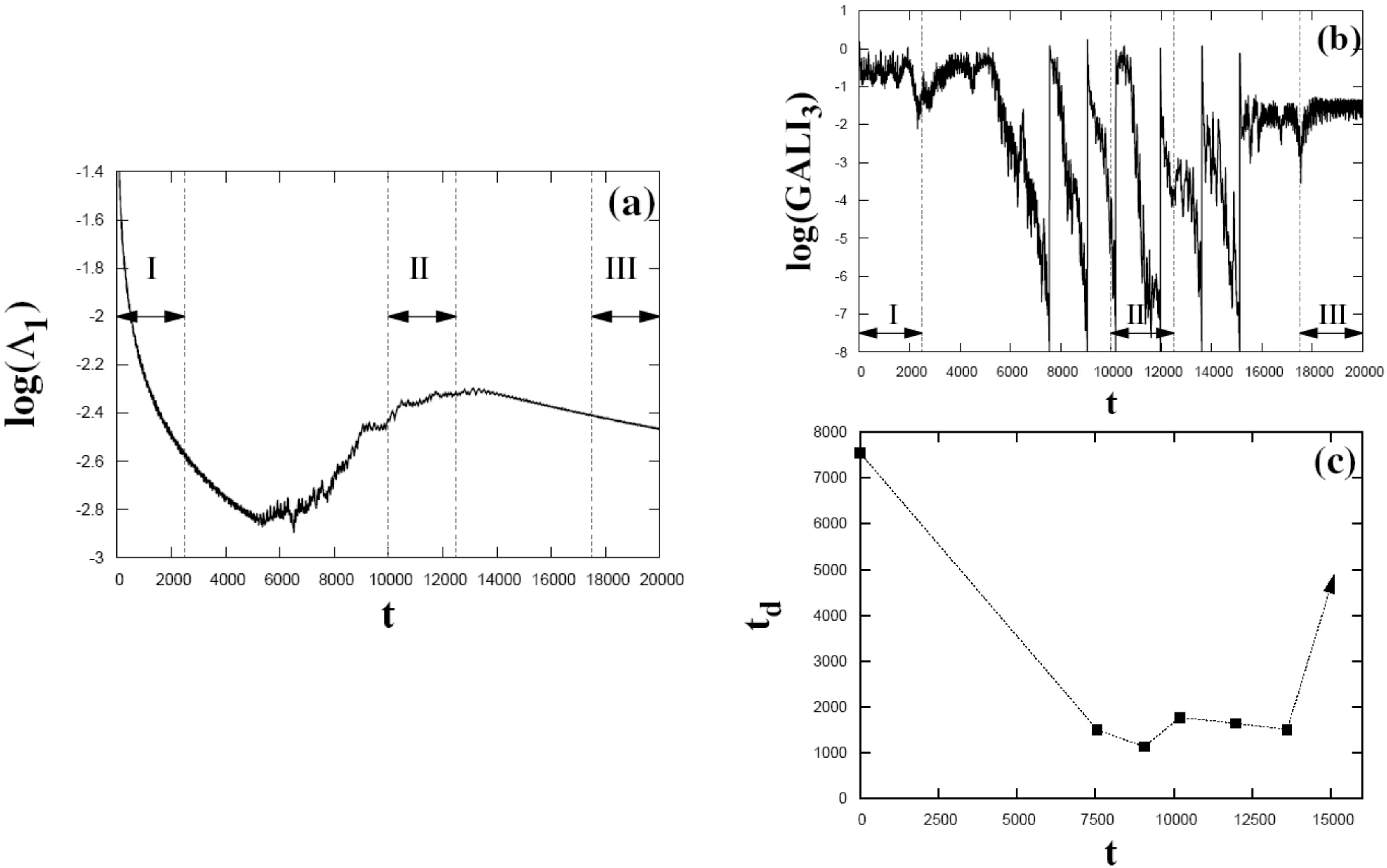

Summary

- **We discussed methods of chaos detection based on**
  - ✓ **the visualization of orbits**
  - ✓ **the numerical analysis of orbits**
  - ✓ **the evolution of deviation vectors (variational equations – tangent map)**

Summary

- **We discussed methods of chaos detection based on**
  - ✓ **the visualization of orbits**
  - ✓ **the numerical analysis of orbits**
  - ✓ **the evolution of deviation vectors (variational equations – tangent map)**
- **The Smaller (SALI) and the Generalized (GALI) ALignment Index methods are fast, efficient and easy to compute chaos indicator.**
- **Behaviour of the Generalized ALignment Index of order k ($GALI_k$):**
  - ✓ **Chaotic motion: it tends exponentially to zero**
  - ✓ **Regular motion: it fluctuates around non-zero values (or goes to zero following power-laws)**

Summary

- **We discussed methods of chaos detection based on**
  - ✓ **the visualization of orbits**
  - ✓ **the numerical analysis of orbits**
  - ✓ **the evolution of deviation vectors (variational equations – tangent map)**
- **The Smaller (SALI) and the Generalized (GALI) ALignment Index methods are fast, efficient and easy to compute chaos indicator.**
- **Behaviour of the Generalized ALignment Index of order k ($GALI_k$):**
  - ✓ **Chaotic motion: it tends exponentially to zero**
  - ✓ **Regular motion: it fluctuates around non-zero values (or goes to zero following power-laws)**
- **$GALI_k$ indices :**
  - ✓ **can distinguish rapidly and with certainty between regular and chaotic motion**
  - ✓ **can be used to characterize individual orbits as well as "chart" chaotic and regular domains in phase space**
  - ✓ **are perfectly suited for studying the global dynamics of multidimentonal systems, as well as of time-dependent models**

Main References I

- **The color and rotation (CR) method**
  - ✓ Patsis P. A. & Zachilas L (1994) Int. J. Bif. Chaos, 4, 1399
  - ✓ Katsanikas M & Patsis P A (2011) Int. J. Bif. Chaos, 21, 467
  - ✓ Katsanikas M, Patsis P A & Contopoulos G. (2011) Int. J. Bif. Chaos, 21, 2321

- **the 3D phase space slices (3PSS) technique**
  - ✓ Richter M, Lange S, Backer A & Ketzmerick R (2014), Phys. Rev. E 89, 022902
  - ✓ Lange S, Richter M, Onken F, Backer A & Ketzmerick R (2014), Chaos 24, 024409
  - ✓ Onken F, Lange S, Ketzmerick R & Backer A (2016), Chaos 26, 063124

- **Frequency Analysis**
  - ✓ Laskar J (1990) Icarus, 88, 266
  - ✓ Laskar J, Froeschle C &Celletti A (1992) Physica D, 56, 253
  - ✓ Laskar J (1993) Physica D, 67, 257
  - ✓ Bartolini R, Bazzani A, Giovannozzi M, Scandale W & Todesco E (1996) Part. Accel. 52, 147
  - ✓ Laskar J (1999) in Hamiltonian systems with three or more degrees of freedom (ed. Simo C / Plenum Press) p 134

- **Lyapunov exponents**
  - ✓ Oseledec V I (1968) Trans. Moscow Math. Soc., 19, 197
  - ✓ Benettin G, Galgani L, Giorgilli A &Strelcyn J-M (1980) Meccanica, March, 9
  - ✓ Benettin G, Galgani L, Giorgilli A &Strelcyn J-M (1980) Meccanica, March, 21
  - ✓ Wolf A, Swift J B, Swinney H L &Vastano J A (1985) Physica D, 16, 285
  - ✓ Ch.S. (2010) Lect. Notes Phys., 790, 63

Main References II

- **0-1 test**
  - ✓ Gottwald G A & Melbourne I (2004) Proc. R. Soc. A, 460, 603
  - ✓ Gottwald G A & Melbourne I (2005) Physica D, 212, 100
  - ✓ Gottwald G A & Melbourne I (2009) SIAM J. Appl. Dyn., 8, 129
  - ✓ Gottwald G A & Melbourne I (2016) Lect. Notes Phys., 915, 221

- **FLI – OFLI – OFLI2**
  - ✓ Froeschle C, Lega E & Gonczi R (1997) Celest. Mech. Dyn. Astron., 67, 41
  - ✓ Guzzo M, Lega E & Froeschle C (2002) Physica D, 163, 1
  - ✓ Fouchard M, Lega E, Froeschle C & Froeschle C (2002) Celest. Mech. Dyn. Astron., 83, 205
  - ✓ Barrio R (2005) Chaos Sol. Fract., 25, 71
  - ✓ Barrio R (2006) Int. J. Bif. Chaos, 16, 2777
  - ✓ Lega E, Guzzo M & Froeschle C (2016) Lect. Notes Phys., 915, 35
  - ✓ Barrio R (2016) Lect. Notes Phys., 915, 55

- **MEGNO**
  - ✓ Cincotta P M & Simo (2000) Astron. Astroph. Suppl. Ser., 147, 205
  - ✓ Cincotta P M, Giordano C M & Simo C (2003) Physica D, 182, 151
  - ✓ Cincotta P M, & Giordano C M (2016) Lect. Notes Phys., 915, 93

- **RLI**
  - ✓ Sandor Zs, Erdi B & Efthymiopoulos C (2000) Celest. Mech. Dyn. Astron., 78, 113
  - ✓ Sandor Zs, Erdi B, Szell A & Funk B (2004) Celest. Mech. Dyn. Astron., 90 127
  - ✓ Sandor Zs & Maffione N (2016) Lect. Notes Phys., 915, 183

Main References III

- **SALI**

  - ✓ Ch.S. (2001) J. Phys. A, 34, 10029
  - ✓ Ch.S., Antonopoulos Ch, Bountis T C & Vrahatis M N (2003) Prog. Theor. Phys. Supp., 150, 439
  - ✓ Ch.S., Antonopoulos Ch, Bountis T C & Vrahatis M N (2004) J. Phys. A, 37, 6269
  - ✓ Bountis T & Ch.S. (2006) Nucl. Inst Meth. Phys Res. A, 561, 173
  - ✓ Boreaux J, Carletti T, Ch.S. &Vittot M (2012) Com. Nonlin. Sci. Num. Sim., 17, 1725
  - ✓ Boreaux J, Carletti T, Ch.S., Papaphilippou Y & Vittot M (2012) Int. J. Bif. Chaos, 22, 1250219

- **GALI**

  - ✓ Ch.S., Bountis T C & Antonopoulos Ch (2007) Physica D, 231, 30
  - ✓ Ch.S., Bountis T C & Antonopoulos Ch (2008) Eur. Phys. J. Sp. Top., 165, 5
  - ✓ Gerlach E, Eggl S & Ch.S. (2012) Int. J. Bif. Chaos, 22, 1250216
  - ✓ Manos T, Ch.S. & Antonopoulos Ch (2012) Int. J. Bif. Chaos, 22, 1250218
  - ✓ Manos T, Bountis T & Ch.S. (2013) J. Phys. A, 46, 254017

- **Reviews on SALI and GALI**

  - ✓ Bountis T C & Ch.S. (2012) 'Complex Hamiltonian Dynamics', Chapter 5, Springer Series in Synergetics
  - ✓ Ch.S. & Manos T (2016) Lect. Notes Phys., 915, 129

A …shameless promotion

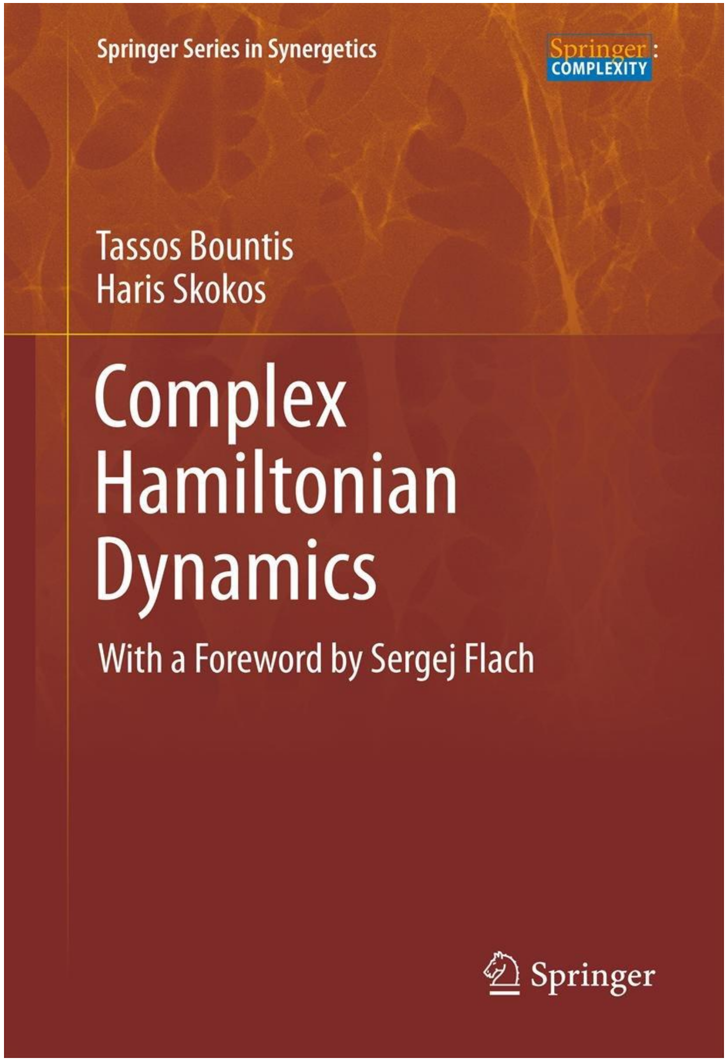

2012, Springer Series in Synergetics

Contents

Another …shameless promotion

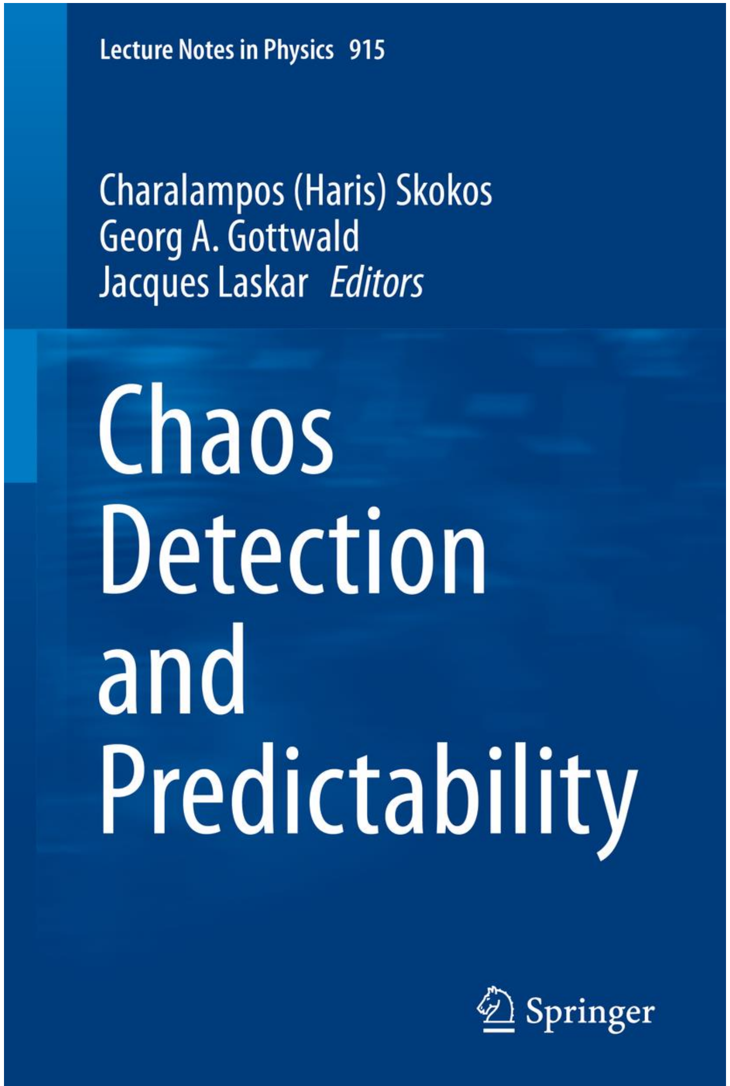

2016, Lect. Notes Phys., 915, Springer

Contents